Unusual negative ions in high pressure electron capture mass spectrometry
by Lyle Joseph Sears

A thesis submitted in partial fulfillment of the requirements for the degree of Doctor of Philosophy in Chemistry
Montana State University

Abstract:
Recent reports and observations of unexpected negative ions in spectra obtained under electron capture (EC) conditions of high pressure mass spectrometry ion sources suggest that secondary processes are operative concurrent with those of electron capture. The EC spectra containing these unusual negative ions may be difficult or impossible to interpret in terms of the well-known EC reactions.

A kinetic model for the chemical events occurring within the high pressure electron capture mass spectrometer (HPECMS) ion source is developed here. It includes four different pathways by which unusual negative ions are produced. The processes involved in these routes to unusual ions include reactions of gas phase free radicals, surface assisted reactions, ion-electron and ion-ion recombination reactions, ion-wall neutralization, and wall assisted transformations of neutrals.

The kinetic model is applied to the explanation of unusual negative ions which occur in EC spectra from various compound classes. These include the trifluoroacetic derivatives of polycyclic aromatic amines, which have been shown to be present in materials derived from liquified coal, and derivatives of hexachlorocyclopentadiene which are used as pesticides.

The efficiency of negative ion formation by secondary processes in high pressure electron capture ion sources can lead to ions of greater abundance than those generated by direct electron capture. This is supported by calculations provided by the model.

Techniques are developed which can control or eliminate the occurrence of unusual negative ions in EC spectra. Carbon dioxide, when used as the buffer gas, can provide EC spectra which are free of ions originating from secondary processes. Equivalent or lower analyte detection limits are demonstrated when carbon dioxide is used as the buffer gas rather than methane.

UNUSUAL NEGATIVE IONS IN HIGH PRESSURE ELECTRON CAPTURE MASS SPECTROMETRY

by

Lyle Joseph Sears

A thesis submitted in partial fulfillment
of the requirements for the degree

of

Doctor of Philosophy

in

Chemistry

MONTANA STATE UNIVERSITY
Bozeman, Montana

March, 1989

APPROVAL

of a thesis submitted by

Lyle Joseph Sears

This thesis has been read by each member of the thesis committee and has been found to be satisfactory regarding content, English usage, format, citations, bibliographic style, and consistency, and is ready for submission to the College of Graduate Studies.

March 23, 1989
Date

Eric Diemond
Chairperson, Graduate Committee

Approved for the Chemistry Department

March 23, 1989
Date

Edwin H. Abbott
Head, Chemistry Department

Approved for the College of Graduate Studies

March 31, 1989
Date

Henry L Parsons
Graduate Dean

STATEMENT OF PERMISSION TO USE

In presenting this thesis in partial fulfillment of the requirements for a doctoral degree at Montana State University, I agree that the Library shall make it available to borrowers under rules of the Library. I further agree that copying of this thesis is allowable only for scholarly purposes, consistent with "fair use" as prescribed in the U.S. Copyright Law. Requests for extensive copying or reproduction of this thesis should be referred to University Microfilms International, 300 North Zeeb Road, Ann Arbor, Michigan 48106, to whom I have granted "the exclusive right to reproduce and distribute copies of the dissertation in and from microfilm and the right to reproduce and distribute by abstract in any format."

Signature L Joseph Soare

Date March 29, 1989

I would like to dedicate this thesis to my wife Katie, who has remained a cheerful and supportive spouse of a graduate student for so many years; my children Steven and Samantha who have sacrificed the most in time forever lost with their father; my mother who has always known that I would accomplish this goal, even when I had my doubts; and my father, who knew and was proud of my pending accomplishments, but did not live to see their completion.

VITA

Lyle Joseph Sears was born on May 19, 1955 in Gothenburg, Nebraska. He is the son of Sam G. Sears and Ella N. Sears. He graduated from Bennett County High School in Martin, South Dakota in 1973. Joe began his undergraduate studies in 1973 at Chadron State College, Chadron, Nebraska and received his Bachelor of Arts Degree in 1977 with majors in Chemistry and Biology. He was accepted into graduate school at Montana State University in 1982 to pursue his Doctor of Philosophy Degree in Chemistry.

He has accepted a position in the Department of Chemistry at Montana State University as the Director of the Mass Spectrometry Facility, beginning in March, 1989.

ACKNOWLEDGMENT

The author expresses his sincere appreciation to Dr. James McCafferty and Dr. Arthur Struempler from Chadron State College, Chadron, Nebraska. These two individuals are responsible for providing an educational atmosphere which nurtured my interest in chemistry. Without the opportunities provided for undergraduate research, support in obtaining employment in chemistry, and their friendship, it is unlikely that I would here completing this docotoral dissertation.

A special thanks goes to Dr. Eric Grimsrud who provided the opportunity for me to stay in graduate school to earn a doctorate degree by way of employment in the mass spectrometry facility. The guidance and constructive criticism he has provided in the course of this thesis work was extremely beneficial and will certainly enhance my professional career.

TABLE OF CONTENTS

LIST OF TABLES

LIST OF FIGURES

ABSTRACT

Recent reports and observations of unexpected negative ions in spectra obtained under electron capture (EC) conditions of high pressure mass spectrometry ion sources suggest that secondary processes are operative concurrent with those of electron capture. The EC spectra containing these unusual negative ions may be difficult or impossible to interpret in terms of the well-known EC reactions.

A kinetic model for the chemical events occurring within the high pressure electron capture mass spectrometer (HPECMS) ion source is developed here. It includes four different pathways by which unusual negative ions are produced. The processes involved in these routes to unusual ions include reactions of gas phase free radicals, surface assisted reactions, ion-electron and ion-ion recombination reactions, ion-wall neutralization, and wall assisted transformations of neutrals.

The kinetic model is applied to the explanation of unusual negative ions which occur in EC spectra from various compound classes. These include the trifluoroacetic derivatives of polycyclic aromatic amines, which have been shown to be present in materials derived from liquified coal, and derivatives of hexachlorocyclopentadiene which are used as pesticides. The efficiency of negative ion formation by secondary processes in high pressure electron capture ion sources can lead to ions of greater abundance than those generated by direct electron capture. This is supported by calculations provided by the model.

Techniques are developed which can control or eliminate the occurrence of unusual negative ions in EC spectra. Carbon dioxide, when used as the buffer gas, can provide EC spectra which are free of ions originating from secondary processes. Equivalent or lower analyte detection limits are demonstrated when carbon dioxide is used as the buffer gas rather than methane.

INTRODUCTION

The use of Chemical Ionization Mass Spectrometry (CIMS) as an analytical technique had its origins with investigations conducted by Munson and Field[1] in the more general area of high pressure gas phase ion chemistry. The initial studies centered on the generation of positive ion signals. A reagent gas, often methane, was introduced to the ion source at pressures of 0.1 to 1.0 Torr. The gas was bombarded by a beam of electrons which provided a series of interactions that led to the formation of a set of reagent ions. An analyte was introduced and the resulting signal reflected the nature of the ion-molecule reaction between the reagent ions and the sample molecules.

It was soon discovered that different reagent gases provided considerably different analytical signals. For example, when methane was used as the reagent gas a proton transfer would often occur from the reagent ion to the analyte[1]. The use of nitrogen would often provide positive ion spectra by electron transfer which were similar to those obtained under electron impact conditions[2]. The result of these initial investigations was the development of a good understanding of positive ion-molecule reactions which occur under chemical ionization mass spectrometry

conditions. An excellent review of the subject of positive ion-molecule reactions has been written by Harrison[2]. A summary of some of these reactions is as follows:

Proton Transfer	$M + XH^+ \longrightarrow MH^+ + X$	(1)
Hydride Abstraction	$M + X^+ \longrightarrow [M-H]^+ + XH$	(2)
Charge Exchange	$M + X^+ \longrightarrow M^+ + X$	(3)
Adduct Formation	$M + X^+ \longrightarrow MX^+$	(4)
Self Clustering	$M + M^+ \longrightarrow M_2^+$	(5)

Initial efforts in CIMS involved only positive ion-molecule reactions. Theory demanded that high pressure ion sources operated at relatively high ion densities ($\geq 10^8$ ions cm^{-3}) exhibit overall charge neutrality. This implied that large densities of negative ions and/or electrons must be present in addition to the commonly observed positive ions. Daugherty[3] was the first to obtain negative ion chemical ioniztion spectra from analytical high pressure ion sources by making modifications to allow a mass spectrometer to detect the negative ions. Daugherty's first experiments involved the use of chloride reagent ions which reacted with the analyte by way of adduct formation.

The majority of the initial negative ion mass spectrometry investigations focused on negative ion-molecule reactions for the generation of ion signals, which greatly increased our understanding of this subject.

A summary of these reactions[2] is provided by the following expressions:

Hydrogen Abstraction	$MH + X^- \longrightarrow M^- + XH$	(6)
Adduct Formation	$M + X^- \longrightarrow MX^-$	(7)
Clustering	$M + M^- \longrightarrow M_2^-$	(8)

It became obvious that certain reagent gas systems yielded only positive ions and electrons upon interaction with an electron beam. This led to the utilization of the electrons as a reagent in the formation of negative ions from an analyte. This process, which is known as electron capture (EC), may occur through resonant (9a) or dissociative (9b) capture of a thermal electron by molecule MX as shown by:

$$MX + e(\text{thermal}) \longrightarrow MX^- \quad (9a)$$

$$MX + e(\text{thermal}) \longrightarrow M + X^- \quad (9b)$$

Thermal electrons are generally produced by interactions of a high energy electron beam with a buffer gas present in the ion source at 0.1 to 1.0 Torr. The buffer gas also serves to provide collisional quenching of the internal energy of the initially formed molecular negative ion, MX^-. The overall process of EC in mass spectrometer ion sources has been termed High Pressure Electron Capture Mass Spectrometry (HPECMS) to provide a unique distinction of

the technique from the more general field of negative ion chemical ionization mass spectrometry.

The minimum requirement for generation of a mass spectrum by HPECMS is that the analyte must have a reasonably large electron affinity (EA). This simple requirement provides a great deal of discrimination in chemical analysis. A limited set of compounds will have EA's large enough to capture thermal electrons to form negative ions having lifetimes of sufficient duration to allow detection. In many instances, EC may be extended to other molecules by simple derivatization procedures with fluorinated reagents. This increases an analyte's EA and its ability to form stable negative ions by electron capture.

It has been demonstrated that exceptionally high sensitivities are often obtainable with EC reactions[4]. A simultaneous comparison of positive ion and EC sensitivities of analytes having fast EC rate coefficients reveals that ion signals can be three orders of magnitude in favor of EC[4]. This is the direct result of the nature of the EC reaction, shown in expression 9, which can have rate coefficients two orders of magnitude larger than those of ion-molecule reactions. If EC is fast, then the majority of the analyte will be consumed by reactions with electrons before positive ion-molecule reactions can occur. This will result in increased signal bias in favor of

negative ions.

High pressure electron capture mass spectrometry has been used for the analysis of various classes of compounds. These have included halogenated hydrocarbons[3,5,6], polynuclear aromatic hydrocarbons[4,7,8] and derivatized alcohols and amines[9-11]. The observed ion signals are usually due to simple dissociative or resonance electron capture. In these cases the observed EC spectrum is easily interpreted in terms of the identity of the analyte molecule.

A careful inspection of the literature provides several examples, however, where the observed EC spectrum is not explainable solely by the resonance or dissociative EC mechanisms shown in reaction 9. One of these examples comes from investigations by Kassel, Kayganich and Watson[12] in which the EC spectra show abundant $[M+Cl]^-$ ions. The spectra were obtained in a methane plasma for compounds which contain little or no chlorine. Another example is the EC spectra of a series of polychlorinated pesticides reported by Stemmler and Hites[6] which contain a prominent series of ions differing by 34 amu; a mass loss which is considered impossible for this particular set of compounds. McEwen and Rudat[13,16] have shown that the EC spectra of the tetracyano derivatives of ethylene, quinodimethane and pyrazine in methane buffer gas include intense ions of the types, $[M+R]^-$ and $[M+R-CN]^-$, where R is

either CH_3 or H. A series of EC spectra of various aromatic hydrocarbons in methane buffer gas have been recently reported by Stockl and Budzikiewicz[7] and by Hilpert, Byrd and Vogt[8] which included ions of the type $[M+CH_2]^-$ and $[M+C_2H_4]^-$. Observations of our own which have been made in the course of this work provide additional examples of unusual negative ions, several of which will be reported here.

These examples of unusual ions in EC spectra demonstrate that secondary processes which provide negative ions of comparable intensity to those generated by direct EC may be very important. These processes are largely unknown. It is, therefore, necessary to reevaluate the overall dynamics of the HPECMS ion source. Particular attention is given to processes which may be kinetically favored over electron capture reactions.

STATEMENT OF RESEARCH OBJECTIVE

The goal of this research is to provide an improved understanding of the events occurring in the high pressure electron capture mass spectrometer ion source, especially those which lead to the production of unexpected negative ions. The goal will be accomplished in three parts. First, a kinetic model will be developed which will incorporate some of the more probable processes occurring in the high pressure electron capture ion source which may lead to generation of unusual ions. The model will incorporate positive ion-electron and negative ion-positive ion recombination reactions, ion-wall neutralization, and wall assisted reactions of neutral species; processes which are often overlooked in the more general field of Chemical Ionization Mass Spectrometry. Second, the model will be used to explain unusual negative ions observed in EC spectra. Examples will be taken from the literature and from observations made during the course of this research. Third, an analytical technique will be presented which is much less prone to complications by unexpected and unusual ion signals while maintaining the sensitivity and selectivity of electron capture reactions.

THEORY

The development of a model which may be utilized to predict the ion signals obtained from a high pressure electron capture mass spectrometer source needs to be concerned with those events that occur within the lifetime of the analyte and all products of the analyte in the ion source volume. Figure 1 shows the various reaction pathways which have been considered in this study as potential routes for the production of unusual negative ions. Two of these pathways, Routes C and D, have been previously reported by others, whereas Routes A and B are proposed here for the first time.

Route C, initially proposed by McEwen and Rudat[13], involves the reaction of analyte, M, with gas phase radicals, R, to form species MR. Their studies included the compounds 7,7,8,8-tetracyanoquinodimethane (TCNQ) and tetracyanoethylene (TCNE). The EC spectra of these two compounds were dominated by ions resulting from apparent radical substitutions for cyano- groups rather that the expected resonance or dissociative electron capture products. McEwen and Rudat pointed out that the source of these unusual ions could not possibly have arisen from negative-ion molecule reactions as no significant levels of

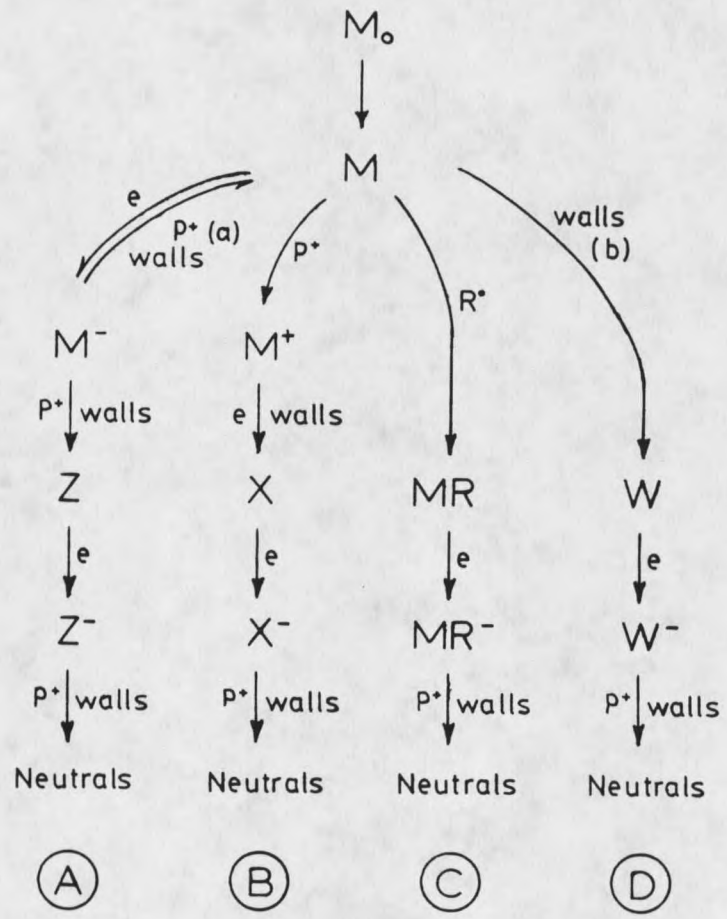

Figure 1. Four mechanisms for the formation of unusual negative ions under typical conditions of high pressure electron capture mass spectrometry.

negative ions are generated from the interaction of electrons with methane. They concluded that TCNE and TCNQ underwent fast radical reactions prior to electron capture.

Route D, initially proposed by Kassel et al.,[12] occurs by the reaction of M on the walls of the ion source to form species W. Species W then goes on to capture an electron to form negative ions, W^-. These negative ions may be vented from the source or undergo neutralization-reionization to form some terminal species. The EC spectra in the study by Kassel et al., showed ions indicating chloride addition to analytes which contained little or no chlorine and which furthermore evolved from plasmas containing no chlorine. The source of chlorine was proposed to be the ion source walls which had been previously exposed to chlorinated solvents. In the theoretical model, a reaction coefficient, b, will be used for the efficiency of product formation at the source walls. A coefficient of b = 0 indicates that no product was formed, whereas, a coefficient of b = 1 indicates that 100% of M was converted to W at the ion source surface prior to electron capture.

The source of unusual negative ions in routes A and B are neutralization reactions involving negative ion-positive ion and positive ion-electron recombination reactions, respectively. In Route B, positive ions, M^+, are generated by the usual positive ion-molecule reactions

occurring in the CI source. Recombination of M^+ with electrons, or neutralization at the source walls, lead to neutral products, X, which may also be susceptible to electron capture, forming X^-.

Route A is the normal electron capture process which gives the expected negative ion, M^-. Recombination of M^- with positive ions from the plasma or neutralization of M^- at the source walls yield neutral product, Z, which in turn may undergo additional electron capture to form Z^-. It is possible that in the neutralization process, M will be regenerated and subsequently undergo electron capture a second time with the same rate coefficient as the first. An enhanced sensitivity will be observed, therefore, for analytes which recycle from M^- to M. For the purpose of later calculations a coefficient of a = 1 will correspond to 100% regeneration of M from neutralization of M^- and a coefficient of a = 0 indicates 0% regeneration of M and 100% formation of Z. Intermediate values of "a" will correspond to the respective quantities of both M and Z.

In the four routes shown in Figure 1, it is assumed that <u>any</u> negative ion formed may be neutralized by recombination with positive ions, P^+, or by neutralization at the ion source walls. Although in some instances this may lead to a species which is no longer active to electron capture, it is conceivable that the neutral product may be able to capture an electron, thereby contributing to the

observed EC spectrum. Neutralization-reionization reactions will continue until the resulting species has been ventilated from the source or has become dead to electron capture.

In consideration of the overall model of the HPECMS ion source, one can see that the spectrum may consist of one or more of the ions M^-, MR^-, W^-, X^-, or Z^- produced in the ionization routes shown in Figure 1. To make qualitative and quantitative predictions on the importance of occurrence of these routes to each other, it is necessary to develop a quantitative model which includes rate constants for the formation and destruction of all ions and neutrals shown in Figure 1. The next section discusses the main fundamental processes involved and the magnitudes of the rate coefficients of these species.

Rate Coefficients of Individual Processes

Ventilation

All processes considered must occur within the lifetime of the analyte in the ion volume. High ventilation rates may favor fast processes, whereas low ventilation rates may provide sufficient time for slower processes. The rate coefficient for ventilation is given by F/V where F(cm^3 sec^{-1}) is the volumetric flow rate of gas through the ion source and V(cm^3) is the source volume. Typical CI ion source volumes are on the order of 1.0 cm^3. The magnitude

of F can be related to the conductance of the source which is in turn related to the sum of the areas of the electron entrance aperture and ion exit slits. Flow of bulk material out of the ion source is independent of the ion source pressure. One must be aware of which region of flow the ion source is operating - viscous flow or molecular flow. Typical source pressures are on the order of 0.1 to 1.0 Torr which is somewhat nearer to molecular flow conditions (mean free path is greater than the diameter of the containing vessel or tube). Dushman[14] provides an estimate of flow when operating under molecular flow conditions:

$$F(cm^3\ sec^{-1}) = 3.64 \times 10^3\ A(T/m)^{.5} \qquad (10)$$

where A is the total area of the source slits, T is the source temperature in degrees Kelvin and m is the molecular weight of the bulk gas in grams per mole. For the ion source initially used in this study the electron entrance aperture had a diameter of 0.8 mm and the ion exit slit had dimensions of 0.27 x 4.8 mm resulting in a total area of .018 cm^2.

The density of reagent species (electrons, positive ions, and radicals) within the ion source will ultimately depend on the rate of ventilation of bulk material. Reasonably accurate knowledge of the flow rate of material out of the ion source is, therefore, essential. Generally

one assumes that the ion source is tight with the only exit of bulk material being through the electron entrance aperture and ion exit slit. If this is not the case, then large errors in the estimation of flow by the above calculation are possible. Consequently an independent experimental method for the determination of F is desirable. This can be accomplished by measuring the total exhaust flow from the source foreline pump at ambient pressure and determining the pressure, P, within the enclosed source. The rate of gas flow, F, from the ion source is then given by

$$F = F_{amb}P_{amb}/P \qquad (11)$$

For our ion source ($F = 337\ cm^3\ sec^{-1}$) a measurement of $F_{amb} = 0.160\ cm^3\ sec^{-1}$ with a source pressure of 0.3 Torr and local atmospheric pressure of $P_{amb} = 630$ Torr would indicate a tight source. Measurements of F_{amb} significantly larger than this would indicate the existence of ion source leaks.

Ionization

In the chemical ionization ion source of about 1 cm internal length operated at 0.1 to 1.0 Torr CH_4, an electron beam of 300 eV is effectively attenuated by interaction with the methane, forming positive ion-electron pairs. Since one ion pair is created for about 35 eV energy of each electron in the beam[15], the total ionization

rate, S_e, is given by:

$$S_e \text{ (pairs sec}^{-1}) = 1.7 \times 10^{11} \text{ (I x E)} \qquad (12)$$

where I (uA) is the intensity of the electron beam entering the source and E (eV) is its energy.

In methane, the positive ions initially formed are rapidly converted by positive ion molecule reactions[1] to the terminal positive reagent ions, CH_5^+ and $C_2H_5^+$, as shown by

$$CH_4 + e \longrightarrow \begin{cases} CH_4^+ + 2e \\ CH_3^+ + H \end{cases} \qquad (13)$$

$$CH_4^+ + CH_4 \longrightarrow CH_5^+ + CH_3 \qquad (14)$$

$$CH_4 + CH_3 \longrightarrow C_2H_5^+ + H_2 \qquad (15)$$

The magnitude of I can be estimated from the filament emission current if the efficiency of electron beam entry into the ion source volume is known. As an approximation, it has been assumed that measurements of emission and trap currents made with an evacuated ion source provide a measure of electron beam entrance efficiency which would also apply to the source filled with methane. For the source used in this study, an electron entrance efficiency of 5 percent was used in all calculations. A value of S_e = 5×10^{14} is predicted for our instrument using settings of emission current of 500 uA (I = 25 uA) and electron energy of 150 eV.

Radical Production

Along with the positive ions produced in a methane system as shown above, there will also be a substantial production of free radicals. These will be formed by interaction of the electron beam with methane by

$$CH_4 \xrightarrow{\text{e-beam}} CH_3^+ + H + e \qquad (16)$$

by ion molecule reactions in methane

$$CH_4^+ + CH_4 \longrightarrow CH_5^+ + CH_3 \qquad (17)$$

and by recombination reactions such as

$$CH_5^+ + e \longrightarrow CH_3 + H_2 \qquad (18a)$$

$$CH_5^+ + e \longrightarrow CH_4 + H \qquad (18b)$$

McEwen and Rudat[16], in the report of their study of radical traps in HPECMS, have provided considerable information on source operating conditions and on the effect of radical-related reactions on the spectrum. Experimental results supported the idea that as the electron emission current is increased, the concentration of radicals increases significantly in the methane plasma. One might initially think that increases in electron and positive ion density. At higher charge densities, however, elimination mechanisms play an increasingly important role (see discussions below on radical processes and recombination reactions). The rate of loss of ions and electrons by

recombination and wall neutralization is considerably faster than the rate of elimination of radicals by radical-radical recombination and wall-induced losses. Therefore, there is a tendency to see a larger contribution of radical related ions in the spectrum with higher emission currents (so long as other parameters remain constant, i.e, sample size, pressure, and temperature).

McEwen and Rudat also provide a semiquantitative estimate of the relative number of radicals produced compared to ion pairs. For the discussion here, it is adequate to assume that for every ion pair produced by the irradiation of methane, about 2 to 4 radicals will be produced. The rate of total radical production can then be estimated by modification of equation 12:

$$S_r \text{ (radicals sec}^{-1}) = 5 \times 10^{11} \text{ (I x E)} \qquad (19)$$

where I is in units of uA (with the electron beam entrance efficiency term) and E in units of eV.

Ion-Molecule and Electron Capture Reactions

Second order rate coefficients for ion molecule reactions[2] involving molecules of molecular weight greater than 30 will approximate the calculated collision rate constants from Average Dipole Orientation theory. Values typically range from 1-3 x 10^{-9} cm^3 $molecules^{-1}$ sec^{-1}, regardless of the neutral molecule and hydrocarbon ion involved, with an average value of 2 x 10^{-9} cm^3 $molecules^{-1}$

sec^{-1}. In contrast, the fastest electron-molecule reactions have rate coefficients of 4 x 10^{-7} cm^3 $molecules^{-1}$ sec^{-1}, more than two orders of magnitude greater[2]. It is for the selective detection of these molecules that high pressure electron capture mass spectrometry has its greatest strengths. Because of the high rates of EC reactions, detection limits in the femtomole and attomole ranges can be realized. It is interesting to note that exothermic electron capture reactions also can be very slow, as shown by NO_2[17] which has a rate coefficient less than those of ion-molecule reactions.

Radical Reactions

The free radical species found in the methane plasma (H, CH_3, and C_2H_5) can react by hydrogen atom abstraction, by addition, or by substitution with a wide range of compounds[18,19]. The significance of gas phase radical reactions and their effect on the resulting spectrum will largely be dependent on the rate coefficients for the above processes as well as the nature of the reacting pair. The rate coefficients of these processes may vary over several orders of magnitude with the fastest of the gas phase radical-neutral reactions[20] having rate coefficients of 1 x 10^{-10} cm^3 $molecules^{-1}$ sec^{-1}. This is about one order of magnitude slower than fast ion molecule reactions. Experiments conducted by McEwen and Rudat[16], in which they

produced methyl radicals by the thermal decomposition of di-tert-butyl peroxide, indicated that addition of CH_3 to TCNE occurs with a rate coefficient of 1×10^{-10} cm^3 $molecules^{-1}$ sec^{-1}. This is of particular interest to this study because TCNE has a high electron affinity[21] and would thus be expected to attach electrons quite readily. As will be shown later, the observed spectrum of this compound does not resemble a simple electron attachment product, but rather is complicated by radical addition and substitution products.

Diffusion of Neutral Species to the Walls

The proposed model suggests that neutral species, including neutral radicals, may undergo various reactions at the walls of the ion source. The importance of these wall related processes must be viewed with respect to the rate coefficient for diffusion to the source boundary. The diffusion of neutrals is given by the collective term, $bD_n\Omega^{-2}$, where b is the efficiency of the wall reaction ($0 \leq b \leq 1$), D_n is the diffusion coefficient of the neutral, and Ω is the characteristic diffusion length[21] of the ion source. The magnitude of the diffusion coefficient will be strongly dependent upon the source temperature, pressure, and mass of the buffer gas. D_n can be readily calculated[23] from the equation

$$D_n = (v_1^2 + v_2^2)^{.5}/(3\pi\beta\delta^2_{12}) \qquad (20)$$

where v_1 and v_2 are the most probable velocities of the buffer gas molecule and neutral of interest, ß is the density of the buffer gas, and δ is the average molecular diameter of the buffer gas molecule and neutral. Equation 20 can be reduced to a more convenient form from which a good approximation of D_n for any relatively large neutral (MW $\geq$ 100 gm mol^{-1}) in methane can be obtained (assuming that $\delta_{12} = 6 \times 10^{-8}$ cm for all neutrals).

$$D_n \ (cm^2 \ sec^{-1}) = 0.063(T/273)^{1.5}(760/P) \qquad (21)$$

For our system, operated at 0.5 Torr methane and a temperature of 423°K, $D_n = 185 \ cm^2 \ sec^{-1}$.

McDaniel[22] provides a calculated value of Ω for a spherical source. For our ion source, a nearly cubical volume, the closest spherical representation is estimated and then Ω is given by the radius divided by π ($\Omega \approx 0.4/\pi = 0.13$ cm). The overall first order rate constant for diffusion of neutrals to the walls of our ion source with 0.5 Torr methane and 150°C will be

$$D_n\Omega^{-2} = 0.063(T/273)^{3/2}(760/P)/(0.13cm)^2 \qquad (22)$$
$$D_n\Omega^{-2} = 1.1 \times 10^4 \ sec^{-1}$$

and will be very dependent on pressure and temperature.

Diffusion of Ions and Electrons to the Walls

Ions and electrons are expected to be neutralized by contact with the metal surface of the ion source.

Therefore, one contribution to their overall loss rate will be their rate of transport to the walls by diffusion through the methane plasma. The rate coefficient for this process is also given by a composite term, $D_a\Omega^{-2}$, where Ω is the same characteristic length that was described above for neutral diffusion to the walls. D_a is the ambipolar diffusion coefficient which applies to both ions and electrons. High electron-ion densities will be present in most commercially available ion sources operated at chemical ionization pressures. This eliminates the use of free diffusion coefficients in describing the transport of oppositely charged species to the walls. The free diffusion coefficient of an electron (D_e) is much greater than that of positive ions (D_+). Therefore, there is a tendency for electrons to escape faster to the walls than positive ions. If electron-ion densities are relatively low ($\leq 10^8$ cm^{-3}), then the difference in transport rates will be unchecked. In situations where the electron-ion density is greater than about 10^8 pairs cm^{-3} (the density in our source is approximately 10^{10} - 10^{11} pairs cm^{-3}), the tendency toward free diffusion is countered by the production of a small positive potential in the central regions of the ion volume. This small positive potential will in turn retard the movement of the electrons. The net result is equalization of the rate of transport of electrons and positive ions. The electrons diffuse more

slowly ($D_a = 10^{-3}D_e$) than under free diffusion conditions, and positive ions diffuse somewhat faster[24], $D_a = 2D_+$. Also, because of the high charge density, the distribution of ions and electrons in the source volume will be relatively unaffected by the application of externally applied repeller fields. Since $D_a = 2D_+$, the ambipolar diffusion coefficient can be determined directly from free diffusion coefficients. These in turn can be evaluated by the application of the Einstein equation[25] to mobility data. Lindinger and Albritton[25] made a study of ion mobilities in which they found the Langevin expression for the mobility of ions to be in good agreement with their experiments. Combining the Einstein and Langevin equations results in a general expression from which D_+ can be evaluated and is written as follows:

$$D_+ = 3.33 \times 10^{-3}T^2/P(\alpha M_r)^{0.5} \qquad (23)$$

where T is the plasma temperature in Kelvin, P is the pressure in Torr, α is the polarizability of the buffer gas in cubic angstroms, and M_r is the reduced mass of the ion and buffer gas. From this the following general expression for D_a of an ion of mass 100 amu in methane ($\alpha = 2.60$ Å^3) is obtained:

$$D_a \ (cm^2 \ sec^{-1}) = 0.11(T/273)^2(760/P) \qquad (24)$$

With a pressure of 0.5 Torr and temperature of 423°K, D_a is found to be 401 cm^2 sec^{-1}. Since the mass of the ion

appears only in the reduced mass term, using the relatively light methane as a buffer gas provides a good approximation of D_a for all ions of mass greater than 50 amu. For CH_5^+, the positive ion of greatest abundance in a CI methane plasma, the coefficient in equation 24 requires slight adjustment from 0.11 to 0.14. The diffusion of negative ions in an ion source having high densities of electrons and positive ions will also be coupled to positive ion diffusion and will be described by D_a. As with diffusion of neutrals, the composite rate coefficient for diffusion of electrons and ions, $D_a\Omega^{-2}$ will be strongly influenced by changes in temperature and pressure. At a pressure of 0.5 Torr and temperature of 150°C, the rate coefficient will be $D_a\Omega^{-2} = 400(0.13)^{-2} = 2.4 \times 10^4$ sec^{-1}.

Radical Losses

Free radicals produced in CI plasmas can potentially be lost by at least three processes which include diffusion to the walls, reaction with a molecular species and by radical-radical recombination. The magnitude of the first two processes have been discussed above. A recombination coefficient for methyl radicals[26] of $R_R = 4 \times 10^{-11}$ cm^3 $particles^{-1}$ sec^{-1} will be used here as a representative value for all radical-radical recombination reactions.

Positive Ion-Electron Recombination

A rather extensive review of positive ion-electron recombination has been provided by Mitchell and McGowan[27]. It was shown that as the complexity of the positive ion increases, the second order rate constant for dissociative recombination tends toward a constant value, irrespective of the species involved. The recombination coefficient for $C_2H_3^+$, which is given by:

$$R_e \ (cm^3 \ particles^{-1} \ sec^{-1}) = 9 \times 10^{-7}(300/T)^{0.5} \qquad (25)$$

is similar to those listed for all other polyatomic organic positive ions. The exception to this trend occurs in cluster positive ions such as $H_3O^+(H_2O)_n$, where n = 2-6, for which R_e increases continuously with n and can be several times greater than that for simple positive ions. Positive ion-electron recombination is a two body process at all relevant pressures. Therefore, R_e does not change with changes in total pressure. At 150°C, equation 25 gives $R_e = 8 \times 10^{-7}$ cm^3 $particles^{-1}$ sec^{-1}. Temperature variations within the typical operating realm of the high pressure EC ion source, will have little effect on the positive ion-electron recombination coefficient.

Positive Ion-Negative Ion Recombination

Biondi[28] and more recently Smith and Adams[29] have reviewed positive ion-negative ion recombination. An interesting feature of recombination between polyatomic

ions is that rate coefficients vary little between ions whether they are small ions or very large cluster ions. Unlike ion-electron recombination, however, ion-ion recombination rates are expected to be significantly altered with changes in pressure over specific ranges of pressure. This is because there is a competition between two body and three body processes in which the latter dominates at higher pressures. At pressures of 1 Torr and below, the two body process, only, is important. Since the pressure range in HPECMS is 0.1 to 1.0 Torr, the second order rate coefficients for ion-ion recombination are essentially constant. The following expression[29] for the recombination of NO^+ and NO^- provides a good estimate of the recombination coefficient, R_-, for any pair of ions in this pressure range.

$$R_- \ (cm^3 \ particles^{-1} \ sec^{-1}) = 6.8 \times 10^{-7} \ / \ T^{0.4} \qquad (26)$$

Thus at 423°K with 0.5 Torr methane, $R_- = 6 \times 10^{-8}$ cm^3 $particles^{-1}$ sec^{-1}, a value about one order of magnitude lower than the coefficient for ion-electron recombination under these conditions. Because the three body process dominates at higher pressures it can be expected that values for R_- will be much larger.

The neutral products generated by ion-ion recombination may have a tremendous effect on predictions of ion source dynamics in HPECMS. However, little is known about the

neutral products of ion-ion recombination of polyatomic species[29]. In Route A from the model in Figure 1 it has been proposed that M^-, formed by the resonance electron capture process, can be converted to an altered neutral, Z, or revert to the molecular species M. A recent report by Valkenburg, Krieger, and Grimsrud[30] on the use of a dual cell electron capture detector suggested that the negative ion, SF_6^-, was converted predominantly to unknown altered species, while c-$C_7F_{14}^-$ (perfluoromethylcyclohexane) was converted primarily back to c-C_7F_{14} upon recombination. One might suspect that a variety of compound dependent fates would be possible in ion-ion recombination reactions.

Conservation Equations

The HPECMS ion source will be considered here to be well mixed with respect to its neutral and ionic constituents. This allows a single expression to be written for the concentration of each species which would adequately describe the presence of that species throughout the ion source. The ion source is a flow-through cell, and the steady state assumption can be applied to all species; the production rate of each species must be equal to the loss rates. If chemical and physical loss rates within the cell are small relative to production rates, loss will then occur primarily by ventilation out of the cell.

In Figure 1, 14 species have been identified which will

be of interest. A conservation equation may be written for each of these which will include the various production and loss parameters which apply to each as previously discussed. These equations may then be manipulated to provide 14 expressions for the steady state concentration of each species. Equations 27 through 39 provide the equilibrium expressions and equations 40 through 52 provide expressions of f_Q values, which indicates the fraction of total analyte which exists in the form Q. All of the various rate coefficients using these expressions have been discussed above with values summarized in Table 1 on page 31. A summary of all the symbols used is provided below for the various species indicated in the equations and represented in Figure 1.

[e] electron concentration (electrons cm^{-3})

$[P^+]$ total reagent positive ion concentration (ions cm^{-3})

[R] total reagent free radical concentration (radicals cm^{-3})

[M] original concentration of analyte compound M in the buffer gas which is entering the ion source.

[Q] steady state concentration of species Q (particles cm^{-3})

f_Q ratio, [Q]/[M]

S_e production rate of positive ions and electrons caused by the electron beam (particles sec^{-1})

S_R production rate of free radicals (radicals sec^{-1})

D_a ambipolar diffusion coefficient of ions and electrons (cm^2 sec^{-1})

Ω characteristic diffusion length of the ion source (cm)

F volumetric flow rate of buffer gas through the ion source (cm^3 sec^{-1})

V volume of the ion source (cm^3)

D_n diffusion coefficient of neutral species (cm^2 sec^{-1})

R_e positive ion-electron recombination coefficient (cm^3 $particles^{-1}$ sec^{-1})

R_- positive ion-negative ion recombination coefficient (cm^3 $particles^{-1}$ sec^{-1})

R_R radical-radical recombination coefficient (cm^3 $particles^{-1}$ sec^{-1})

a efficiency of regeneration of molecular species M from neutralization of M^- by either positive ions or contact with the source walls (0 - 1; a = 0, species Z is formed)

b efficiency of conversion of species M to W by collision with the source walls (0 - 1; b = 0, no W found)

k_R rate constant for gas phase reaction of reagent radical with analyte M (cm^3 $particles^{-1}$ sec^{-1})

k_+ rate constant for reaction of reagent positive ions with analyte M (cm^3 $particles^{-1}$ sec^{-1})

$k_{e,q}$ rate constant for reaction of thermal electrons with species Q (cm^3 $particles^{-1}$ sec^{-1})

As stated at the beginning of this section, the development of a model which may be used to predict and evaluate high pressure electron capture mass spectrometry ion signals needs only to be concerned with those events that occur within a reasonable time frame of ventilation of the ion source. The steady state equations will also reflect only those processes which may occur within the

ventilation time constant, although it may be possible to describe other production and loss steps. Table 1 lists the rate coefficients and time constants under an established set of standard operating conditions as a reference and guide for the development of the steady state equations.

It has been assumed in these calculations that the analyte concentration, $[M]_o$, entering the ion source is sufficiently small so as not to adversely perturb the steady state concentrations of the three reagent species, [e], $[P^+]$, and [R]. By making this restriction, one is able to make predictions of relative sensitivity which would apply to signals at the detection limit up through about the lower 20% of the dynamic range of the system under a given set of conditions.

Table 1. Standard Conditions, Concentrations, Rate Coefficients and Time Constants for Evaluation of the Concentration Equations.

Standard Conditions

Buffer gas = Methane	P = 0.5 Torr
Mass of Analyte = 200 amu	T = 150°C
Emission Current = 0.50 mA	V = 1.0 cm^3
Electron Energy = 150 eV	Ω = 0.13
Electron Entrance Efficiency = 5%	
Area of Source Slits = 0.018 cm^2	

Concentration of Reagent Species

$S_e = 5 \times 10^{14}$ particles cm^{-3}
$[e] = [P^+] = 1.4 \times 10^{10}$ particles cm^{-3}
$S_r = 1.5 \times 10^{15}$ particles cm^{-3}
$[R] = 3.2 \times 10^{12}$ particles cm^{-3}

Rate Coefficients	Time Constants (u sec)
$F/V = 337\ cm^3\ sec^{-1}$	2967
$k_{e,m} = 3 \times 10^{-7}\ cm^3\ sec^{-1}$	240
$k_+ = 2.0 \times 10^{-7}\ cm^3\ sec^{-1}$	35,714
$k_R = 1.0 \times 10^{-10}\ cm^3\ sec^{-1}$	3125
$R_R = 4.0 \times 10^{-11}\ cm^3\ sec^{-1}$	7812
$R_e^- = 8.0 \times 10^{-7}\ cm^3\ sec^{-1}$	89
$R_-^- = 6.0 \times 10^{-8}\ cm^3\ sec^{-1}$	1190
$D_a\Omega^{-2} = 2.4 \times 10^4\ sec^{-1}$	42
$D_n^a\Omega^{-2} = 1.1 \times 10^4\ sec^{-1}$	91

Equilibrium Expressions

P^+, e: $$S_e = R_e[P^+][e] + D_a\Omega^{-2}[e] + FV^{-1}[e] \quad (27)$$

R: $$S_r = R_r[R][R] + D_n\Omega^{-2}[R] + FV^{-1}[R] \quad (28)$$

M: $$FV^{-1}[M]_o + aR_-[P^+][M^-] + aD_a\Omega^{-2}[M^-] = k_+[M][P^+] + k_R[M][R] + FV^{-1} + bD_n\Omega^{-2}[M] \quad (29)$$

M^-: $$k_{e,m}[M][e] = R_-[M^-][P^+] + FV^{-1}[M^-] + D_a\Omega^{-2}[M] \quad (30)$$

$$Z: \quad (1-a)R_{-}[M^{-}][P^{+}] + (1-a)D_a\Omega^{-2}[M^{-}] = k_{e,z}[Z][e] + k_{+}[Z][P^{+}] + FV^{-1} \tag{31}$$

$$Z^{-}: \quad k_{e,z}[Z][e] = R^{-}[Z^{-}][P^{+}] + D_a\Omega^{-2}[Z^{-}] + FV^{-1} \tag{32}$$

$$M^{+}: \quad k^{+}[M][P^{+}] = R_e[M^{+}][e] + D_a\Omega^{-2}[M^{+}] + FV^{-1} \tag{33}$$

$$X: \quad R_e[M^{+}][e] + D_a\Omega^{-2}[M^{+}] = k_{+}[X][P^{+}] + k_{e,x}[X][e] + FV^{-1} \tag{34}$$

$$X^{-}: \quad k_{e,x}[X][e] = R_{-}[X^{-}][P^{+}] + D_a[X^{-}] + FV^{-1}[X^{-}] \tag{35}$$

$$MR: \quad k_R[M][R] = k_{e,MR}[MR][e] + FV^{-1} \tag{36}$$

$$MR^{-}: \quad k_{e,MR}[MR][e] = k_{-}[MR^{-}][P^{+}] + D_a\Omega^{-2}[MR^{-}] + FV^{-1}[MR^{-}] \tag{37}$$

$$W: \quad bD_n\Omega^{-2}[M] = k_{e,M}[W][e] + FV^{-1} \tag{38}$$

$$W^{-}: \quad k_{e,W}[W][e] = k_{-}[W^{-}][P^{+}] + D_a\Omega^{-2}[W^{-}] + FV^{-1}[W^{-}] \tag{39}$$

Concentration Expressions

$$[e] = [P^{+}] = \{-(D_a\Omega^{-2} + FV^{-1}) + [(FV^{-1})^2 + 4R_eS_eV^{-1}]^{.5}\}(2R_e)^{-1} \tag{40}$$

$$[R] = -(FV^{-1}) + [(FV^{-1})^2 + 4R_RS_RV^{-1}]^{.5}(2RR)^{-1} \tag{41}$$

$$f_M = FV^{-1}\{k_{e,M}[e] + bD_n\Omega^{-2} + k_{+}[P^{+}] + FV^{-1} - ak_{e,M}[e](R_{-}[P^{+}] + D_a\Omega^{-2})(R_{-}[P^{+}] + D_a\Omega^{-2} + FV^{-1})^{-1}\}^{-1} \tag{42}$$

$$f_{M-} = f_M k_{e,M}[e]\,(R_-[P^+] + D_a\Omega^{-2} + FV^{-1})^{-1} \quad (43)$$

$$f_Z = f_{M-}(1-a)\,(R_-[P^+] + D_a\Omega^{-2})\,(k_{e,Z}[e] + k_+[P^+] + FV^{-1})^{-1} \quad (44)$$

$$f_{Z-} = f_Z k_{e,Z}[e]\,(R_-[P^+] + D_a\Omega^{-2} + FV^{-1})^{-1} \quad (45)$$

$$f_{M+} = f_M k_+[P^+]\,(R_e[e] + D_a\Omega^{-2} + FV^{-1})^{-1} \quad (46)$$

$$f_X = f_{M+}(R_e[e] + D_a\Omega^{-2})\,(k_+[P^+] + k_{e,X}[e] + FV^{-1})^{-1} \quad (47)$$

$$f_{X-} = f_X k_{e,X}[e]\,(R_-[P^+] + D_a\Omega^{-2} + FV^{-1})^{-1} \quad (48)$$

$$f_{MR} = f_M k_R[R]\,(k_{e,MR}[e] + FV^{-1})^{-1} \quad (49)$$

$$f_{MR-} = f_{MR} k_{e,MR}[e]\,(R_-[P^+] + D_a\Omega^{-2} + FV^{-1})^{-1} \quad (50)$$

$$f_W = f_M bD_n\Omega^{-2}\,(k_{e,W}[e] + FV^{-1})^{-1} \quad (51)$$

$$f_{W-} = f_W k_{e,W}[e]\,(R_-[P^+] + D_a\Omega^{-2} + FV^{-1})^{-1} \quad (52)$$

From the f_Q values, one may predict mass spectral ion intensities, I_Q, with the additional consideration of flow parameters such that

$$I_{Q-} = [M]_o f_{Q-} F_{ie} \quad (53)$$

where I_Q is the observed ion signal, $[M]_o$ is the concentration of analyte entering the ion source, f_{Q-} is the fractional amount of $[M]_o$ existing as species Q^-, and F_{ie} is the conductance ($cm^3\ sec^{-1}$) of the ion exit slit. Since $[M]_o$ and F_{ie} will be the same for all species, it is

obvious that the relative magnitudes of f_{Q^-} determined from the above calculations also provide predictions of relative ion beam currents.

Predictions of Ion Signals for Selected Cases

In Tables 2-5, predictions of the relative concentration (f_Q x 100) for all neutral and ionic species shown in Figure 1 are listed for various selected conditions for the model under consideration.

The Standard Condition

Case A0 listed in Table 2 is defined to be the standard case of operating conditions and events by which all other examples in Tables 2-5 will be compared. In Case A0, the only means of forming a negative ion is electron capture by M to form M^-. The standard set of conditions selected for this case are: P = 0.5 Torr CH_4, T = 150°C, V = 1 cm^3, Ω = 0.13, emission current = 500 uA ($S_e = 5 \times 10^{14}$ and $S_r = 1.5 \times 10^{15}$ particles cm^{-3}), $k_{e,m} = 3 \times 10^{-7}$ cm^3 $molecules^{-1}$ sec^{-1}; all other rate constants $K_{e,Q}$, K_+ and K_R have been set to 0 as well as the efficiency coefficients, a and b. The magnitudes of the diffusion and recombination coefficients have been set according to the relationship previously described. Under these conditions, the positive ion and electron densities will be $[e] = [P^+] = 1.4 \times 10^{10}$ particles cm^{-3} and the radical density will be $[R] = 3.2 \times 10^{12}$ particles cm^{-3}.

Table 2 indicates that for the standard condition 1.2% of the analyte will exist as M^-; the expected electron capture signal of this compound. It is important to note that [M] is only 7.3% as great as $[M]_o$. This is an expected result as the electron capture rate constant is fast and the electron density is large, resulting in a rapid depletion of M by electron capture reactions. The sum total of species relating to M is only 8.5%. This means that most of the analyte (91.5%) has been converted to species Z by recombination of M- with positive ions from the plasma or by diffusion of M^- to the source walls where it is neutralized and converted to species Z. In the Case of A0, Z is considered to be inactive toward additional electron capture.

Route A to Unusual Ions (Table 2)

By altering Case A0 to allow species Z of Route A to capture electrons at the same rate as the original parent compound M ($k_{e,z}$ = 3 x 10^{-7} cm^3 $molecules^{-1}$ sec^{-1}), the theory predicts that a new and unexpected ion, Z^-, will be present in the spectrum. It is interesting to note that the concentration of Z^- is nearly as great as M^- (1.1% and 1.2% respectively).

The time constants in Table 1 suggest that this chain of events in Route A might continue to occur to form species Z^-, Z_2^-, Z_3^-, Z_n^-, so long as the electron capture rate constants for the respective species remain fast.

Calculations indicate only a modest decrease in concentration of species Z_n with increasing n, thus enabling significant contributions to the spectrum's total ion current from unusual ions arising from this route.

Table 2. Relative Amounts ($f_o x10^2$) of Neutral and Ionic Species Predicted to be Present in Route A.

Case	Major Change	M	M^-	Z	Z^-
A0	Std. Cond.	7.3	1.2	91.5	-
A1	$k_{e,z}=3x10^{-7}$	7.3	1.2	6.6	1.1
A2	V/8	22	2.4	17	1.8
A3	Fx2	20	1.1	16	0.88
A4	S/10	36	0.88	23	0.55
A5	S/100	84	0.22	13	0.033
A6	$k_{e,M}/10$	44	0.76	4.0	0.69
A7	a=1	85	15	0.0	0.0
A8	a=0.5	13	2.3	6.1	1.0

A feature of the calculations employed for the prediction and occurrence of ion signals is the ability to modify the source geometry to optimize the overall signal. In Case A2, the ion source volume has been reduced by a factor of 8 by halving its linear dimensions (Ω is halved also). It is seen that this change increases both f_M and f_{M^-} by factors of 3 and 2, respectively. This result is consistent with previous calculations by Siegel[30], who concluded that the conventional CI source is too large for the optimum detection of strongly electron-capturing molecules. It is also noted in Case A2 that a smaller source tends to weaken the intensity of unusual ion Z^- relative to that of M^-. The above effects of volume are

expected due to the shortened residence time (F/V is 8 times greater) of the analyte in the smaller ion source.

Ion source residence time can also be decreased by increasing the area of the ion exit slit. In Case A3 the slit area has been doubled and, so that the manifold pressure and total gas throughput is unchanged, the ion source pressure has been halved. This change results in f_{M^-} = 1.1%, about the same as for the standard condition. However, due to the greater conductance of the ion exit slit in Case A3, the ion beam intensity derived from M^- will be about twice that of Case A0.

Cases A4 and A5 predict the effect of lowering the electron beam intensity by one and two orders of magnitude, respectively. Because of the attendant lowering of electron concentration, these changes cause large increases in f_M and a decrease in f_{M^-}. However, for Case A4, the decrease in f_{M^-} is relatively small (from 1.2 to 0.88%), suggesting that use of the intermediate level of filament emission current causes little harm to the detection of strongly responding compounds. Since the response to weakly responding compounds will be decreased roughly in proportion to the decrease in filament emission current, this change to a lower level of emission current in Case A4 is expected to result in increased detection bias for strongly responding compounds. As is clearly indicated by the magnitude of f_{Z^-} in Cases A4 and A5, use of lower

emission currents tends to decrease the importance of unusual ion Z^- in the mass spectra of strongly responding compounds.

In Case A6 the magnitude of $k_{e,M}$ is decreased to 3×10^{-8} cm^3 $molecules^{-1}$ sec^{-1} while the magnitude of $k_{e,Z}$ is held constant at 3×10^{-7} cm^3 $molecules^{-1}$ sec^{-1}. It is seen that even though $k_{e,Z} > k_{e,M}$, the concentration of Z^- still does not exceed that of M^-. Therefore, a general rule for assignment of Route A to the formation of unusual ions can be stated, that is, that the intensity of the suspected unusual ion Z^- can not exceed that of its suspected precursor ion, M^-. Also, it is important to note in Case A6 that the sensitivity to M via formation of M^- is decreased only by a factor of two relative to Case A0 in which $k_{e,M}$ was ten times greater. This observation is an important one; it indicates that under typical conditions of HPECMS, sensitivity to M is not strongly dependent on the EC rate constant as long as it is in the 10^{-8} to 10^{-7} cm^3 sec^{-1} range and if the coefficient a is given by a = 0.

In Case A7 the fate of M^- upon neutralization is to be converted entirely back to the molecular species (a = 1). This possibility applies only to M^- ions high have been formed by the resonance EC process. It is seen that both f_M and f_{M-} are increased about one order of magnitude by this mechanism relative to Case A0 in which M^- was converted to Z. Case A8 gives predictions for the

intermediate possibility in which a = 0.5. One half of the M^- ions are restored to M upon neutralization and the remaining half is converted to Z. As expected, the relative prominence of unusual ion Z^- in the mass spectrum of M is strongly decreased as the factor, a, is made larger.

Route B to Unusual Ions (Table 3)

If the standard condition, Case A0, is altered by allowing a positive ion molecule reaction of M to occur with a rate constant of $k_+ = 2 \times 10^{-9}$ cm^3 $molecules^{-1}$ sec^{-1}, and to allow neutral X to capture electrons at a rate of $k_{e,x} = 3 \times 10^{-7}$ cm^3 $molecules^{-1}$ sec^{-1}, the predictions shown in Table 3 for Case B1 will result. Almost no change in the electron capture spectrum of M is observable; f_{M^-} is still 1.2% and the potential unusual ion in Route B, X^-, is more than two orders of magnitude less than $[M^-]$.

Table 3. Relative Amounts ($f_0 \times 10^2$) of Neutral and Ionic Species Predicted to be Present in Route B.

Case	Major Change	M	M^-	Z	M^+	X	X^-
A0	Std. Cond.	7.3	1.2	91.5	-	-	-
B1	$k_+=2\times10^{-9}$	7.2	1.2	84	0.00059	0.044	0.0076
B2	$k_{e,M}=2\times10^{-9}$	85	0.098	6.6	0.070	0.52	0.090

The coefficients assigned to the reactions forming M^+ and X^- are as large as can be expected for these processes. Therefore, it is concluded that Route B cannot compete

significantly with fast electron capture reactions in the formation of negative ions. However, if $k_{e,M}$ is not fast, Route B may then in fact generate competitive negative ion signals. This is shown in Case B2 where the EC rate coefficient for M has been reduced to $k_{e,M} = 2 \times 10^{-9}$ cm^3 $molecules^{-1}$ sec^{-1}, the same magnitude as K_+ for the competing positive ion molecule reaction. Now, as seen in Case B2, the unusual ion, X^-, is nearly as abundant as M^-. Also, $F_{X^-} = 0.09\%$ is only about one order of magnitude lower than F_{M^-} reported in Case A0. Of significant interest is the observation that the abundance of X^- may actually exceed that of its precursor, M^+, by a small amount. This is attributed to the fact that the rate coefficient for recombination of positive ions with electrons is about an order of magnitude faster than the coefficient for negative ion-positive ion recombination, resulting in a faster loss rate of M^+.

Route C to Unusual Ions (Table 4)

Unusual ions observed by this pathway would be initiated by gas phase reactions of reagent free radicals with the analyte. Case C1 in Table 4 shows the expected result if the standard condition, A0, is altered to allow a relatively fast radical reaction. The rate coefficient for molecule-radical reactions has been set to $k_R = 1.0 \times 10^{-10}$ cm^3 $molecules^{-1}$ sec^{-1} and the rate coefficient for electron capture of the corresponding unusual species in Route C is

$k_{e,MR}$ = 3.0 x 10^{-7} cm^3 $molecules^{-1}$ sec^{-1}. It is seen that even with these optimal choices of rate coefficients, that Route C is not predicted to be competitive with fast electron capture reactions; the abundance of MR^- is one order of magnitude less than that of M^-. As in Route B, however, Route C can provide sensitive signals which can dominate the spectrum of M if the electron capture rate coefficient of M is not appreciably large.

Table 4. Relative Amounts ($f_Q x10^2$) of Neutral and Ionic Species Predicted to be Present in Route C.

Case	Major Change	M	M^-	Z	MR	MR^-
A0	Std. Cond.	7.3	1.2	91.5		
C1	k_R=1x10^{-10}	6.8	1.2	85	0.47	0.081
C2	$k_{e,M}$=2x10^{-9}	49	0.056	4.1	3.4	0.59

In Case C2, $k_{e,M}$ has been changed from 3.0 x 10^{-7} cm^3 $molecules^{-1}$ sec^{-1} to 2 x 10^{-9} cm^3 $molecules^{-1}$ sec^{-1}. The resulting predictions are values of f_{MR-} = 0.6% and f_M = 0.05%. Therefore, Route C appears to be potentially important for a unique class of molecules which react with radicals extremely rapidly but attach thermal electrons with only modest speed. Species MR, however, must have a large rate coefficient for electron capture.

Route D to Unusual Ions (Table 5)

In this pathway to unusual ions a reaction of the analyte is allowed to occur on the walls of the ion source. In Case D1 the standard conditions have been altered by

setting the efficiency coefficient, b, for surface reaction of M to unity and by setting $k_{e,W} = 3 \times 10^{-7}$ cm^3 molecules^{-1} sec^{-1}. The resulting values of $f_{M^-} = 0.37\%$ and $f_{W^-} = 0.88\%$ indicate that wall related processes can compete quite favorably with fast electron capture reactions. The diffusion rate coefficient shows a large dependence on pressure. Therefore, by simply reducing the ion source pressure, as in Case D2 in which it has been halved, the abundance of W^- with respect to M^- should be further increased. The results do indeed show this with $f_{W^-} = 0.54\%$ and $f_{M^-} = 0.076\%$. For molecules which do not have appreciably fast electron capture rates, but do undergo wall sensitization by Route D, one might expect very sensitive mass spectral signals of the type W^-. This can be verified by Case D3 in which the rate coefficient for electron capture by M has been set to zero. The abundance of W^- produced here by favorable Route D is as great as that of M^- in Case A0.

Table 5. Relative Amounts ($f_o x 10^2$) of Neutral and Ionic Species Predicted for Route D.

Case	Major Change	M	M-	Z	W	W-
A0	Std. Cond.	7.3	1.2	91.5	-	-
D1	b=1	2.2	0.37	27	5.1	0.88
D2	P/2	1.3	0.076	11	9.6	0.54
D3	$k_{e,M}=0$	3.0	-	-	7.0	1.2

EXPERIMENTAL

All mass spectra reported in this study were obtained on a medium resolution, double focusing mass spectrometer (VG Analytical, model 70E-HF). Ionization of the reagent gas was accomplished by the use of 150 eV electrons generated from either a tungsten or tungsten-rhenium (97%:3%) filament with typical emission currents of 0.1 to 1.0 mA. Most experiments were conducted with the standard vendor supplied ion source, although in some instances the electron entrance aperture and ion exit slits were modified to control ion source conductance and electron and positive ion densities. Ion source pressures were measured with a capacitive manometer (MKS, model 270B) and typically maintained at 0.1 to 0.5 Torr. Gases used in this study included methane, iso-butane, ammonia, xenon and carbon dioxide (Matheson, 99.995% purity) as well as nitrogen and argon which were obtained locally. All gases were passed through oxygen, molecular sieve, and water traps (Alltech Associates) where appropriate. Ion source temperatures were monitored by the use of a thermocouple attached directly to the ion block. The repeller was grounded to the ion source block in an effort to minimize the occurrence of any electric fields within the ion volume

which might affect relative ion populations. Ions were accelerated into the analyzer region with an energy of 5000 or 6000 eV. Ion detection was accomplished by the use of an off-axis stainless steel conversion dynode operated at a potential of +5000 volts and a 19 stage discrete dynode analog electron multiplier (ETP, model AEM-1200) or, alternatively, by the use of an on-axis faraday cup. Ion signals were typically recorded by the use of the associated interface and data system (VG software, based on the DEC PDP 11/73 series computer). All ion signals were amplified by the instruments electrometer which was found to be linear over its entire range of amplification (0.2×10^{-9} to 1.0×10^{-4} amps full scale).

The mass scale in negative ion mode was calibrated by using a mixture of perfluorokerosene (SCM Specialty Chemicals) and 1-chloro-2-bromo-butane (Aldrich), which provided the low mass reference ions necessary for low mass calibration when the instrument is scanned exponentially. Positive identification of the composition of the observed unusual ions was made by accurate mass measurements at resolutions of five to ten thousand using the reference mixture mentioned above for real time mass assignments.

Samples were typically introduced to the mass spectrometer by a gas chromatograph (Varian, model 3700) equipped with a capillary column (J&W Scientific, DB-5 30m x 0.25mm) interfaced directly to the mass spectrometer ion

source. High purity helium was used as the carrier gas after having been first passed through oxygen, water and molecular sieve traps. Typical carrier gas flow rates were 30 cm sec^{-1}, adjusted at a temperature of 200°C. Samples were also introduced by the direct probe in those instances where sample volatility or polarity precluded the use of the gas chromatograph.

Some of the primary amines used in this work were derivatized with trifluoroacetic or pentafluoropropionic anhydride (Aldrich) by appropriate methodologies[32] to give the respective mono-derivatized amides. All compounds used were obtained from commercial sources with the exception of some of the isomers of aminoanthracene and aminophenanthrene, which were obtained from Milton Lee, Department of Chemistry, Brigham Young University.

APPLICATIONS OF THE MODEL TO ELECTRON CAPTURE SPECTRA

Reagent Ion, Radical and Electron Density

Three and possibly all four of the routes to unusual ions discussed in Figure 1 are thought to be capable of producing intense negative ion signals. This is possible, only due to the relatively high concentrations of electrons, positive ions, and radicals believed to be present in the source plasma of the HPECMS. Because of the importance of this, it is necessary to justify, by experimental verification, the density of ions within the source. This is readily done by biasing the ion focusing plates with -27 volts to collect all positive ions drifting out of the ion exit slit. The ion block was maintained at ground potential and the positively biased side of the potential source was connected to the instrument's electrometer. A positive ion current due to the collection of all positive ions passing through the ion exit slit was subsequently observed. The measurements were conducted at source pressures ranging from 0.05 Torr to 0.5 Torr at various emission currents, electron energies, and temperatures. As an example, Figure 2 shows a comparison of experimental vs. calculated ion current at a temperature

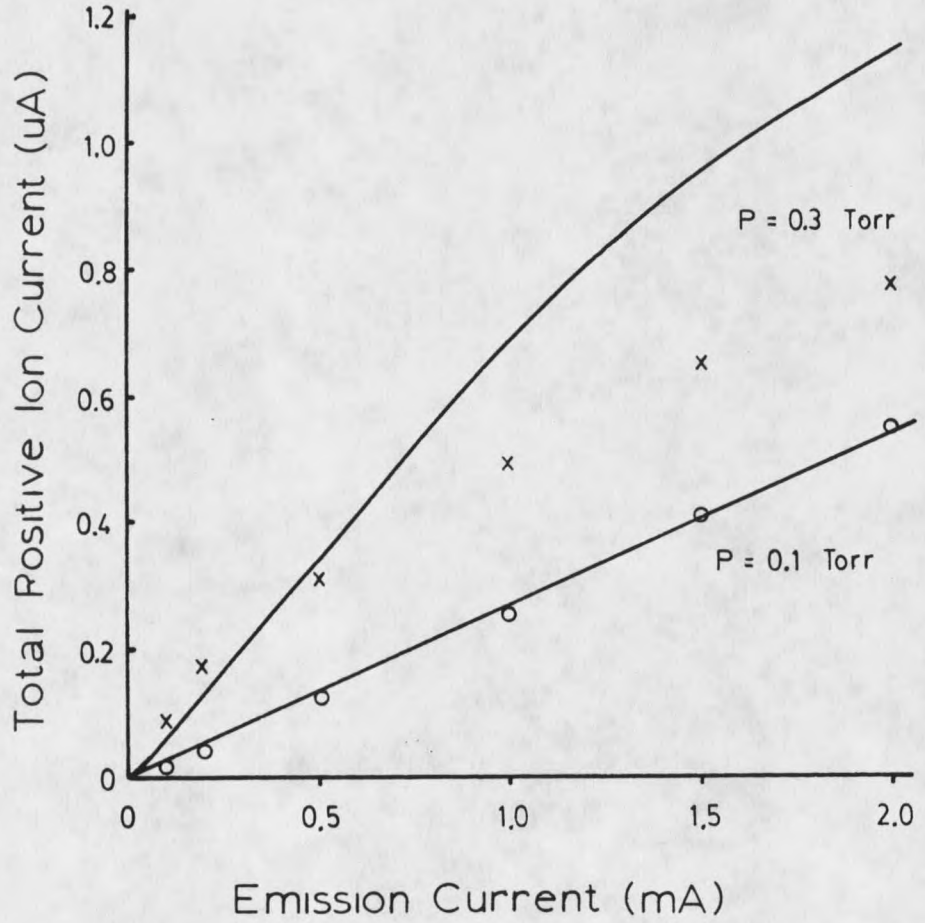

Figure 2. Measurements of total positive ion current emerging from the ion source as a function of filament emission current. Ion source pressure (methane) is 0.1 torr (O) and 0.3 torr (X). Temperature is 150°C. The solid lines shown are the predicted positive ion currents obtained from the model.

of 150°C at 0.1 and 0.3 Torr methane as a function of emission current at constant electron energy of 150 eV. The continuous lines are the predictions for the positive ion currents obtained from $I^+ = [P^+]F$, where $[P^+]$ is calculated from equation 40 of the model and $F = 243\ cm^3\ sec^{-1}$ is the calculated flow from the ion exit slit (in determining D_a for the relatively light positive ions present in a pure methane plasma, it is important to note the effect of the reduced mass term in equation 24; CH_5^+ was considered to be the only positive ion present). It is clear from Figure 3 that the actual magnitude of the positive ion current is very close to that predicted by the model. Note that a curvature is predicted for the higher pressure and also observed experimentally whereas a near linear relationship between I^+ and emission current is both predicted and observed at the lower pressure. The nonlinear behavior at the higher pressure is expected due to an increase in the relative importance of second order ion-electron recombination relative to the first order diffusional loss of ions.

Electron and radical densities are expected to be coupled to the positive ion density by processes described in the previous section. It may be assumed that they will also be as large as predicted by the model. Nevertheless, to confirm the presence of methane derived free radicals in the ion source, the HPECMS spectrum of tetracyanoethylene

(TCNE) and tetracyanoquinodimethane (TCNQ) were obtained and are provided in Figure 3.

McEwen and Rudat have shown that TCNE, TCNQ and a few

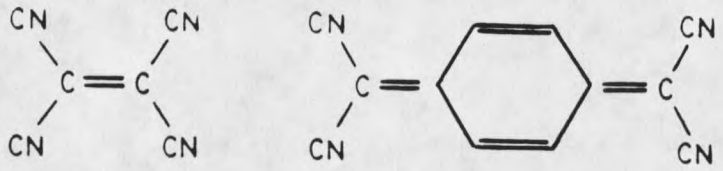

TCNE TCNQ

other select compounds act as free radical traps so that their EC spectrum is greatly influenced by prior reactions with the radicals present, as was shown symbolically in Route C of Figure 1. Although the spectra in Figure 3 would seem to provide convincing evidence of the presence of H, CH_3 and C_2H_5 radicals in the irradiated methane of our source. Additional proof was obtained by conducting an accurate mass experiment which allowed the determination of the elemental composition of each ion.

Table 6. Accurate Mass Data for Tetracyanoquinodimethane. Resoulution Equals 7500.

m/z	Composition	origin	Observed Mass	ppm dev.
168	$C_{10}H_6N_3$	$[M+CH_3-C_3HN_2]$	168.0563	0.6
193	$C_{12}H_7N_3$	$[M+CH_3-CN]$	193.0637	-1.5
204	$C_{12}H_4N_3$	M	204.0436	-1.0
205	$C_{12}H_5N_4$	[M+H]	205.0511	1.0
207	$C_{13}H_9N_3$	$[M+2CH_3-HCN]$	207.0798	1.0
221	$C_{14}H_{11}N_3$	$[M+3CH_3-H_2CN]$	221.0948	-1.8
223	$C_{14}H_{13}N_3$	$[M+3CH_3+2H-CN]$	223.1109	-0.5
235	$C_{15}H_{13}N_3$	$[M+4CH_3-H_3CN]$	235.1109	2.1
248	$C_{15}H_{12}N_4$	$[M+4CH_3-4H]$	248.1063	0.4

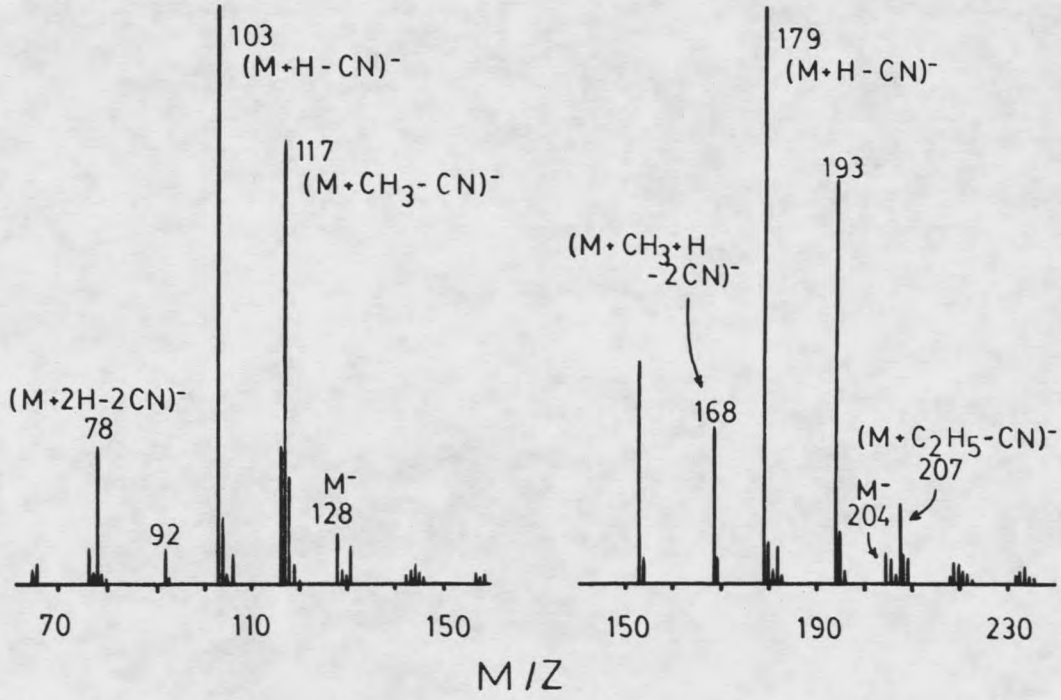

Figure 3. The HPECMS spectra of tetracyanoethylene and tetracyanoquinodimethane in 0.3 Torr (methane) the and Temperature of 180°C.

It can be seen from the results in Table 6 that the composition of each ion from the EC spectrum of TCNQ does indeed reflect the addition and elimination reactions by the suspected free radicals in the source plasma. As an example, m/z = 193 is shown to have an elemental composition of $C_{12}H_7N_3$, which considering the nature of the methane plasma, must originate from $[M+CH_3-CN]^-$.

Polyhalogentated Unsaturated Hydrocarbons

Stemmler and Hites[6] recently reported the HPEC spectra of 24 hexachloropentadiene derivatives. An observation made in that study was the occurrence of a series of unusual ions of the type $[M+nH-nCl]^-$, or a series of ions differing by 34 mass units, $[+nH-nCl]^-$, where n = 1 to 4 were observed for most compounds. In the course of this study, the EC spectra of some of these compounds were obtained on the VG 70E-HF mass spectrometer. One of these measurements for Pentac is shown in Figure 4 and is in good agreement with that reported by Stemmler and Hites.

No molecular ion of Pentac is observed. Ions due to $[M-Cl]^-$ and $[M-2Cl]^-$, mass 435 and 400 respectively, are present, as well as an ion at mass 235 which is simply the rupture of the center carbon-carbon bond. These ions are easily rationalized by dissociative electron capture processes. Of interest here is the series of ions, beginning at mass 400 and differing by 34 amu. These ions

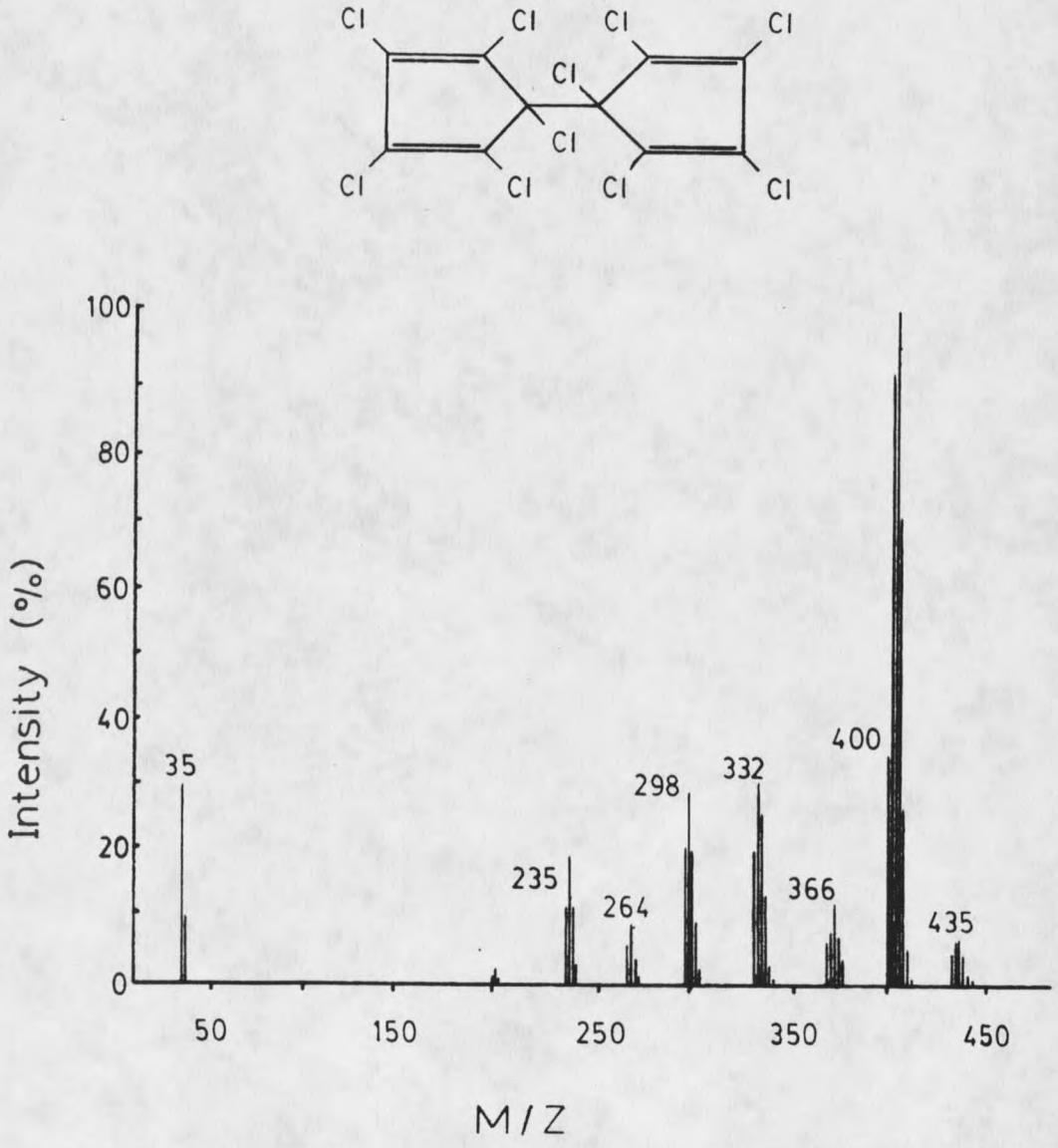

Figure 4. The HPECMS spectrum of Pentac. The pressure is 0.3 torr (methane) and the temperature is 180°C.

present a considerable challenge in attempts at explaining the basis for their occurrence.

During the course of this study, a second set of compounds was found to have EC spectra which exhibit a similar series of mass losses as the pentadiene derivatives of Stemmler and Hites. The EC spectra of fluoranil and chloranil are shown in Figure 5 where it is seen that ions

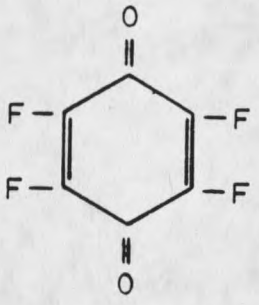

Fluoranil

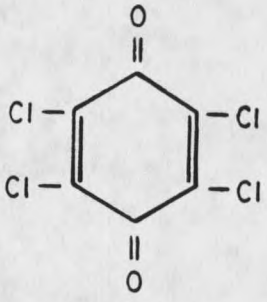

Chloranil

of type M^-, $[M+H-X]^-$ and $[M-2X]^-$, where X is either fluorine or chlorine, are observed for both compounds. In addition to these ions, chloranil also shows a species due to $[M+2H-2Cl]^-$. Here, as with the examples of TCNQ and the TFA derivatives of the AA and AP isomers (shown later), accurate mass analysis have substantiated the elemental composition of the observed ions. The general appearence of these spectra are not altered by changes in temperature. The temperature stable EC spectra were also reported for the cyclopentadiene derivatives[6]. Since these simple molecules appear to mimic the unusual features of the more complex molecules studied by Stemmler and Hites, an attempt

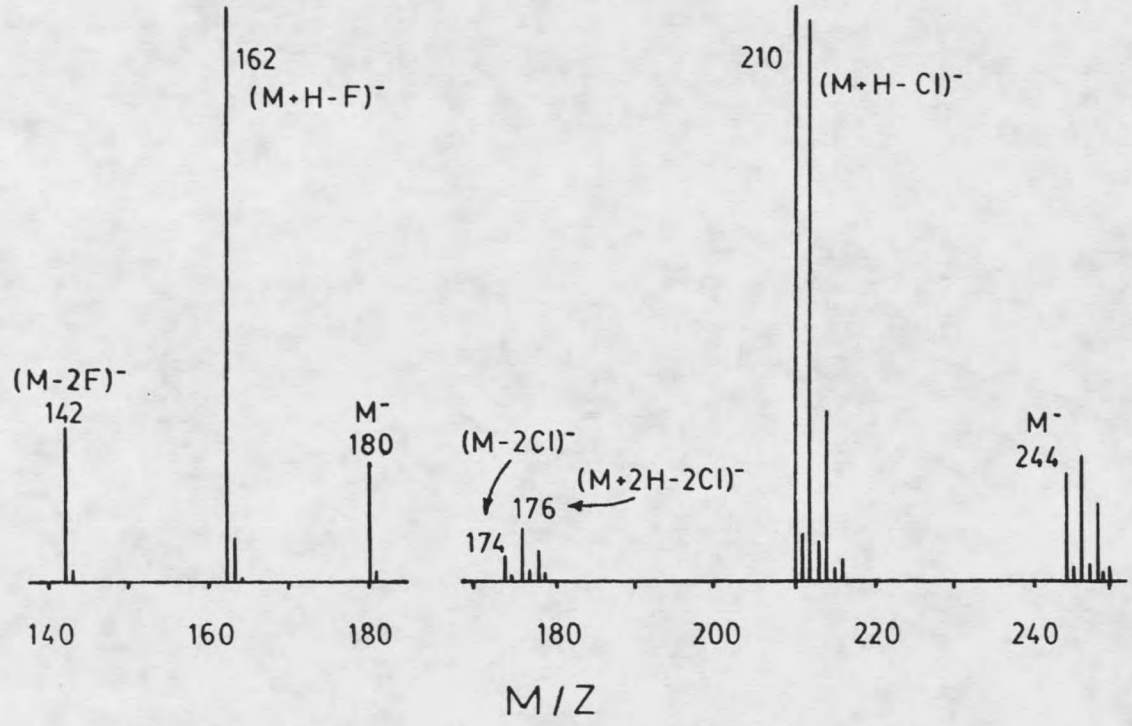

Figure 5. The HPECMS spectra of fluoranil and chloranil. The pressure is 0.3 Torr (methane) and the ion source temperature is 100°C for fluoranil and 180°C for chloranil.

was made to understand the basis of the EC spectra of fluoranil and chloranil.

Prior to the development of the model, it was believed that Route A was the likely possibility for the occurrence of the unusual ions in the spectra of these two compounds. However, the model developed here clearly indicates that Route A cannot be the pathway toward generation of these signals since the precursor ion, that which occurs by a simple resonance or dissociative electron capture processes, must be larger than any unusual ions, Z^-. Both spectra in Figure 6 are dominated by signals due to $[M+H-X]^-$ which greatly exceed that due to the M^- ion. Route B was tested, as described later in greater detail for the trifluoroacetic anhydride derivatives of the aminoanthracene and aminophenanthrene isomers, by adding triethylamine (TEA) to the buffer gas. In this case, TEA had no effect on the observed spectra, which was expected.

Route B toward generation of unusual negative ions is only feasible when the rate coefficient for electron capture is of the same magnitude as that for ion-molecule reactions. Fluoranil and chloranil are believed to have very fast EC rate coefficients due to their extremely high electron affinities[21,43]. Route C is also not expected to be operative since it was shown by the model not to be competitive with fast EC. Also, if Route C were operative, one might expect to see other gas phase radicals, such as

CH_3 and C_2H_5, present in the spectrum, as seen from the examples of TCNE and TCNQ in Figure 3. This leaves Route D which has been shown by Cases D1 and D2 to be potentially competitive with fast EC if a wall reaction does occur with high efficiency and if the altered neutral species, W^-, attaches electrons rapidly.

Convincing evidence of efficient wall reactions by both fluoranil and chloranil under HPEC conditions has been obtained by a series of separate experiments. The first of those is illustrated in Figure 6 where four electron impact (EI) spectra of fluoranil in the mass range m/z = 150-190 are shown. Spectrum A was obtained from a recently cleaned and baked ion source. The predominant ion is the expected one of m/z = 180 due to the molecular species. Note that the $[M+1]^+$ ion abundance reflects the normal isotopic distribution of ^{13}C found in fluoranil. Electron impact spectrum B was obtained ten minutes later under identical conditions, but just after the source had been operated under typical HPEC conditions for a period of two minutes and then returned to EI mode. It is seen from spectrum B that a substantial increase in the intensity of ion m/z = 182 has occurred due to the species $[M+2H]^+$ (confirmed by accurate mass measurements). In spectrum C, the same experiment was repeated, this time using a five hour period of exposure to irradiated high pressure methane. It is seen that a further increase in the $[M+2H]^+$ ion has

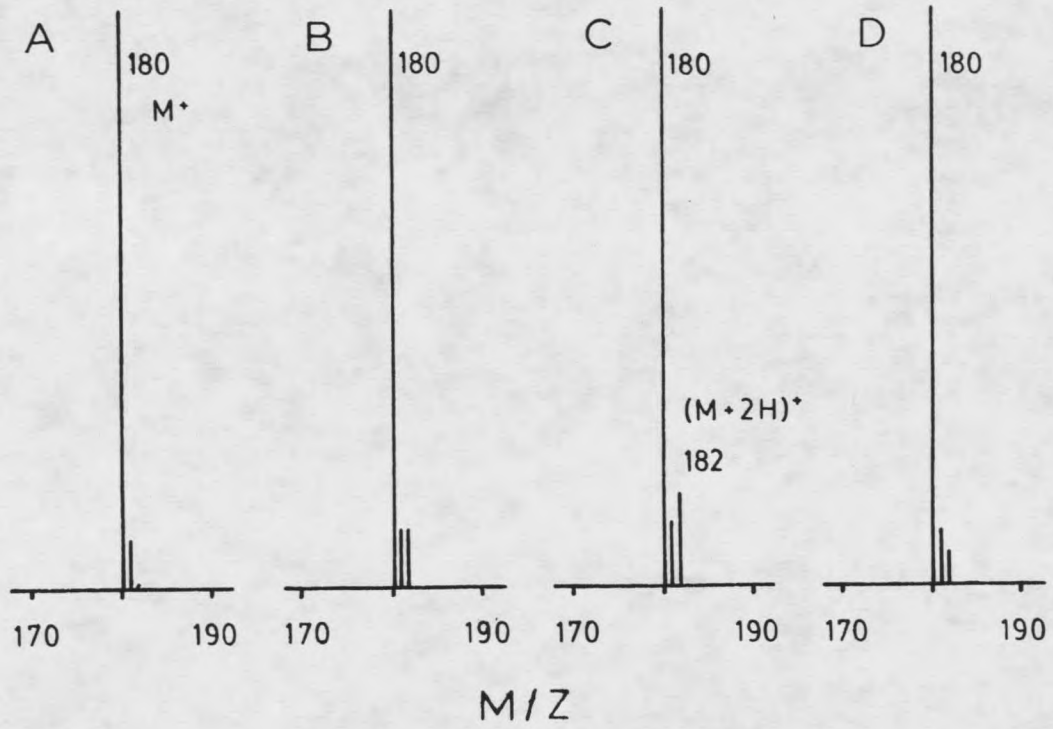

Figure 6. The electron impact spectra of fluoranil measured (A) immediately after cleaning the ion source, after subjecting the ion source to CH_4/HPEC conditions (B) for 2 minutes and (C) for 5 hours, and (D) after allowing the ion source to remain gas- and sample-free for 12 hours. The temperature is 150°C.

occurred. The ion source was allowed to remain sample and methane free overnight at a temperature of 150°C. Twelve hours after the five hour irradiation period, EI spectrum D was obtained in which it is seen that the $[M+2H]^+$ ion has been diminished, but not entirely eliminated.

In the wall sensitized spectra of fluoranil, it is interesting to consider where the two hydrogen atoms add to the fluoranil molecule. Fluoranil and chloranil are often used in condensed phase reactions to aromatize other molecules. For example, by adding fluoranil to tetrahydrofuran, one can generate fluoranol and furan as shown by

Fluoranil and fluoranol can be readily separated by gas chromatography. Therefore, the possibility of co-elution resulting in the increase in the $[M+2H]^+$ species is eliminated. A prominent ion in the fluoranol EI spectrum is that which is due to $[M-OH]^+$. There is no evidence of the occurrence of a $[M-OH]^+$ ion in the EI spectrum of fluoranil in Figure 7. This indicates that the wall induced addition of the hydrogen atoms is not at the site of the carbonyl oxygens. The two hydrogens may add to

eliminate a carbon-carbon double bond. This would facilitate the loss of a HF neutral, thereby providing an ion in the EC spectrum corresponding to $[M+H-X]^-$.

Identical EI experiments were conducted with chloranil which provided similar spectra. The results clearly indicate that a wall reaction tends to hydrogenate fluoranil and chloranil and that activation by hydrogen loading of the ion source walls is caused by irradiation of methane under normal HPEC conditions. These experiments strongly point to the occurrence of Route D in the ionization of fluoranil and chloranil and also suggest that the species corresponding to W in Figure 5 for these cases is [M+2H]. This clue provides additional insight into the origin of the fragment ions of fluoranil and chloranil shown in Figure 5. It means that the ions of the types $[M+H-X]^-$ and $[M-2X]^-$ are more descriptively written as $[M+2H-HX]^-$ and $[M+2H-2HX]^-$, respectively.

The suggestion that the two fragment ions just mentioned come from a single species, [M+2H], finds additional support in the experiment shown in Figure 7. The reconstructed single ion chromatograms of a fluoranil sample introduced by gas chromatography is shown. It is seen that the chromatographic peak, as indicated by the near gaussian profile of the M^- signal, reflects the expected passage of the sample through the detector. The other two ions, however, exhibit distorted time profiles

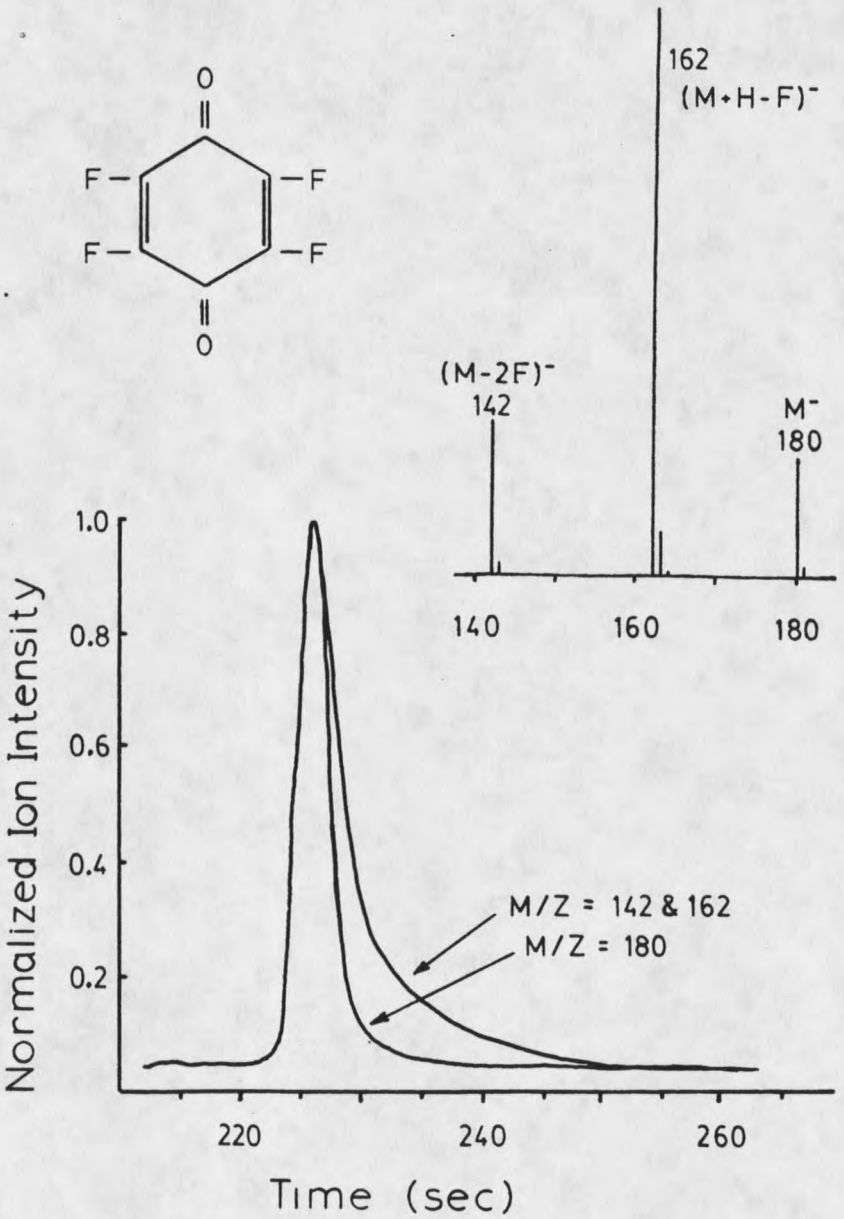

Figure 7. The single ion reconstructed chromatograms in the HPECMS analysis of fluoranil. Pressure is 0.3 torr (methane) and the temperature is 100°C.

which tail significantly after the chromatographic peak due to M^- has passed. The neutral, which upon EC provides ions m/z = 162 and 142, tends to stick to the wall of the ion source. Ventilation out of the source is thereby delayed in time as shown. Since the two ions of m/z = 162 and 142 have the same distorted time profiles, Figure 7 also suggests that these two ions come from a branched EC reaction of the same neutral species, presumed here to be [M+2H]. The corresponding experiment has also been performed with chloranil as shown in Figure 8. These results also show a similar time distortion for the corresponding $[M+2H-HX]^-$ and $[M+2H-2HX]^-$ in fluoranil, in this case m/z = 210 and 174. Therefore, these ions are thought to be formed from the same type of precursor, [M+2H], as previously seen for fluoranil. Figure 8 also provides additional significant information; the ion of m/z = 176 due to $[M+2H-2Cl]^-$ has a unique time dependence and is therefore not formed by EC of [M+2H].

Conclusions concerning the M^-, $[M+H-X]^-$, and $[M-2X]^-$ ions in the HPEC mass spectra of fluoranil and chloranil are summarized by the following sequence

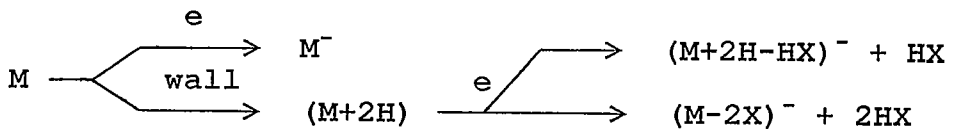

(54)

As stated in the discussion of Figure 8, the formation of species $[M+2H-2X]^-$ does not originate from the [M+2H]

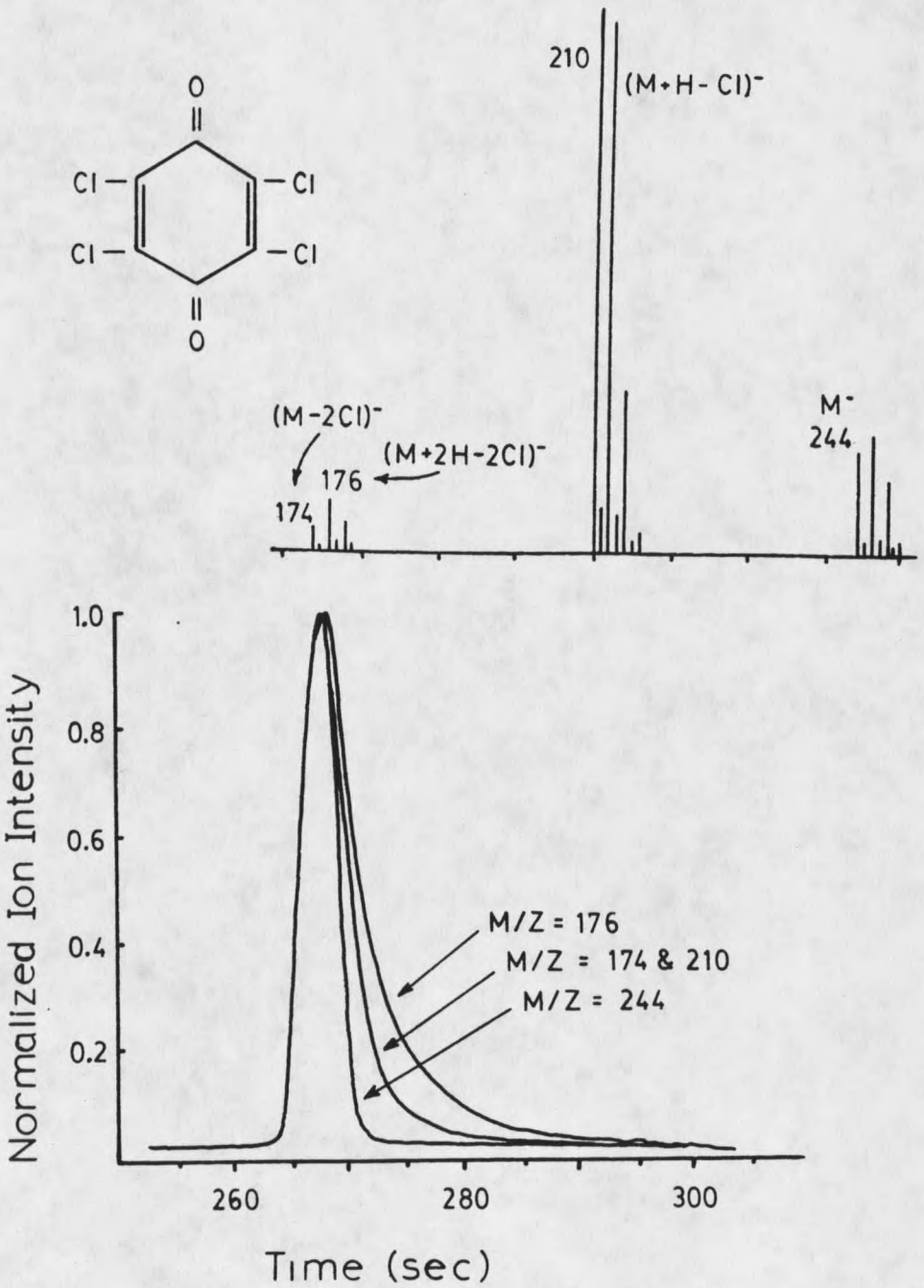

Figure 8. The single ion reconstructed chromatograms in the HPECMS analysis of chloranil. Pressure is 0.3 torr (methane) and the temperature is 180°C.

neutral. The formation of a [M+4H] neutral is not supported by experiments shown in Figure 6. Therefore, the following sequence is thought to occur from the continued reaction of the wall enhanced route in expression 54 leading to the $[M+2H-2Cl]^-$ ion.

$$[M+2H-HCl]^- \xrightarrow[\text{wall}]{P^+} [M+2H-HCl] \xrightarrow{\text{wall}} [M+3H-Cl]$$

$$\xrightarrow{e} [M+2H-2Cl]^- + HCl \qquad (55)$$

The first two steps in sequence 55 may occur as a single step if neutralization and hydrogen addition can occur with a single interaction of $[M+2H-HCl]^-$ upon recombination with positive ions or diffusion to the ion source walls.

Returning to the cyclopentadiene derivatives of Stemmler and Hites, with the insight gained from the experiments conducted with fluoranil and chloranil, it is seen from Figure 9 that the same types of explanations can readily be applied to the EC spectrum of Pentac.

The most intense ion in Figure 9, due to $[M-2Cl]^-$, could readily come from the dissociative electron capture of M, but could also be produced by dissociative electron capture of species [M+2H], formed by a wall reaction, to form the ion $[M+2H-2HCl]^-$. In either case, the same ion of m/z = 400 (for ^{35}Cl - containing ions) is produced. Also the ions at m/z = 35, 235, and 435 are probably formed by EC of M as shown in Figure 9. The question remaining is,

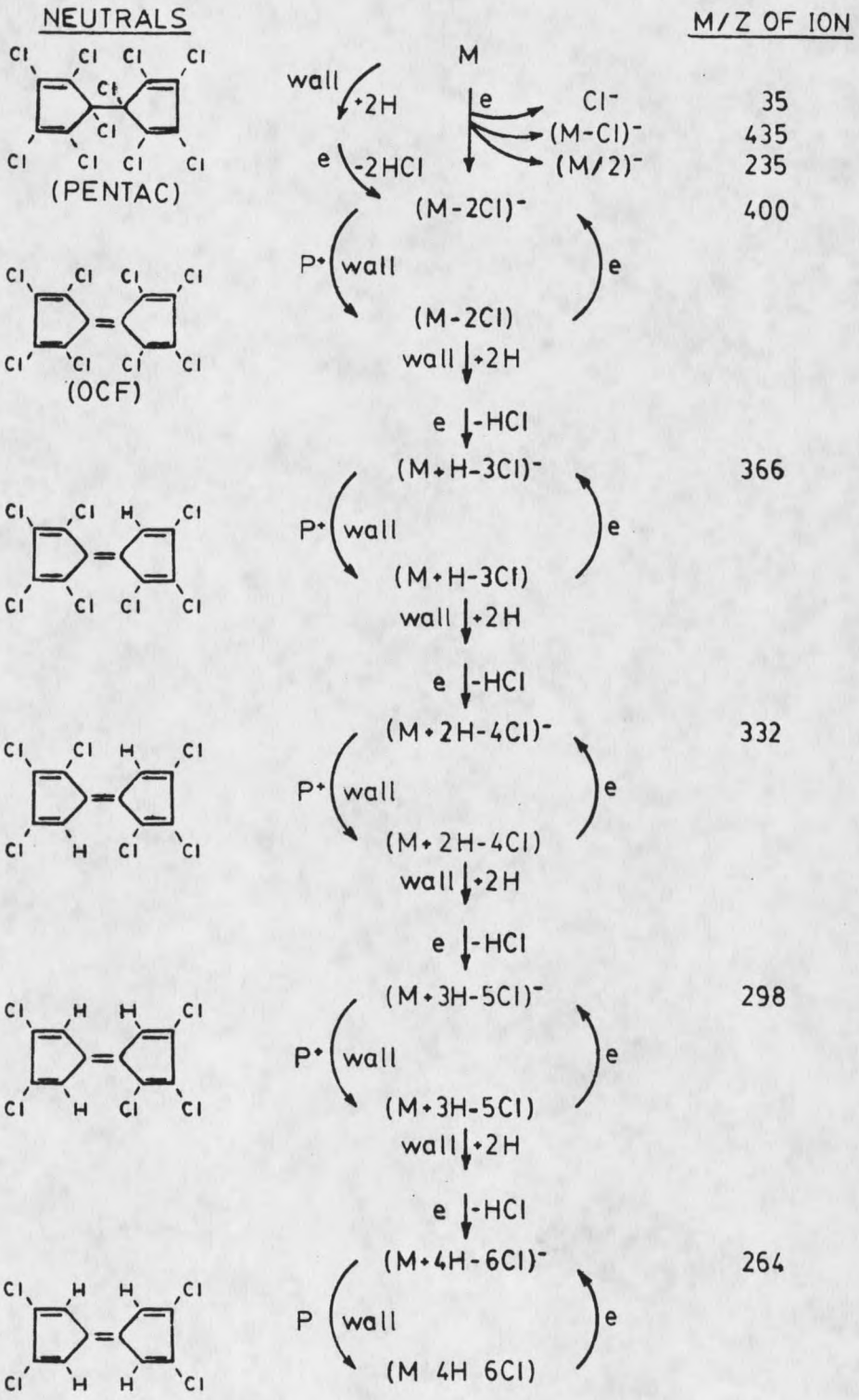

Figure 9. A suggested mechanism for the HPECMS spectrum of Pentac shown if Figure 4.

how are the ions of m/z = 366, 332, 298, and 264 formed? One possibility is the following: if neutralization of the $[M-2Cl]^-$ ion by recombination or by contact with a wall produces a neutral species which resembles or is equivalent to octachlorofulvalene (OCF), then the sequence of ions observed from m/z = 264 to 400, differing by 34 amu seen in Figure 5 might be expected. This is because OCF itself, produces an HPEC spectrum[6] which is in near-perfect accord with that of Pentac in this mass range.

These ions could be formed from OCF by a repeated sequence of reactions involving wall activation (hydrogenation), dissociative electron capture, and then neutralization as was deduced by experiments for the case of chloranil discussed above. If so, the total ionization sequence of Pentac represented in Figure 9 would occur, producing the unusual ions of 366, 332, 298, and 264. With the formation of the final neutral, [M+4H-6Cl], no unsaturated sites would have two chlorine atoms and either wall activation or electron capture no longer occurs. The suggested mechanism in Figure 9 constitutes a combination of steps shown in Routes A and D of Figure 1. It is seen that the intensities of the ions forming the sequence from m/z = 400 to 264 are in reasonable agreement with general diagnostic predictions developed in theory for Route A; that is the intensity of an unusual ion can be approximately equal to, but should not exceed, the

intensity of the precursor ion. While some modifications of the details of Figure 9 may be necessary as experiments provide additional information concerning the four proposed routes seen in Figure 1 toward unusual ions in HPECMS, the sequence shown is viable in view of existing evidence. The evidence is 1) the ionization mechanism demonstrated here for fluoranil and chloranil provide precedents for the mechanism and 2) the predictions concerning Routes A and D in theory indicate that these two processes are sufficiently fast as to allow all of the steps shown in Figure 9 to occur during the passage of Pentac through the ion source.

Pentafluoropropionic (PFP) and Trifluoroacetic (TFA) Anhydride Derivatives of the Aminoanthracene (AA) Aminophenanthrene (AP) Isomers

In the trace analysis of environmentally important compounds it is often necessary to be able to distinguish between positional isomers. This is especially true when the position of a substituent is important in the determination of carcinogenic or physiological activity. The amines of anthracene and phenanthrene provide a challenging group of structurally similar isomers for study due to their mutagenic activity and their presence in the environment as the result of coal related processes[32]. The isomers of AA and AP can be sensitively detected by HPECMS if they are first derivatized by reaction with a

perfluorinated anhydride[33]. The purpose of this step is to

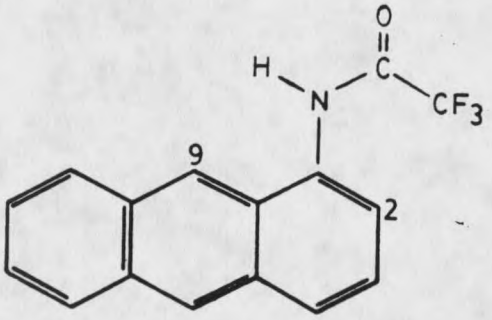

1-AA-TFA

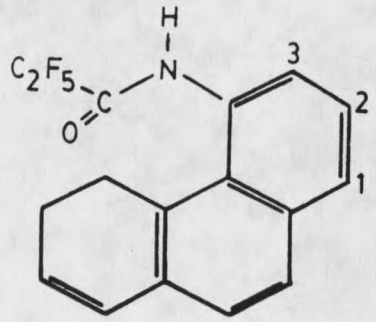

4-AP-PFP

increase the propensity of the molecule toward electron capture by increasing its electron affinity.

Initial efforts in the HPECMS analysis of these compounds was directed toward the generation of EC spectra which would provide unequivocally unique identification of each positional isomer. The results obtained with the PFP derivatives which are shown in Figure 10 are those which would be expected; very sensitive signals due predominantly to ions of the type $[M-HF]^-$. Ions of the type M^- and $[M-2HF]^-$ also contributed to the EC mass spectra. However, as can be seen from Figure 10, there are inadequate differences for absolute differentiation. These three ions are commonly observed in the spectra of PFP derivatives of amines[35] and are thought to result from a single, branched

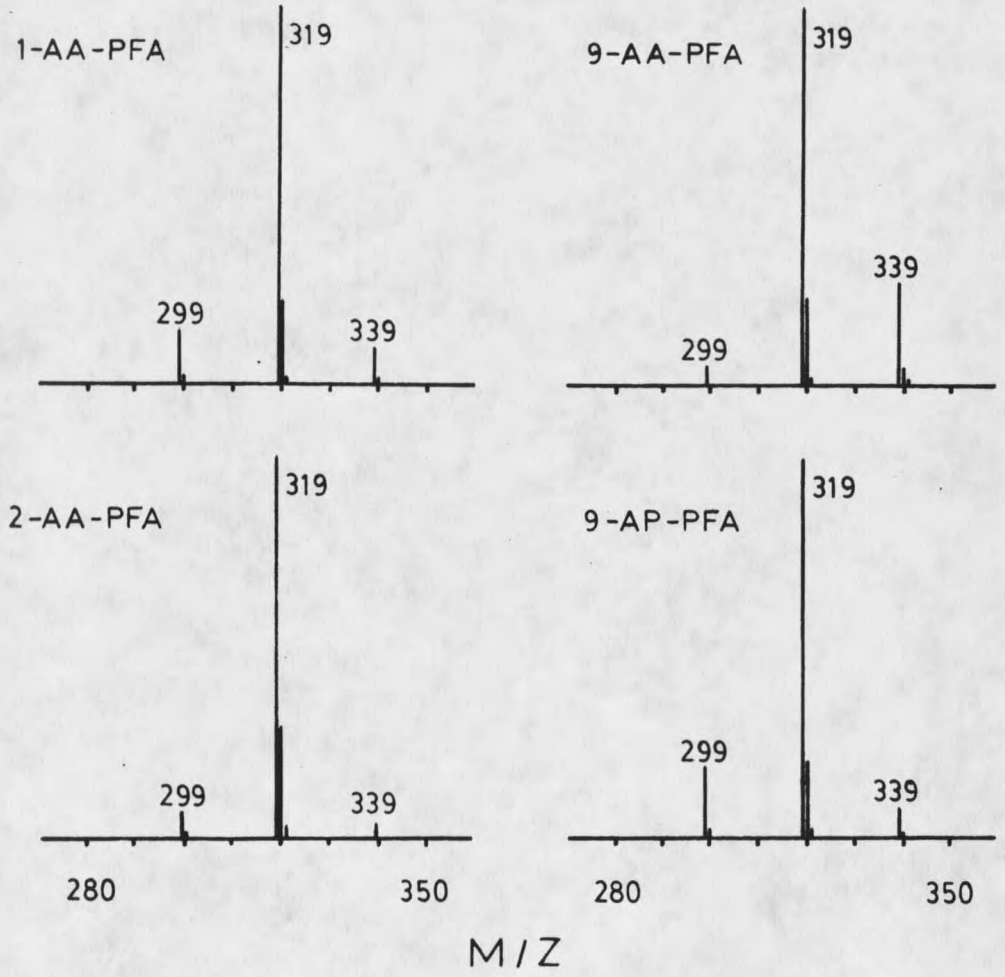

Figure 10. The HPECMS spectra of the pentafluoropropionic anhydride derivatives of 1-, 2-, 9-aminoanthracene and 9-aminophenanthrene. The pressure is 0.3 Torr (methane) and the temperature is 180°C.

EC reaction leading to both resonance and dissociative products.

Analysis by HPECMS of the TFA derivatives of AA and AP, on the other hand, did result in a more complex spectrum which, as seen in Figure 11, provided useful unique information for each isomer. The dominating ion in the spectra of the AP isomers is due to an apparent $(M-16)^-$ species which is also present to a certain extent in the spectra of the AA isomers. This ion was completely unexpected as were the ions of $(M+14)^-$, $(M-86)^-$, and $(M-18)^-$, although it should be noted that the expected ions M^- and $[M-HF]^-$ from the simple EC process are observable in each case. Accurate mass experiments were performed, the results of which are shown in Table 7, which provided information as to the identity of the observed unusual ions.

The composition of m/z = 273, from Table 7, was determined to be an oxygen loss from the molecular species. While precedence exists for some of these ions, the ion corresponding to $[M-O]^-$ was particularly difficult to rationalize. It is believed that this ion has not been previously reported in the EC spectrum in which the only oxygen present occurs as a carbonyl functionality. The sensitivity of detection allowed by the $[M-O]^-$ ions is about an order of magnitude less than that offered by the $[M-HF]^-$ of the PFP derivatives shown in Figure 10. This

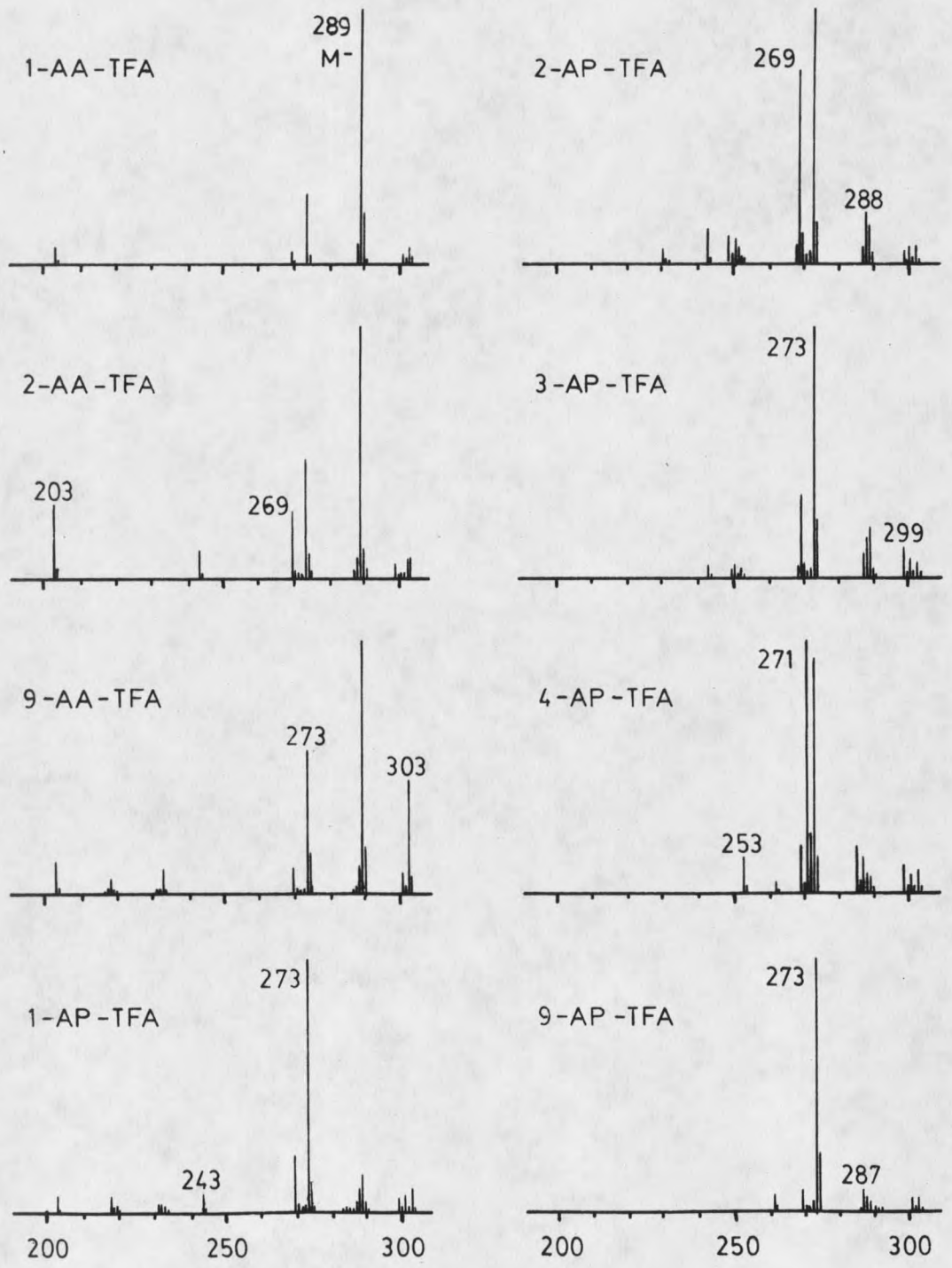

Figure 11. The HPECMS spectra of the trifluoroacetic anhydride derivatives of the isomers of aminoanthracene and aminophenanthrene. The pressure is 0.3 Torr (methane) and the temperature is 180°C.

level of sensitivity is, nevertheless, substantial and suitable for the trace analysis of these compounds. The strong dependence of the spectra in Figure 11 on isomeric structure also suggests a potential use of the TFA derivatives for their HPECMS isomer-specific analysis.

Table 7. Accurate Mass Data of the Unusual Ions in the Spectra of the Trifluoroacetic Anhydride Derivatives of the Aminoanthracene and Aminophenanthrene Isomers.

m/z	Composition	Origin	Observed Mass	ppm dev.
113	$C_2H_2ONF_3$	$[M-C_{14}H_8]$	112.9843	2.8
203	$C_{15}H_9N$	$[M-CHOF_3]$	203.0706	14
269	$C_{16}H_9ONF_2$	[M-HF]	269.0636	-13
271	$C_{16}H_8NF_3$	$[M-H_2O]$	271.0645	5.5
273	$C_{16}H_{10}NF_3$	[M-O]	273.0776	11
289	$C_{16}H_{10}ONF_3$	M	289.0682	3.0
303	$C_{17}H_{12}ONF_3$	$[M+CH_2]$	303.0852	-4.0

In attempting to define the origin of the $[M-O]^-$ ions, the four candidate routes to unusual ions in Figure 1 have been considered. Route A can be immediately eliminated as a possibility because in it the unusual ion Z^- must be accompanied by a precursor ion, M^-, which is at least as intense as Z^-. For the AP isomers in Figure 11, the $[M-O]^-$ ion greatly exceeds the intensity of any ion which could conceivably be its precursor. The spectra suggest that Route C might be operative to some degree whereby EC of these molecules follow a prior gas phase radical reaction. As mentioned in the discussion of Route C in the previous section, in order for competitive signals to be generated,

the EC rate coefficient for M^- must be low. This certainly seems to apply here where the $[M+CH_2]^-$ signal is a sizable percentage of that of M^-. It is difficult to envision, however, how the more prominent ions of the type $[M-O]^-$ could be produced by this sequence. Because the positive ionization of the AA and AP derivatives by CH_5^+ reagent ions is expected to occur with the usual rate of a fast ion molecule reaction, Route B seems particularly worthy of consideration, especially since the EC rate coefficient for the TFA derivatives is considered to be slow. A recent report by Morton[34] provides evidence that the site of protonation of these derivatives is at the carbonyl oxygen rather than the nitrogen. Neutralization of the protonated molecule, followed by electron capture would easily result in an apparent oxygen loss in the EC spectrum.

Investigations by Grimsrud[35,36], in the study of the response of anthracene in the electron capture detector, have shown that triethylamine (TEA) is an effective reagent for blocking positive ion-molecule reactions. This is made possible by creating a thermodynamically stable set of terminal reagent positive ions which do not react with the analyte. An additional feature of TEA is that it does not disturb the electron density by the formation of reagent negative ions, therefore allowing the desired EC reactions to occur as they would in a pure methane plasma. The results of this sort of an experiment are shown in Figure

12 in which the EC spectrum of 9-AP-TFA was obtained with and without TEA doped into the methane buffer gas by way of the heated expansion volume accessory on the mass spectrometer. Spectrum A of Figure 12 shows the very dominant $[M-O]^-$ ion observed for this derivative together with ions M^- and $[M-HF]^-$ of about an order of magnitude lower intensity. Spectrum B, with TEA doped into the source, is quite different; the $[M-O]^-$ ion is now a minor ion and those due to $[M-HF]^-$ and M^- (the expected electron capture products) are dominant. Also, the total ion sensitivity to 9-AP-TFA under condition B was about an order of magnitude less than in condition A. Clearly the effect of the TEA in this experiment has been to reduce the $[M-O]^-$ ion to a small percentage of the total ion current as compared to standard conditions, whereas the intensity of ion M^- and $[M-HF]^-$ has not been strongly affected by the presence of TEA. The corresponding experiment performed on several of the remaining TFA derivatives also resulted in strong and selective attenuation of the $[M-O]^-$ ion.

In the examples of fluoranil and chloranil we have seen that certain unusual negative ions can be traced to a particular neutral. This was done by comparing the reconstructed ion chromatograms of the various negative ions. Different temporal profiles indicated that different neutrals, which had been adsorbed on the source walls, were responsible for the observed negative ions. The same test

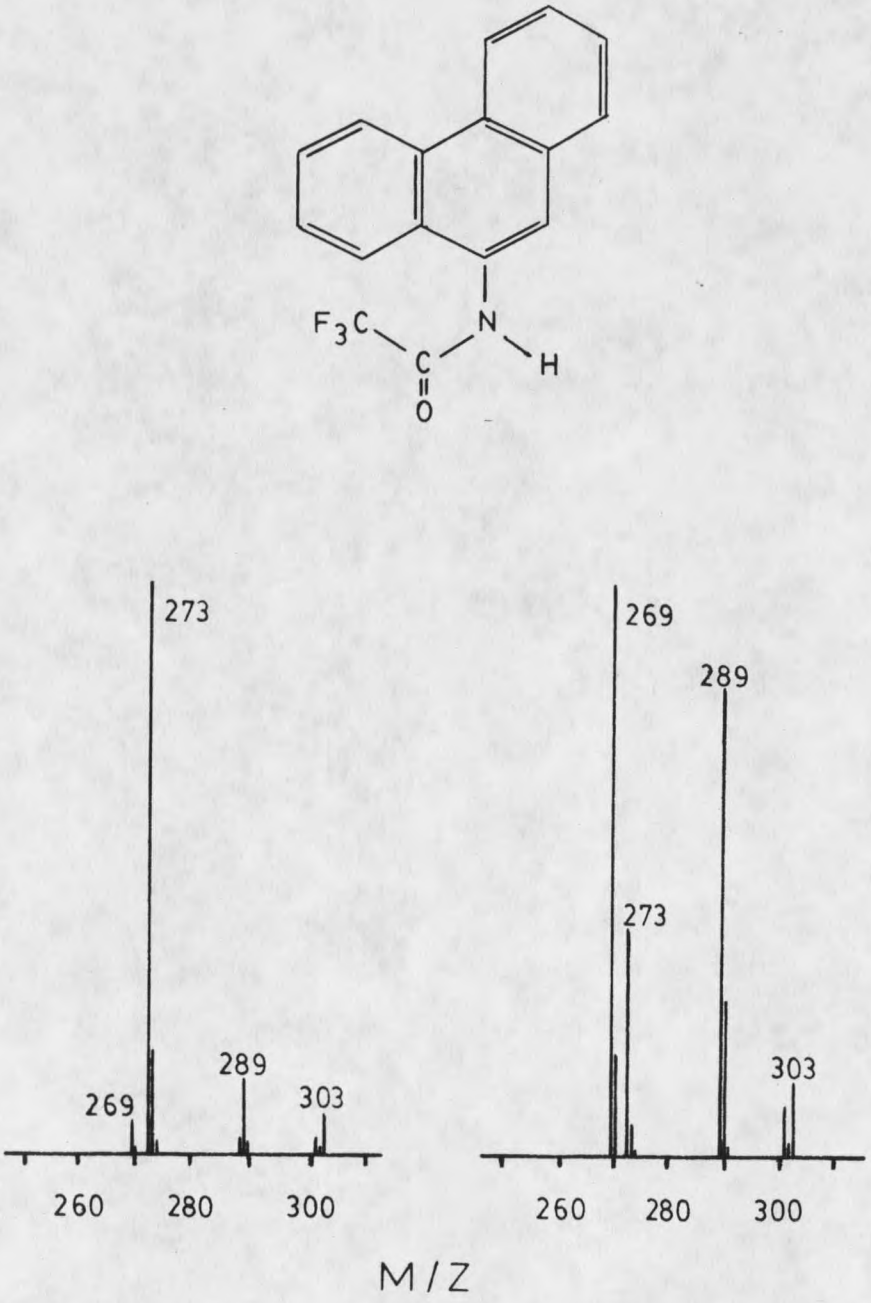

Figure 12. The HPECMS spectra of the trifluoroacetic anhydride derivative of 9-aminophenanthrene (A) under normal CH_4 and (B) with about 5% triethylamine added to the buffer gas. The pressure is 0.3 Torr and the temperature is 180°C.

for wall adsorbed neutrals as used in the EC of fluoranil and chloranil may be used here, that is the degree of overlap of the reconstructed ion chromatograms. The results of the application of this test to the ion signals generated from electron impact and positive chemical ionization, as seen in Figure 13, show that the ion traces provide excellent overlap. The indication is that all ions of lower mass are the result of normal fragmentation of the ion generated from the molecular species. Altered neutrals which may be retained by the walls are not precursors of positive ions observed in these spectra. This is, however, expected as ions which originate as gas phase fragments of a parent ion must have the same temporal profile as that parent ion.

In Figure 14, presenting the corresponding results of this test as applied under EC conditions, show substantial retardation in the overlap of the signals arising from the unusual ions. Although we see differences in the temporal profile of the ions in the EC spectrum of 3-AP-TFA, it does not necessarily indicate that a Route D process has occurred. It simply indicates that some altered neutral, regardless of its origin, has been absorbed on the surface of the walls. If two ion traces would provide perfect overlap, this may indicate that the ions originate from the same neutral. The $[M-O]^-$ ion, which has been shown by Route B to be the result of positive ion-molecule

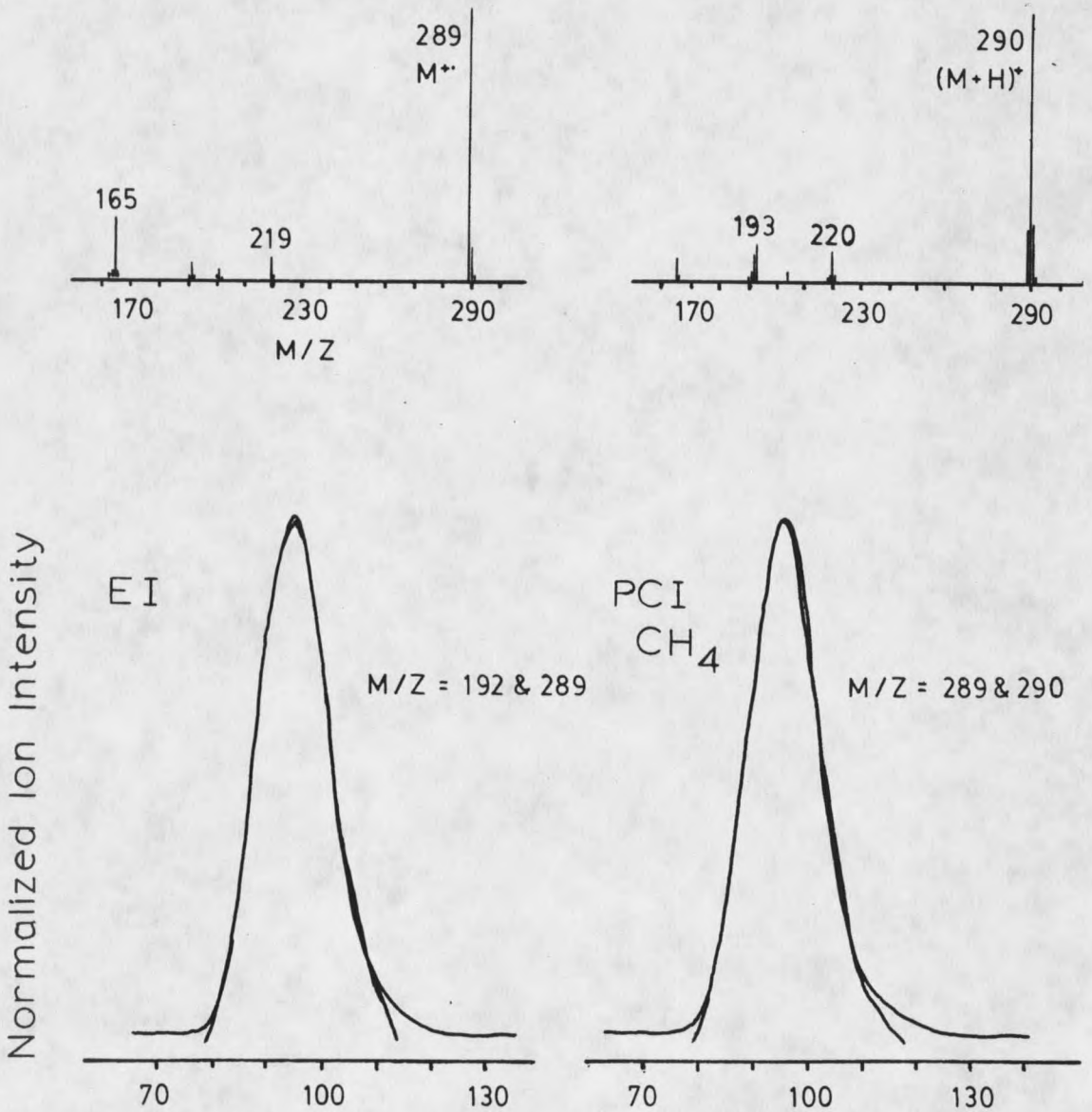

Figure 13. The single ion reconstructed chromatograms in the EI (temperature is 200°C) and PCI (methane) spectra of the trifluoroacetic anhydride derivative of 3-aminophenanthrene. The PCI pressure is 0.3 Torr and the temperature is 250°C.

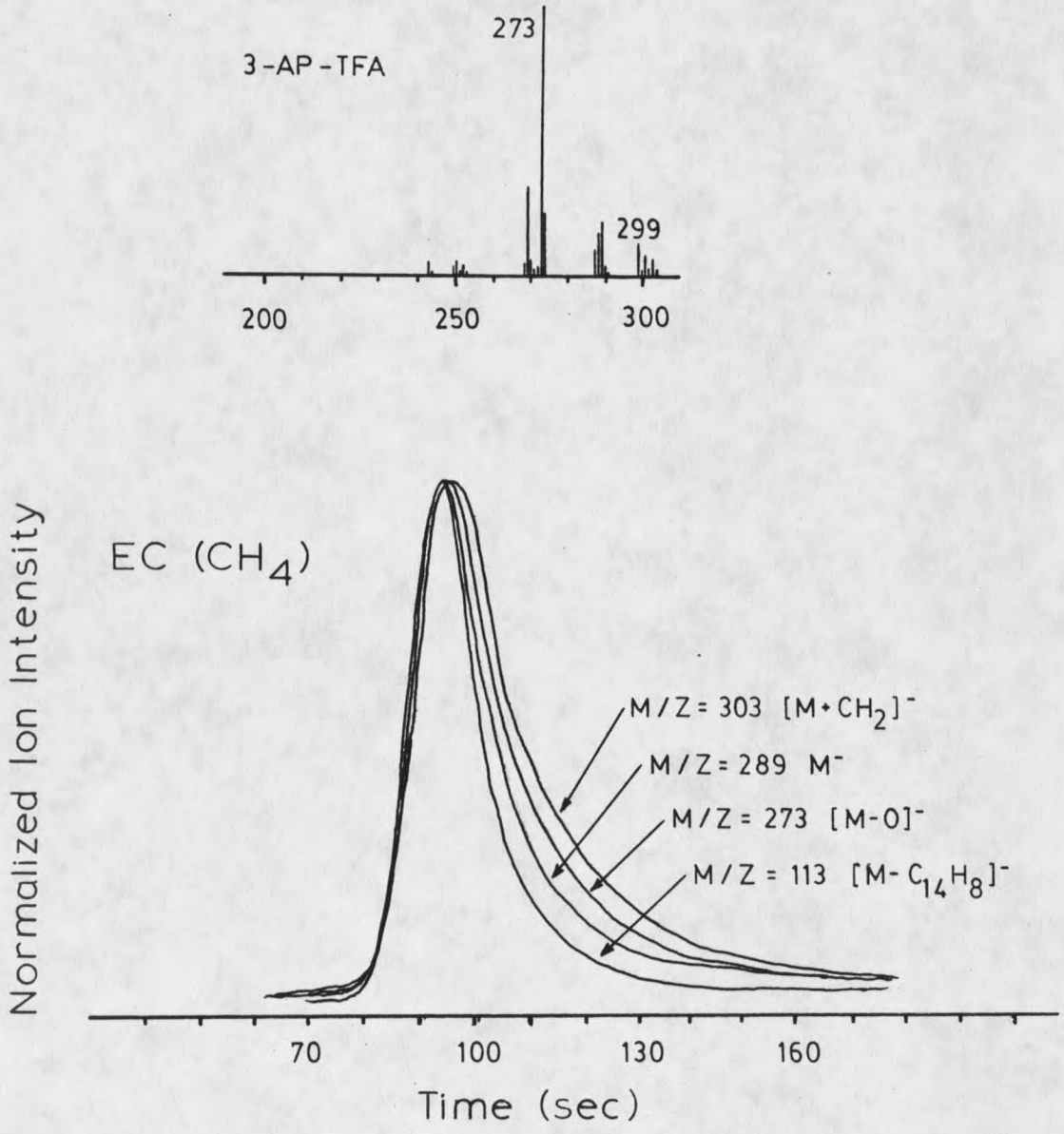

Figure 14. The single ion reconstructed chromatograms in the HPECMS analysis of the trifluoroacetic anhydride derivative of 3-aminophenanthrene. The pressure is 0.3 Torr (methane) and the temperature is 250°C.

reactions, shows significant retardation by the source walls as does the $(M+14)^-$ ion, believed to arise through Route C as the result of molecule-radical reactions. In these two cases, altered neutrals apparently stick to the source walls and are later desorbed and capture an electron.

It has been shown that the kinetic model developed here provides a valuable guide for the interpretation of spectra containing unusual and unexpected negative ions. The remainder of this study will deal with techniques and experiments which attempt to eliminate the occurrence of the unusual negative ions in HPECMS.

THE ELIMINATION OF UNUSUAL IONS IN HPECMS

Ion Source Surface Modifications

The prior discussion of the occurrence of unusual negative ions in HPECMS revealed that reactions at the ion source walls may result in the production of altered neutral species, W. If W is EC active, unusual ions, W^-, will be generated and contribute to the overall spectrum. As mentioned in Case D of Table 5, this wall-related process can provide ion signals which are quite competitive with those generated from fast EC reactions. The contribution of wall-related reactions was effectively demonstrated by experiments conducted with fluoranil and chloranil.

An obvious question to consider with respect to wall-related ion signals is what effect does the wall material itself have on the generation of unusual neutrals and ions? The role of the wall in the reaction may be that of a catalyst or an adsorbate which retains the analyte and/or reactive radical species for a sufficient period of time to allow a reaction to occur. By changing the surface characteristics, it may be possible to alter the outcome of any processes taking place at that surface.

A modification of the ion source surfaces was accomplished by depositing a layer of gold on the cleaned stainless steel surface with a gold sputter coater. All source parts, which might be exposed to the analyte, were also coated with gold. The coating chamber was evacuated to 10 Torr with a vacuum pump and then purged with argon. This evacuation/purging procedure was repeated two additional times to ensure that all oxygen was removed from the chamber. The controls of the sputter coater were adjusted to 1.2 KeV and argon was introduced into the chamber to maintain a discharge current of approximately 20 mA. Gold was allowed to deposit for a period of 10 minutes. Calculations indicated the thickness of deposited gold to be approximately 1200 angstroms. A magnifying lens was used to inspect all coated surfaces. A smooth, evenly distributed layer of gold had been deposited leaving no exposed stainless steel. The ion source was reassembled, installed in the mass spectrometer's source vacuum chamber and baked at 300°C overnight.

The series of spectra previously shown in Figure 6 indicated that the EI spectrum of fluoranil, obtained after a stainless steel ion source had been exposed to irradiated methane, provided evidence of a surface related reaction. Two hydrogen atoms had been added to fluoranil which was observed in the EI spectrum as an $[M+2H]^+$ ion. The same experiment was also conducted with the gold coated ion

source. First, the walls of the ion source were exposed to irradiated methane under HPEC conditions for a period of one hour. Spectrum A of Figure 15 provides the EC spectrum of fluoranil obtained after the one hour irradiation. The wall-related negative ions, $[M+2H-HF]^-$ and $[M+2H-2HF]^-$, which were previously observed from the stainless steel source, are still prominent in the EC spectrum from the gold source. The ion source was evacuated and the EI spectrum of fluoranil was obtained after a period of two minutes. In spectrum B of Figure 15 we see that the EI spectrum of fluoranil from the gold source provides evidence of the same $[M+2]^+$ ion previously observed from the stainless source.

An additional experiment was conducted to determine if perhaps the gold surface would change the absorption characteristics of the altered neutral, believed to be [M+2H]. Figure 16 provides a direct comparison of EC spectra and the temporal profiles of the reconstructed ion chromatograms from the stainless steel and gold sources. The ions of m/z = 162 and 142 are believed to arise from EC by the altered neutral, [M+2H], and m/z = 180 is the molecular ion of fluoranil. We see that nearly identical results are obtained when both sources are operated under identical HPEC conditions.

The evidence presented in Figures 15 and 16 clearly indicates that coating the ion source with gold was not an

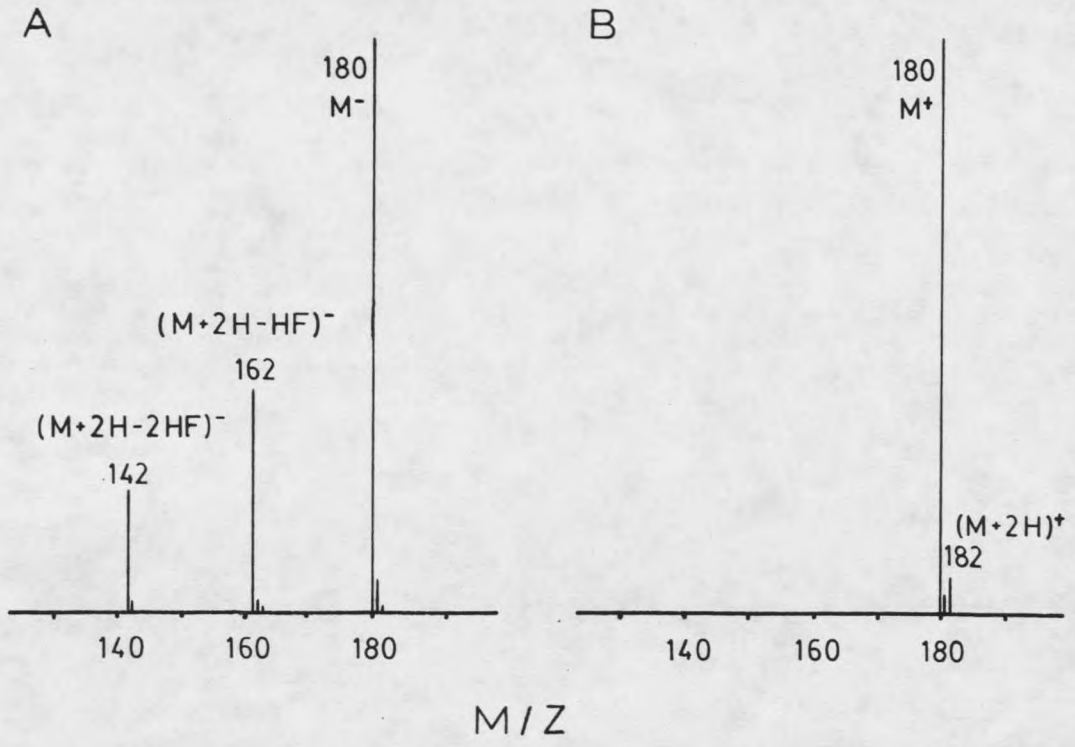

Figure 15. The HPECMS spectrum of fluoranil (A) obtained from a gold coated source exposed to irradiated methane for 1 hour (pressure is 0.5 Torr methane, temperature is 150°C) and (B) the EI spectrum obtained two minutes later.

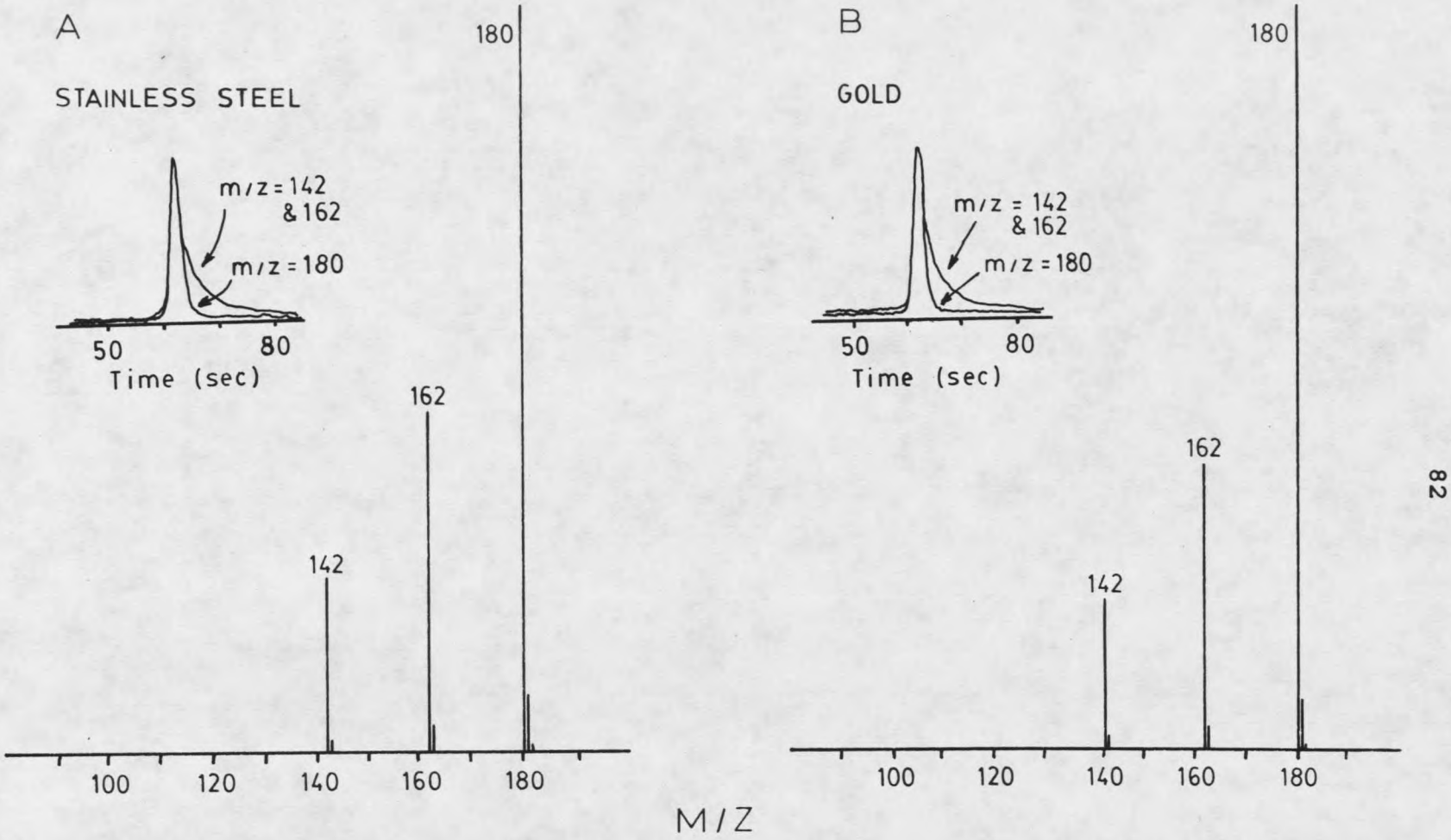

Figure 16. The HPECMS spectrum of fluoranil from (A) the stainless steel and (B) the gold ion source. In both spectra the pressure is 0.5 torr methane and the temperature is 150°C.

effective solution for the elimination of wall related negative ions.

Buffer Gases Other Than Methane

The objective in this study for using buffer gases other than methane is to eliminate the occurrence of unusual ions which are often observed in EC spectra from methane plasmas. In all the examples presented in prior discussions, the observed unusual negative ions could be attributed to reactions involving some species arising from the interaction of the electron beam with methane. Therefore, a logical solution to these problems was sought by the use of buffer gases which do not provide these reactive products when irradiated with electrons.

It is apparent that the hydrocarbon gases in general will result in large densities of free radicals and hydrogen atoms. This was confirmed by obtaining the EC spectra of several of the compounds presented in this study in iso-butane. The results were comparable to those from methane. It was also observed that ammonia provided reactive products, most notably hydrogen atoms, which strongly influences the EC spectrum of fluoranil. Generally, it may be surmised that any buffer gas used to eliminate unusual negative ions in HPECMS applications must be free of hydrogen. Other considerations of a more general nature are the requirements that the gas should not

be a strong oxidizer (shortens filament lifetimes) and that it should not form long lived negative ions, thereby decreasing the overall electron density in the ion source. These criteria suggest that nitrogen, carbon dioxide, and the noble gases might be suitable alternatives. Of these, the EC spectra obtained in carbon dioxide were found to be the only ones which were free of unusual negative ions. Also, detection sensitivities obtained in CO_2 were found to be suitable for trace analysis. Some of the results in CO_2 are reported below.

Comparison of EC Spectra From Carbon Dioxide and Methane

Examples From Route D Processes

The EC/CH_4 spectra of fluoranil and chloranil have been shown to be dominated by unusual negative ions which occur from wall related generation of altered neutrals. Since the reactions resulting in the transformed neutrals have involved hydrogen atoms, it is expected that the products of this reaction would be eliminated by the use of CO_2. The EC spectra in Figure 17 provide a comparison of ion signals of fluoranil and chloranil in CO_2 and CH_4. Spectra A and B are the EC results of fluoranil in CO_2 and CH_4, respectively, and spectra C and D are the respective EC results of chloranil. The visual evidence alone is quite convincing of the usefulness of CO_2 in the simplification of the EC spectra of these two compounds. It is clear

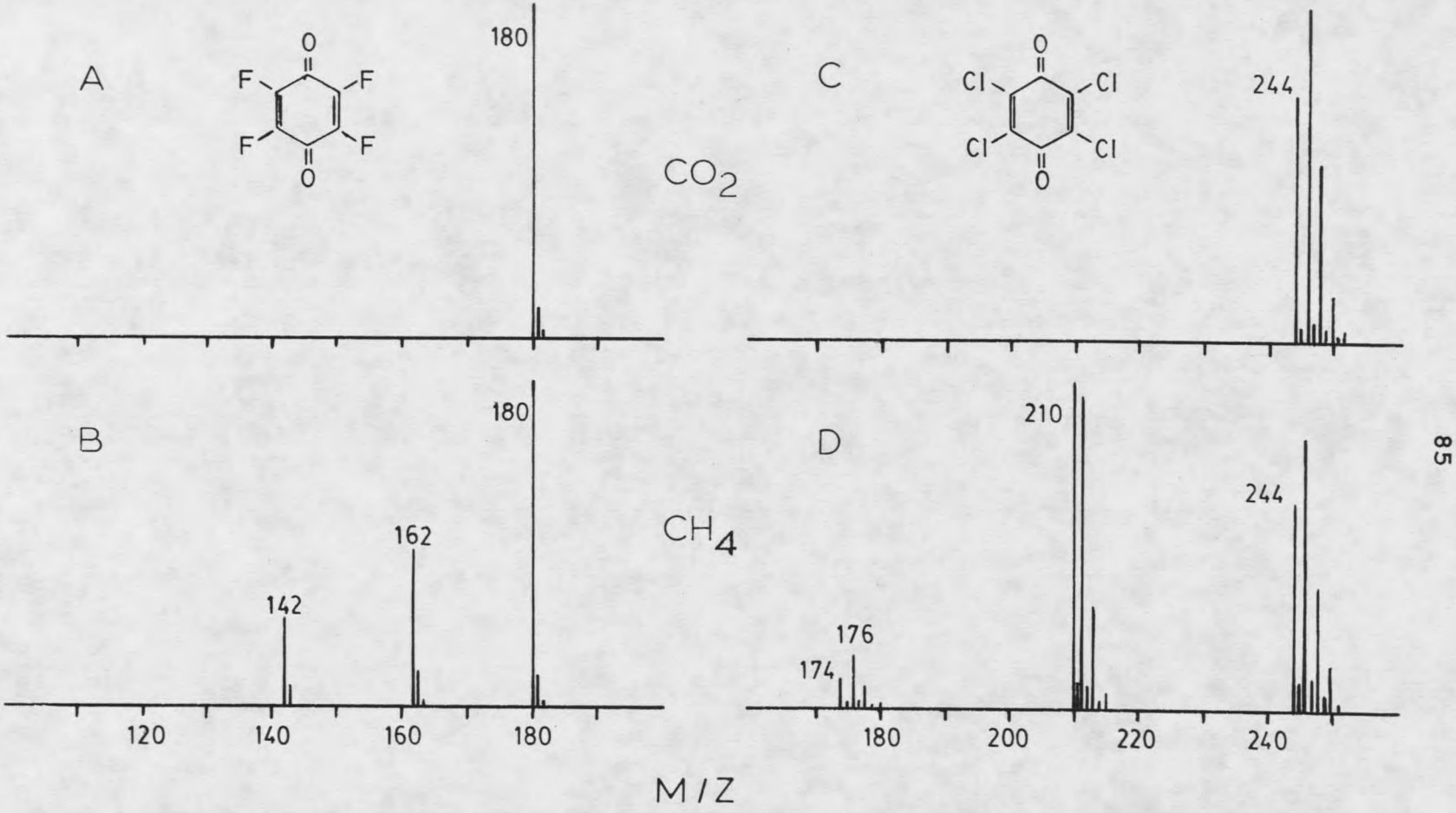

Figure 17. The HPECMS spectra of fluoranil in (A) CO_2 and (B) CH_4, and chloranil in (C) CO_2 and (D) CH_4. The pressure is 0.5 Torr and the temperature is 150°C.

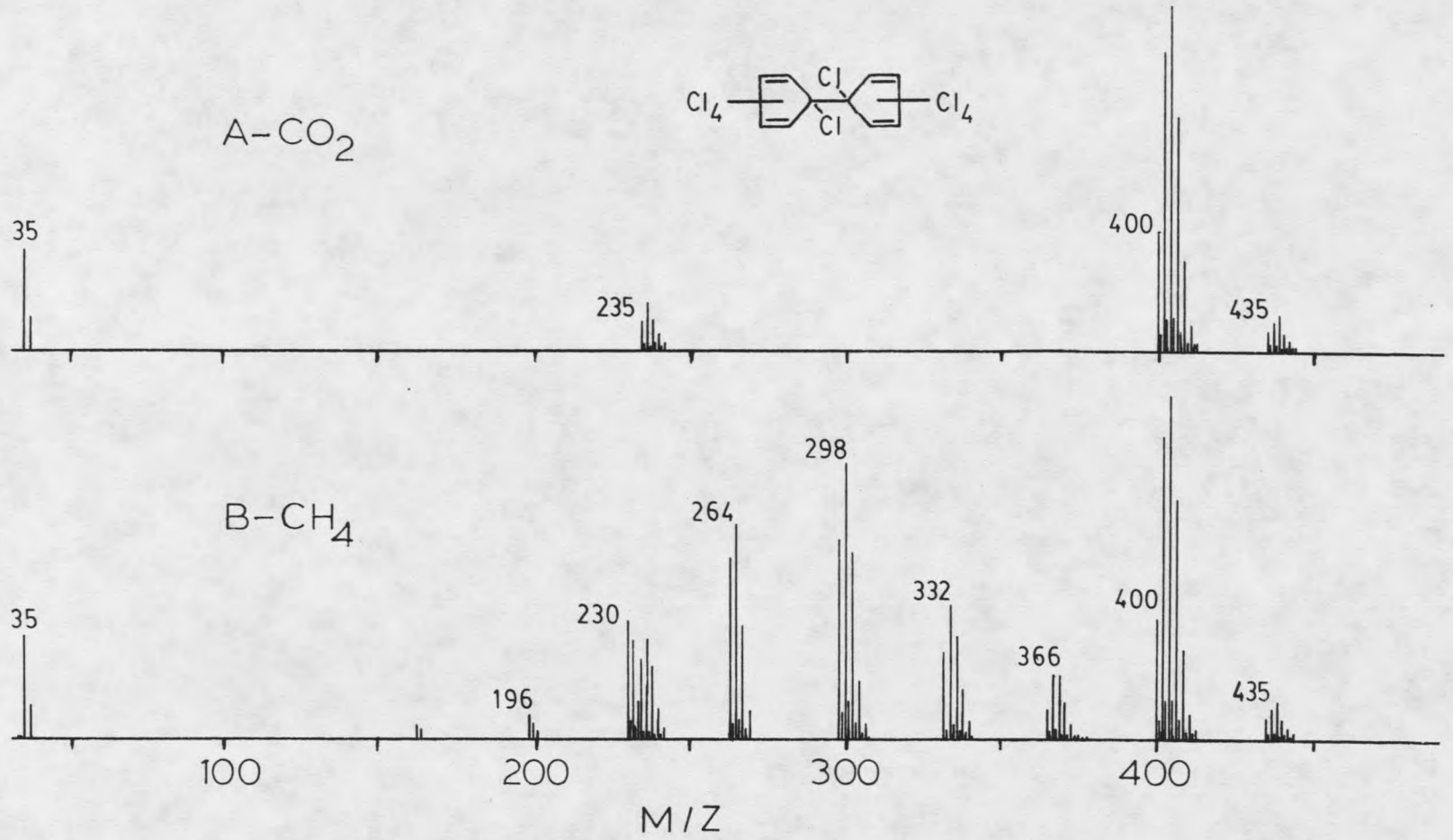

Figure 18. The HPECMS spectra of Pentac in (A) CO_2 and (B) CH_4. The pressure is 0.5 Torr and the temperature is 150°C.

that use of CO_2 as a buffer gas in HPECMS does not result in production of any negative ions related to wall transformations of neutrals.

Similar results are observed in the case of Pentac, shown in Figure 18, where the unusual negative ions observed from methane are believed to be related, in part, to a Route D mechanism. The EC/CO_2 spectrum provides negative ions which are readily predictable from dissociative or resonance EC of the molecule.

In the cases of the halogenated quinones and Pentac, the sensitivity based on the ions arising from dissociative and/or resonance electron capture in CO_2 are equivalent to or greater than the respective ions in CH_4.

Examples From Route C Processes

It has been shown that TCNE and TCNQ are extremely effective trapping agents for hydrocarbon based gas phase free radicals. The EC/CH_4 spectra of TCNE and TCNQ are nearly totally obscured by radical related reactions as seen in Figure 19b and 19d. In contrast, the EC/CO_2 spectra of these compounds, in Figure 19a and 19c, show only the expected dissociative and resonance EC products. All spectra were recorded under identical conditions of pressure, temperature, electron energy and beam current, and sample concentration. No gas phase free radical reactions with TCNE and TCNQ prior to EC are indicated in these spectra.

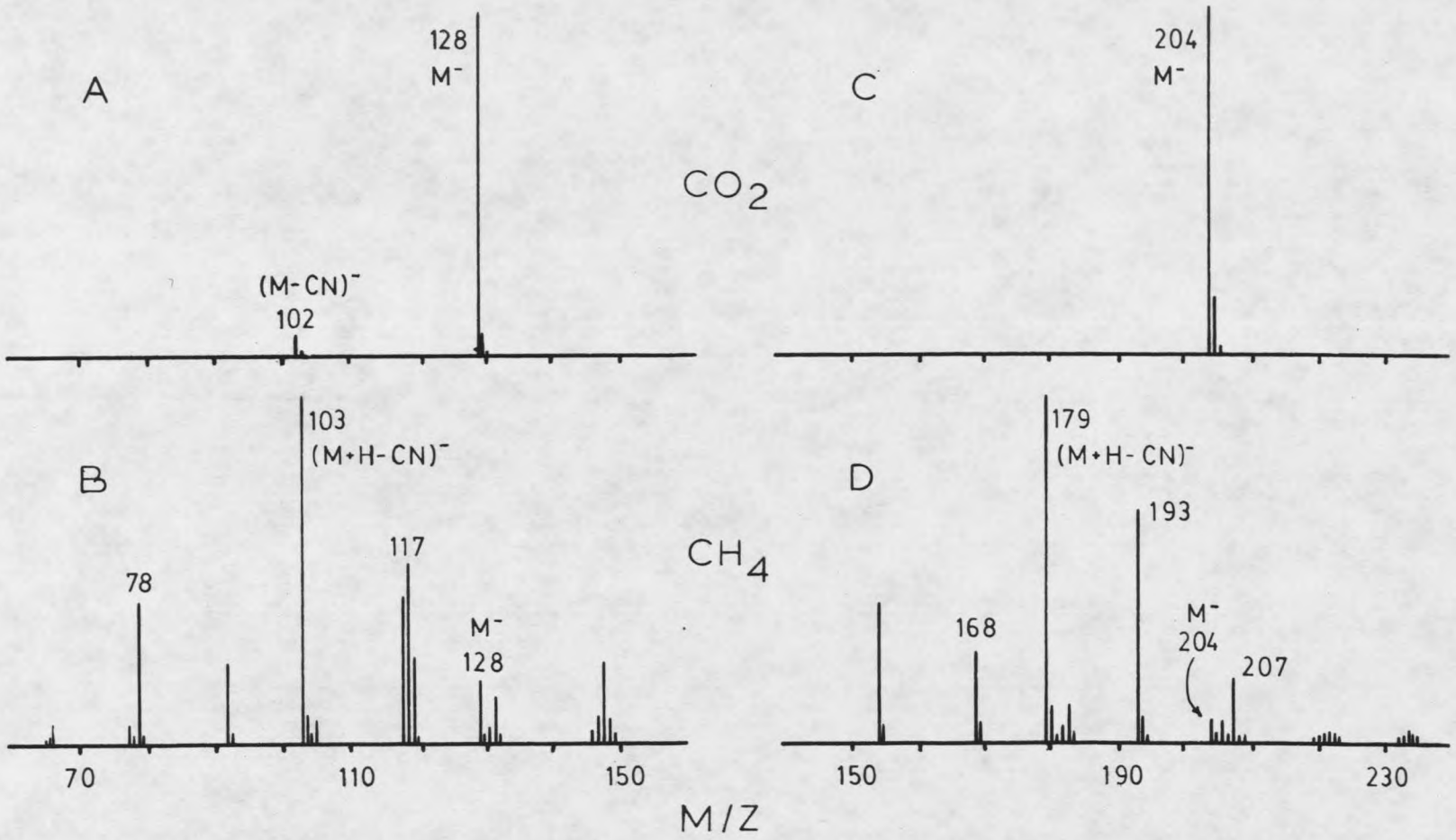

Figure 19. The HPECMS spectrum of tetracyanoethylene in (A) CO_2 and (B) CH_4, and tetracyanoquinodimethane in (C) CO_2 and (D) CH_4. The pressure is 0.5 Torr and the temperature is 150°C.

Examples from Route B Processes

The TFA derivatives of AA and AP have been demonstrated to undergo positive ion-molecule reactions followed by neutralization by either recombination with electrons or diffusion to the walls. The result of the neutralization was the generation in the EC spectrum of an unusual ion of $[M-O]^-$, a loss which would not normally be expected, especially from a carbonyl oxygen. Contributions to the negative ion signal through Route B can only be significant if EC is slow, thereby making positive ion-molecule reactions competitive. With this in mind, it follows that for compounds which attach electrons slowly, Route B will have the potential to remain active irregardless of the gas used to pressurize the source. The difference will lie in the product formed as the result of the initial positive ion-molecule reaction.

A comparison of results of the EC spectra of the trifluoroacetic anhydride derivative of 3-aminophenanthrene (3-AP-TFA) obtained in CH_4, CO_2, N_2, and $N(C_2H_5)_3$ is presented in Figure 20. In spectrum A, m/z = 273 has been found to be due to an oxygen loss, initiated by a prior positive ion-molecule reaction.

The CO_2 spectrum of 3-AP-TFA, as seen in spectrum B, provides us with an ion at m/z = 303 which is believed to have a composition of $[M-H+O]^-$ which might be more descriptively written as $[M+CO_2-H_2CO]^-$. The ion at

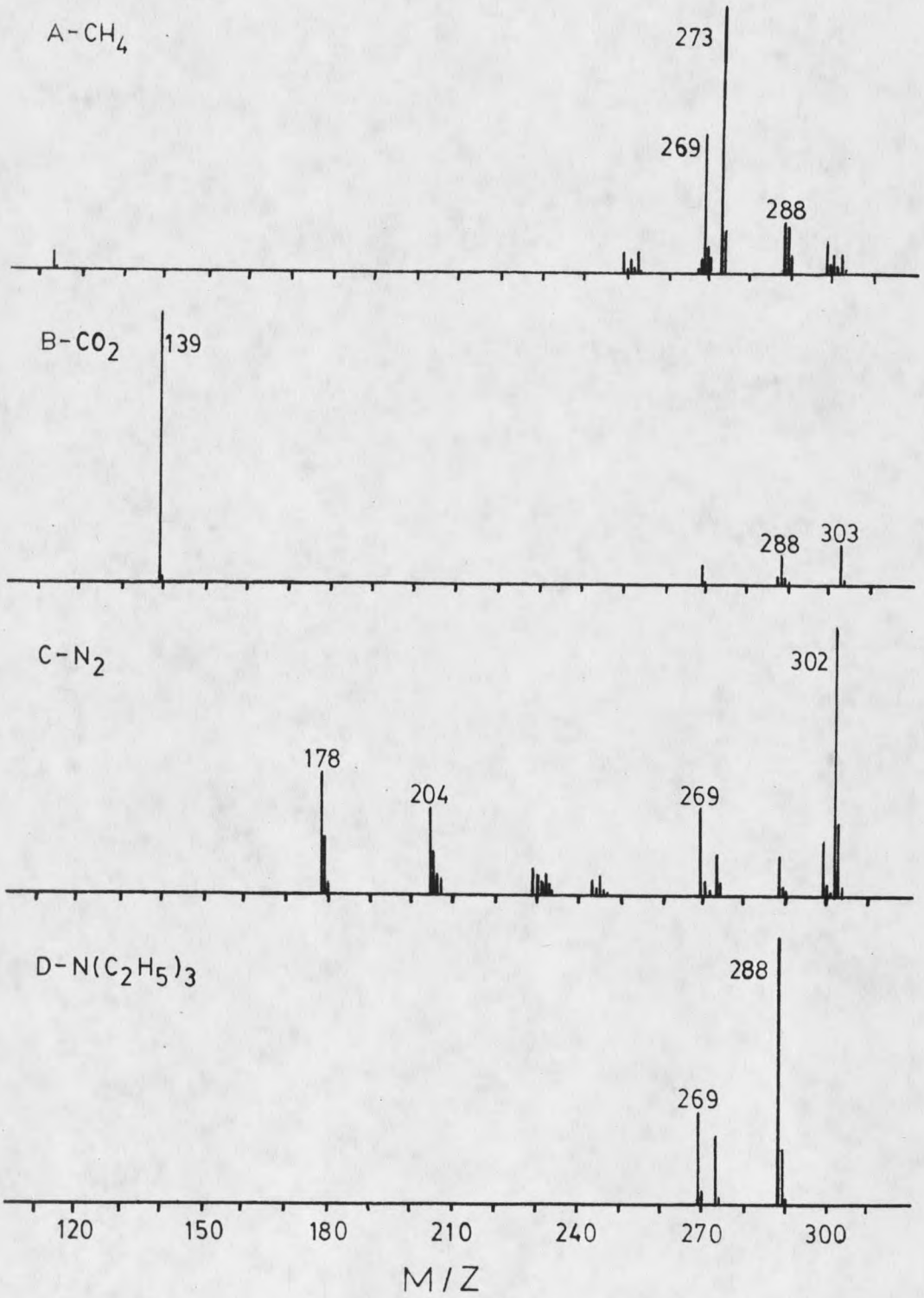

Figure 20. The HPECMS spectrum of the trifluoroacetic anhydride derivative of 3-aminophenanthren in (A) CH_4, (B) CO_2, (C) N_2, and (D) $N(C_2H_5)_3$. The pressure is 0.5 Torr and the temperature is 150°C.

m/z = 139 is due in part to the side chain functionality of 3-AP-TFA, and has the probable composition of $[NCO_2CF_3]$. This ion probably originates from fragmention of m/z = 303 by the sequence of M + CO_2 - $C_{14}H_9CO$. Again, these ions are likely the result of prior positive ion-molecule reactions involving CO_2^+, followed by neutralization and then electron capture.

Spectrum C is the net EC result when using N_2 as the buffer gas. Here, the primary reagent positive ion is N_2^+. The dominant ion in spectrum C is m/z = 302 which has been determined by accurate mass measurements to be $[M+N-H]^-$. The ions of m/z = 178 and 204 have been found to contain nitrogen originating from the ion source plasma. These ions are also thought to originate from prior ion-molecule reactions of 3-AP-TFA with positive reagent ions. The final gas used in this comparison was $(C_2H_5)_3N$, which as seen in D, provides a spectrum which has the closest resemblance to the desired EC reaction. The transfer of a proton from the reagent ion to 3-AP-TFA is not expected to occur as the result of differences in proton affinities. It may, however, be reasonable to expect adduct formation of the type MBH^+ or MB^+ where BH and B are the protonated and non-protonated buffer gas molecule respectively. Upon neutralization and electron capture it would be conceivable to generate a species such as $[M-H]^-$ as observed in spectrum D.

The spectra in Figure 20 indicates that CO_2 does not eliminate the occurrence of unusual negative ions for this set of compounds. Additionally, Figure 20 effectively demonstrates that in order to achieve ion signals representative of only EC for molecules that follow Route B processes, it may be necessary to eliminate the occurrence of positive ion-molecule reactions.

The discussion and comparison of EC spectra from CO_2 and methane has indicated that CO_2 may be well suited as a buffer gas in HPECMS. The occurrence of unusual negative ions has generally been eliminated by the use of CO_2. The observed sensitivity in CO_2 has been found to be equal to or better than the sensitivity in CH_4. A point to consider is why CO_2 is such a good candidate for a buffer gas in HPECMS? The next section will answer this question through a discussion of the role of the buffer gas in HPECMS ion sources.

THE ROLE OF THE BUFFER GAS IN HPECMS

Two general requirements of the buffer gas in HPECMS have already been briefly mentioned. These are 1) its inability to form long-lived negative ions which perturb the electron density in the ion source and possibly lead to negative ion-molecule reactions, and 2) it should not present a highly oxidative environment which would tend to shorten filament lifetimes and result in possible side reactions with the analyte. Assuming that these general requirements have been met, there are three additional considerations for selection of a buffer gas in HPECMS. One of these involves the principle subject of this study; that is the ability of the gas to minimize the occurrence of unusual negative ions. The other two considerations involve more fundamental characteristics of the gas itself and are discussed below.

Attenuation of the Energy of the Electron Beam

The thermalization of the electron beam may be divided into four distinct steps characterized by the energy range over which they occur. These are 1) ionization ($\geq$ 35 eV), 2) sub-ionization relaxation (1 - 35 eV), 3) sub-excitation relaxation (0.10 - 1.00 eV), and 4) relaxation of electrons

having energies below vibrational or rotational thresholds of the moderator gas (0.00 - 0.10 eV).

The initial step involves energy loss through the ionization process by

$$B + e_i \quad > \quad B^{+\cdot} + e_B + e_i \qquad (56)$$

where B is the buffer gas molecule, e_i is the ionizing electron (assumed to have an energy of 150 eV), and e_B is the electron removed from B in the ionization process. In high pressure sources it typically requires 30 - 35 eV to create an ion pair. This quantity of energy, lost from the ionizing electron, will be divided between the formed ion pair. The radical cation, $B^{+\cdot}$, will distribute its excess energy through fragmentation processes and collisions with the buffer gas and e_B will lose its excess energy in one of the succeeding relaxation steps. The ionizing electron, e_i, retains sufficient energy to create an additional 3 - 4 ion pairs.

Ions and electrons generated in the initial step of electron thermalization contribute to the steady-state equilibrium as defined by the system dynamics. The attenuation of electron energy by ionization of the buffer gas will be expected to proceed with nearly equal rates and efficiency for most gases used in HPECMS. Differences will be minor and will reflect the relative electron impact cross sections of each species, provided that pressures are

relatively high and equivalent for each gas.

The second step, defined here as relaxation of electrons having subionization energies, involves a series of elastic collisions. At this level of the overall thermalization process, differences in the ability of various buffer gases to attenuate the electron energy will become apparent. The differences will be characterized by the ability of the gas to absorb energy in the range of 1 to 35 eV. The rate of energy transfer from the electron to the buffer gas during an elastic collision would provide valuable insight for the selection of appropriate buffer gases for use in HPECMS ion sources. Perhaps as important would be knowledge of the relative time constants for electron energy exchange at a given pressure. The time constants may be compared directly with the time constants in Table 1 for the various processes which are expected to occur in a well thermalized ion source.

Warman and Sauer[37] have provided calculations of thermalization times, σ_{th}. These times have been determined over the energy range of the electrons, beginning at the time following ionization and ending at the time where reactions of the electrons may proceed by attachment or recombination at their thermalized rates. Values for thermalization times at 1 Torr are listed in Table 8 and were obtained by the relationship

$$\sigma_{th} = 2.303(k_u \times N_m)^{-1}[1+\log(\mu_o\mu_{th}^{-1} - 1)] \qquad (57)$$

where k_u is the energy exchange rate coefficient, N_m is the concentration of the buffer gas, $\mu_o\mu_{th}^{-1}$ is the ratio of the energy of the electron just following ionization to the energy at approximately 10% of the mean energy of the medium. Warman and Sauer base the magnitude of this ratio on experimental observations. It was found to have an approximate value of 25.

The energy exchange rate coefficients for CO_2 and NH_3 are an order of magnitude greater than those observed for CH_4. This suggests that CO_2 and NH_3 may be exceptionally efficient as attenuators of electron energy. The corresponding rates of the monatomic gases are quite slow. The time constants for thermalization by these simple gases suggest that the mean energy of the electrons in the ion source may be far from thermal. Therefore, less than optimum conditions will be provided by the monatomic gases for efficient electron capture.

Overall rate coefficients for electron attachments are typically dependent upon electron energy[39], particularly in the region close to thermal energies. The electron capture cross sections of most molecules possessing positive electron affinities substantially increases with decreasing electron energies. This enables an apparent faster rate of attachment with subsequent increases in signal intensities. A potential problem in the EC process arises when the time for energy relaxation of the electrons becomes comparable

to the time required for electron capture. An interesting series of experiments conducted by Warman and Sauer[37] using CCl_4 ($k_{e,CCl4} = 3 \times 10^{-7}$ cm^3 sec^{-1}) as an energy probe in argon, a gas which was determined to have a slow energy exchange coefficient ($k_{\mu,Ar} = 1.3 \times 10^{-13}$ cm^3 sec^{-1}), confirmed that signal intensities improved considerably as one changes to a fast electron energy exchange gas.

Table 8. Energy Exchange Coefficients, Thermalization Times, and Collision Efficiencies of Selected Gases.

Gas	k_μ[a], cm^3 sec^{-1}	σ_{th}[a], sec Torr^{-1}	Z[b]
Ar	1.3×10^{-13}	1.3×10^{-3}	77
Ne	2.5×10^{-13}	6.7×10^{-4}	100
He	6.4×10^{-12}	2.6×10^{-5}	150
N2	2.2×10^{-11}	7.6×10^{-6}	70
CH_4	8.6×10^{-10}	2.0×10^{-7}	40
CO_2	5.8×10^{-9}	2.9×10^{-8}	18
NH_3	5.9×10^{-9}	2.8×10^{-8}	-

[a] Warman and Sauer[37]
[b] Ahmad and Dunbar[41]

The third step in the relaxation process occurs for electrons having energies between thermal conditions and a few tenths of an eV; a region which provides direct vibrational and rotational excitation of the buffer gas molecule. Christophorou, et.al.,[39] has shown by calculations that the time required to thermalize an electron is constant for electrons having initial energies of 0.2 to 1.2 eV. The thermalization rate, however, increases rapidly as the energy of the electron approaches

the vibrational excitation threshold of the moderating gas. The vibration excitation threshold of CO_2 and CH_4 are 0.085 eV and 0.162 eV respectively. It is expected that those moderators having the lowest thresholds would be more effective at providing a large population of electrons of thermal energies, assuming that vibrational excitation of the moderator is the final mode of energy loss from the electron.

At energies between thermal and 1.0 eV, the mobility of the electron in the particular buffer gas should be considered with respect to capture by the analyte. Highly mobile electrons would tend to be less amenable to capture than those of lower mobility. Calculations have been provided by Christophorou[39] who has considered the mobility of electrons in various gases at 1 Torr. Of significance here is that the mobility, u, in CO_2 remains relatively constant and low (0.5 to 0.8) over the energy range of .04 to 1.0 eV. This is contrary to the mobilities of the electron in various hydrocarbon gases, including methane which ranged from $u = 8$ at 0.04 eV, to $u \approx 20$ at 0.14 eV (very near the vibrational excitation threshold of CH_4), and falling to a value of about $u = 4$ at 1.0 eV. The mobility of the electron at thermal energies is over an order of magnitude lower in CO_2 than methane, suggesting a possible enhancement of the electron capture process when using CO_2 as the buffer gas. An important point to

consider is the correlation between the electron mobility and the ambipolar diffusion coefficient, D_a. A decrease in the mobility of the electron must result in a decrease in the rate at which ions and electrons migrate to the walls of the ion source. The number of ions lost by wall-related neutralization will be decreased, thereby providing the potential for increased detection of negative ions related to the analyte.

The final step which may be of importance with some buffer gases is their ability to capture electrons into very short-lived states which rapidly undergo autodetachment. The attachment-autodetachment will not affect the electron density, provided the intermediate negative ion has a sufficiently short lifetime ($< 10^{-7}$ seconds). This process may, however, contribute substantially to electron energy thermalization by "indirect" vibrational excitation of the buffer gas. Indirect vibrational excitation can occur by the formation of intermediate compound-negative ion resonance states. Electrons that autodetach from these resonance states will have energies considerably lower than electrons which had induced direct vibrational excitation. The ultimate rate and degree of thermalization may not be determined by the actual vibrational excitation threshold of the buffer gas, but rather on the ability of the buffer gas to form these compound-negative ion resonance states. Although not all

gases used to thermalize electrons would be expected to provide this mode of energy relaxation, there is evidence available which supports this process in the case of CO_2[40]. Christophorou[39] notes that such processes would possibly occur with very high crossections, providing an extremely efficient mechanism in electron energy attenuation.

Collisional Stabilization Efficiency of the Negative Ion

In addition to the efficiency of thermalization, careful consideration must be given to the ability of the buffer gas to stabilize the initially formed molecular negative ion through collisional quenching. Ahmed and Dunbar[41] have recently discussed this subject and provided information as to the relative efficiency of various gases as quenching media. Their experiments involved the formation of bromobenzene positive ions in an ion cyclotron resonance cell by two-photon dissociation in the presence of a specific pressure of quenching gas. By monitoring a predetermined energy loss with respect to time at a known orbiting velocity, they were able to determine the absolute number of collisions required to provide the necessary quenching. The results of their experiments are provided in Table 8 for the gases of interest in this study. The value, Z, is the absolute number of collisions required to reduce an ion's energy from 2.48 eV to 0.35 eV. Although the absolute values will vary considerably under different

operating conditions, the important point is that relative values when comparing one gas to another should remain constant under identical conditions.

Experiments Involving Potential HPECMS Buffer Gases

Gregor and Guilhaus[42] have evaluated the use of various gases in terms of their abilities to provide maximum EC signals. Their investigations utilized anthraquinone and bis(N,N-diethyldithiocarbamato)-nickel(II) as electron capturing agents, both of which provide about 98% of the analytical signal as M^- in well thermalized systems. The results indicated that for these two probes the optimum signal was obtained by the use of CO_2 as the moderator. The other gases considered followed the general series of

$$He < Ne \approx N_2 < CH_4 \approx Ar \approx Kr < Xe < i\text{-}C_4H_{10} < CO_2$$

A study of electron attachment to NO_2 has been conducted by Christodoulides et.al,[38] in a series of charge exchange gases. Although the EC rate coefficient for NO_2 is not exceptionally fast, the relative signal intensities may still provide a useful guide to the use of these gases under EC conditions. The observed ion intensity in the gases considered in their study follow the order of

$$He < Xe < Kr < Ne < Ar < N_2$$

The work of Christodoulides and Gregor concerning the

relative utility of various buffer gases for providing intense EC ion signals provides useful experimental evidence concerning the overall processes of electron energy attenuation and collisional quenching of the negative ion. To complement the data, similar experiments were performed which involved selected compounds and buffer gases. Seven compounds were chosen which were anticipated to have relatively fast EC rate coefficients and large positive electron affinities. The eighth compound, azulene, was chosen because it is known to be sensitive to temperature variations of the ion source through thermal autodetachment of the electron as thermal conditions are altered[43]. The temperature of the ion source and pressure of the buffer gas were carefully adjusted to 130°C and 0.450 Torr respectively. Each compound listed in Table 9 was introduced to the ion source by the gas chromatograph at a concentration of 10 ng per component. Relative signal intensities of each component in the individual buffer gases were reported by measuring the total ion current of the chromatographic profile.

An interesting observation of the data in Table 9 is that for every compound, the relative signal intensity is larger in argon than helium. This might suggest, based on the information in Table 8, that the efficiency of collisional stabilization may be a more important parameter for consideration of optimization of signal intensities

than that of electron energy exchange rates. The general trend in the data is for increased signal intensities when going from poor electron energy exchange and collision stabilization gases to good energy exchange and collision stabilization gases (Z is not known for NH_3). The two exceptions are nitrobenzene and p-bromo-nitrobenzene. Here the EC signals are less than those obtained in methane but still substantially larger than any other non-hydrogen containing gas. These two exceptions certainly do not warrent the exclusion of CO_2 in HPEC.

Table 9. Comparison of Relative HPECMS Signal Intensities with the use of Different Electron Energy Moderating Gases. Temperature is 130°C, Pressure is 0.45 Torr, and the Concentration of Each Component is 10 ng.

Compound[a]	XE	He	Ar	N_2	NH_3	CH_4	CO_2
Fluoranil	.0004	.011	.039	.120	.540	.903[b]	1.000
m-CF_3-NO_2benzene	.0013	.007	.026	.037	.346	.854	1.000
p-F-NO_2-benzene	.0012	.005	.017	.035	.605	.984	1.000
NO_2-Benzene	.0006	.005	.011	.026	.852	1.000	.852
m-Cl-NO_2-Benzene	.0010	.009	.071	.037	.492	.926	1.000
p-Br-NO_2-Benzene	.0003	.007	.050	.038	.535	1.000	.820
p-$(NO_2)_2$-Benzene	-	.012	.041	.019	.302	.516	1.000
Azulene	.0002	.0014	.004	.004	1.000	.913	.001

[a] The electron affinities (eV) of each compound are as follows in order of their appearance in the table: 2.27[44], 1.34, 1.05, 0.96 , 1.19, -- , 1.89, 0.75.
[b] Value based on m/z=180; including the unusual ions, the value is 2.021.

The remaining case of azulene is somewhat of a mystery. Azulene follows the same general trend of increasing sensitivity as we go from slow electron energy exchange and

collision stabilization gases to fast energy exchange and collisional stabilization gases, until we come to CO_2. Here it is only a marginally responding compound. The signal intensities observed in CH_4 and NH_3 suggest that the rate coefficient for EC is certainly adequate for detection, and that conditions of thermalization and collisional stabilization would also seem to be adequate. From these considerations, azulene should provide an EC signal in CO_2 at least equivalent to those observed in CH_4 and NH_3 and yet it does not; the signal resembles those of the other charge exchange gases. The experimental data at hand does not provide sufficient clues for the solution to this unexpected result. A couple of points, however, should be elaborated upon.

First, for whatever significance, all gases in which azulene gave poor signals are typically used as charge exchange gases in positive chemical ionization ion sources. Second, the relative quenching efficiency, Z, was determined specifically for the bromobenzene positive ion. Generally, positive ions are more stable than the corresponding negative ion. It may be reasonable to expect collisional stabilization efficiencies to be somewhat different for negative ions than positive ions. Also, individual negative ions may show a preference for increased stability in one gas over another. Therefore, the poor sensitivity for azulene in CO_2 may be due to poor

thermalization of this negative ion in CO_2.

Additional Experiments Using Carbon Dioxide

It has been shown that irradiation of methane by the electron beam has resulted in the generation of a variety of reactive products. These reactive species from the methane plasma have been observed in the EC spectra of several compounds presented in this study. The irradiation of CO_2 by electrons is expected to yield several neutral and ionic species, yet it has been shown that EC/CO_2 spectra are generally free of species originating from the CO_2 plasma. To understand why the products of irradiated CO_2 are not seen in subsequent EC spectra, it is necessary to provide a brief discussion of the various reactions which lead to a steady-state condition in the CO_2/HPECMS ion source.

Meisels et al.[45] have described the interaction of the ionizing electron with CO_2 at pressures used in CI sources in addition to the normal fragment formation as the result of ionization by high energy electrons. Expected products of low pressure EI ionization are

$$CO_2 + e \;>\; CO_2^+ + 2e \qquad (58)$$

$$CO_2^+ \;>\; CO^+ + O \qquad (59a)$$

$$>\; CO\cdot + O^+ \qquad (59b)$$

Reactions at CI pressures would include

$$CO_2 + e \longrightarrow CO^+ + O^- + e \quad (60)$$

$$CO_2 + e \longrightarrow CO + O + e \quad (61)$$

$$O + e \longrightarrow O^- \quad (62)$$

$$CO_2^{+\cdot} + CO_2 \longrightarrow (CO_2)_2^{+\cdot} \quad (63)$$

Oxygen atoms and O^+ ions, CO molecules CO^+ ions, and $CO_2^{+\cdot}$ dimers are all possible. The oxygen atoms are expected to be extremely reactive and would, therefore, be rapidly lost by

$$O + CO_2 \longrightarrow CO_3 \quad (64)$$

$$O + e \longrightarrow O^- \quad (65)$$

$$O + O \longrightarrow O_2 \quad (66)$$

Although reaction 66 could certainly occur, the abundance of oxygen atoms in the gas phase is expected to be quite low, thereby reducing the significance of O_2 formation. Support for this is provided by observations of the negative ion background of CO_2 which is void of O_2^-. Present in a small amount is O^- which is shown to occur by reaction 65, and CO_3^- which may occur by the EC of CO_3 produced in reaction 64. It is anticipated that the majority of the oxygen atoms formed in the plasma will be found as CO_3 and CO_3^- species and therefore will not be available for reactions with analytes which exist in concentrations orders of magnitude less than CO_2. Although

CO_3^- is present as a reagent ion in the CO_2 plasma, calculations have shown that it contributes to approximately 2 - 5% of the total negative species in the steady-state system. This density of reagent negative ions is not expected to provide competitive signals from negative-ion molecule reactions with strongly responding EC compounds. The only perturbation expected would be in quantitative curves at higher analyte concentrations where electron densities would be depleted at a somewhat faster rate causing a loss of linearity. This is not considered to be a problem for trace analysis.

It has been previously shown that fluoranil is altered at the ion source walls by a reaction involving two hydrogen atoms. These hydrogen atoms, which originate from a hydrocarbon plasma, were apparent in the EI spectrum of fluoranil as a $[M+2H]^+$ ion. The EC spectrum of fluoranil provided negative ions which are believed to be due to the wall-altered neutral. An experiment is reported here which evaluates the effects of irradiated CO_2 on the EI and EC spectra of fluoranil after the ion source had been exposed to irradiated CH_4. Spectrum A of Figure 21 shows the EC spectrum of fluoranil obtained after the source walls had been exposed to irradiated methane for a period of 1 hour. The unusual ions of m/z = 162 and 142 contribute a substantial amount to the total ion current. To show the lingering effects of methane irradiation, the electron

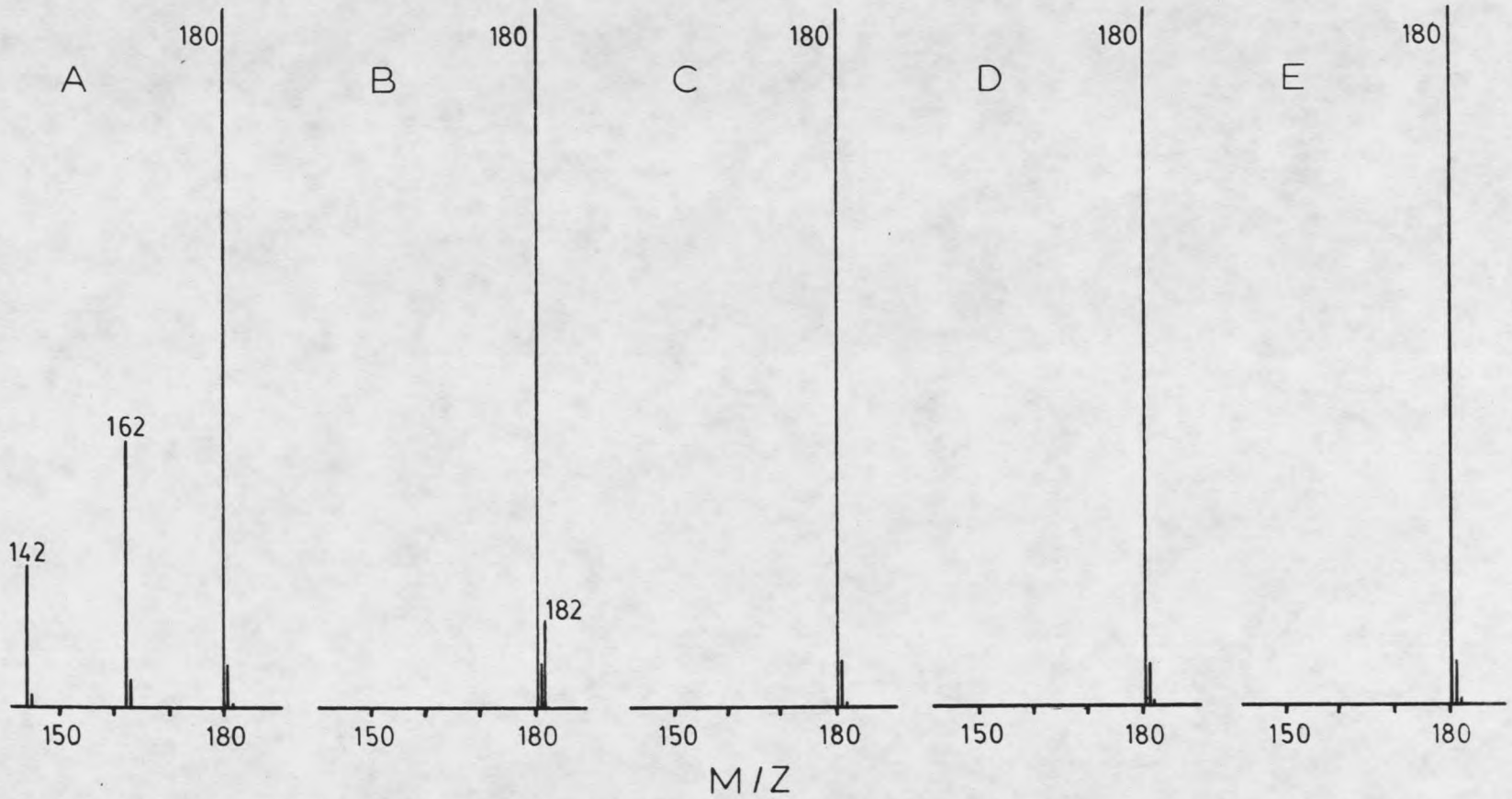

Figure 21. The HPECMS spectrum of fluoranil after (A) the ion source had been irradiated with CH_4 for 1 hour under HPEC conditions, (B) the EI spectrum two minutes later, (C) the HPECMS spectrum after 1 hour irradiation of CO_2, (D) the EI spectrum immediately after the CO_2 exposure, and (E) the EI spectrum of fluoranil after the ion source had been exposed to non-irradiated CH_4 for 1 hour. The pressure for HPECMS is 0.5 Torr and the temperature is 150°C.

impact spectrum was obtained which, as seen in spectrum B, provided comparable results to the same experiment previously conducted; that is, there is a substantial elevation of the $[M+2]^+$ signal due to the attachment of 2 hydrogen atoms to the fluoranil neutral.

Previous experiments, the results of which were presented in Figure 6, have shown that the $[M+2H]^+$ ion persists in the EI spectrum of fluoranil for as long as twelve hours. During that 12 hour time period the source was free of sample and buffer gas. Here, rather than remaining gas free, the ion source was exposed to irradiated CO_2. This exposure was conducted for a period of 1 hour under the same EC conditions which preceded spectrum A of Figure 21. Spectrum C shows the EC/CO_2 results of fluoranil after the 1 hour CO_2 irradiation. It is totally void of any of the unusual ions associated with CH_4 and provides only the expected EC response. A continuation of this experiment provides the EI spectrum of fluoranil obtained immediately following the CO_2 irradiation. It is seen in spectrum D that there are no lingering effects of the prior use of CH_4 or CO_2.

To confirm that the wall contamination arises from products generated by the interaction of the e-beam with methane, the ion source was exposed to 0.5 Torr of non-irradiated methane for a period of 1 hour. The EI spectrum of fluoranil was then obtained, and as seen from spectrum E

of Figure 21, there is no indication of the prior presence of methane. This result confirms that the source wall effects observed in the spectra of fluoranil and chloranil are indeed due to products of irradiated methane.

An interesting question arises with regard to the time required for removal of all effects of irradiated CH_4 from the source walls by exposure to irradiated CO_2. The combined data presented in Figures 22 and 23 represent a series of experiments which begins with exposing the ion source walls to irradiated CH_4 at 0.5 Torr for a period of 1 hour. After the one hour time period the system was switched to CO_2 at the same pressure and e-beam intensity used with CH_4. Spectrum A of Figure 22 provides the observed EC spectrum of fluoranil as obtained after the 1 hour CH_4 exposure (labeled as time 0). The three succeeding spectra, B, C, and D, provide the EC results obtained as a function of total exposure time of irradiated CO_2; 0.5, 1.25, and 2.75 minutes, respectively. As observed in this series of spectra, there is a substantial decrease in the occurrence of the wall related ions in a relatively short period of CO_2 irradiation.

A more significant representation of this "cleansing" effect of CO_2 is the plot of the background ion current as seen in Figure 23. The background negative ion signal was measured as a function of time when switching from 0.5 Torr CH_4 to 0.5 Torr CO_2 under identical electron currents and

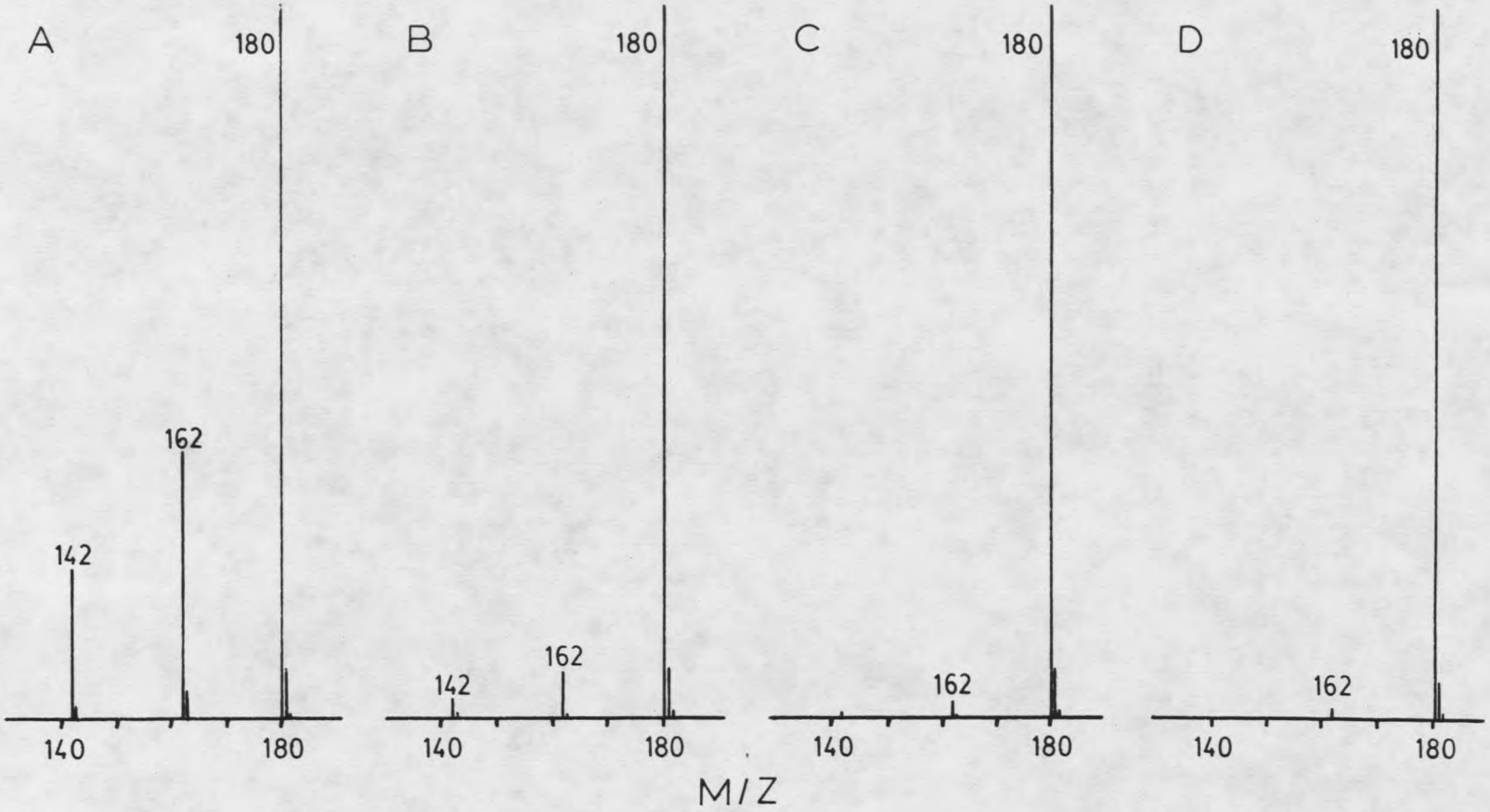

Figure 22. The HPECMS spectrum of fluoranil (A) in methane after the ion source had been irradiated for 1 hour, and the HPECMS spectra of fluoranil in CO_2 (B) 0.5 minute, (C) 1.25 minutes, and (D) 2.75 minutes after the methane exposure. The pressure is 0.5 Torr and the temperature is 150°C.

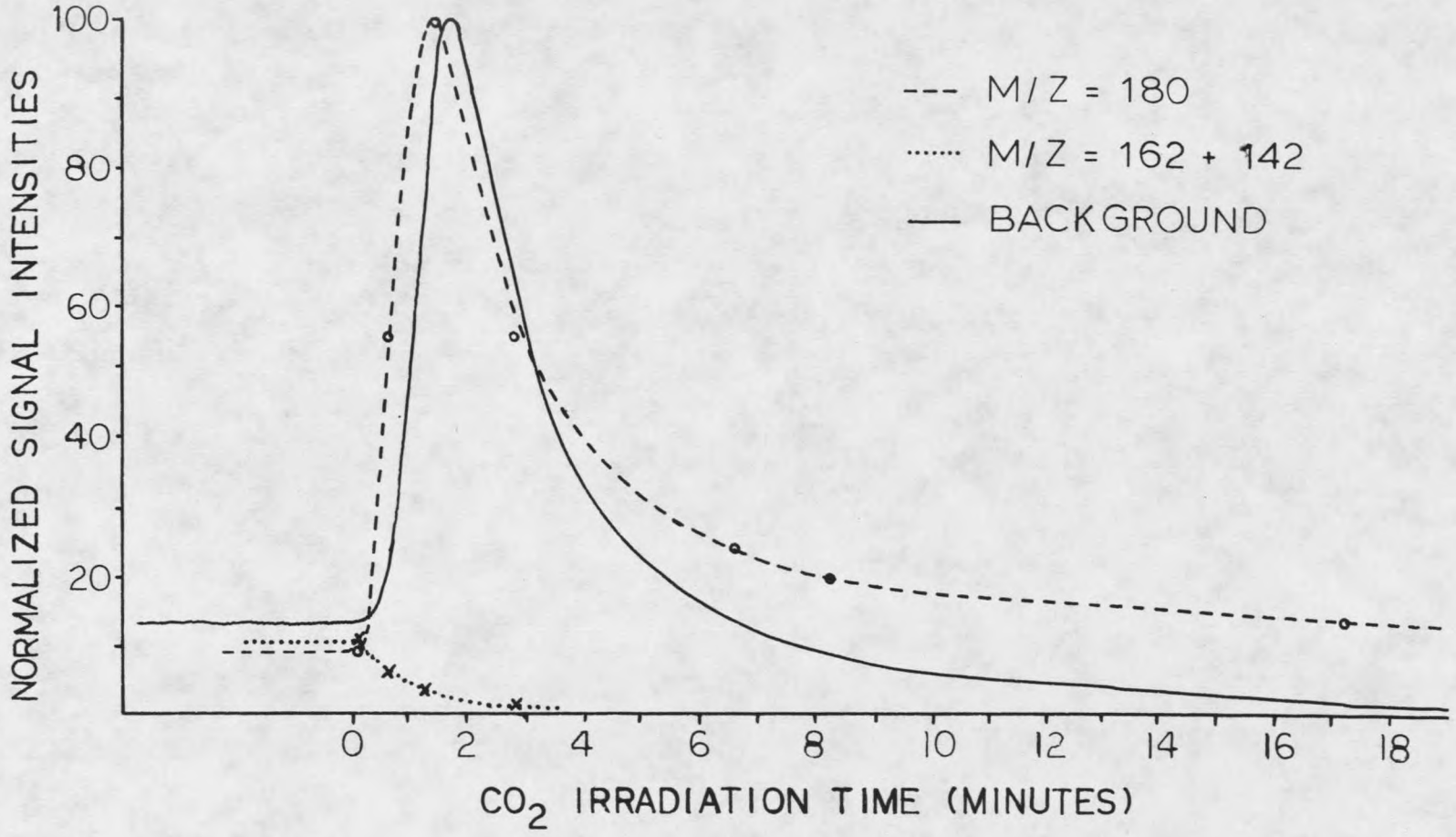

Figure 23. The normalized signals of the HPECMS negative ions background (solid line), m/z = 180 from the EC spectra of fluoranil (dashes) and the sum of the ion currents of m/z = 162 and 142 (dots). The data represents the observed signals when switching from CH_4 buffer gas (time 0) to CO_2 (time 0-18 minutes). The pressure is 0.5 Torr and the temperature is 150°C.

energies. As seen from the solid line, the background increases rapidly at time zero when CO_2 is initially introduced, to a value of nearly an order of magnitude larger than experienced with CH_4. It then falls over a period of 18 minutes at a near exponential rate to a level which is an order of magnitude less than the initial CH_4 background. The spectrum obtained of the background at maximum intensity as scanned over the mass range of 70 - 250 amu is provided in Figure 24. The background spectrum is indicative of a hydrocarbon homologous series differing by 14 mass units. Presumably these negative ions occur by some interaction of the CO_2 plasma with products contained on the source walls from irradiated methane, followed by electron attachment.

Presented with the background data in Figure 23 is the ion current of m/z = 180 (dashes) and the combined ion currents of the unusual ions, m/z = 162 and 142 (dots). These plots were obtained from the total GC peak profile of fluoranil as a function of time of exposure of the walls to irradiated CO_2. This data set is more revealing as to the true relationship of the relative ion signals of the EC spectra seen in Figure 22. Rather than remaining constant, the signal due to m/z = 180 follows the same pattern exhibited by the background negative ions. We see a substantial increase in the observed intensity for the molecular ion of fluoranil with sustained exposure to CO_2.

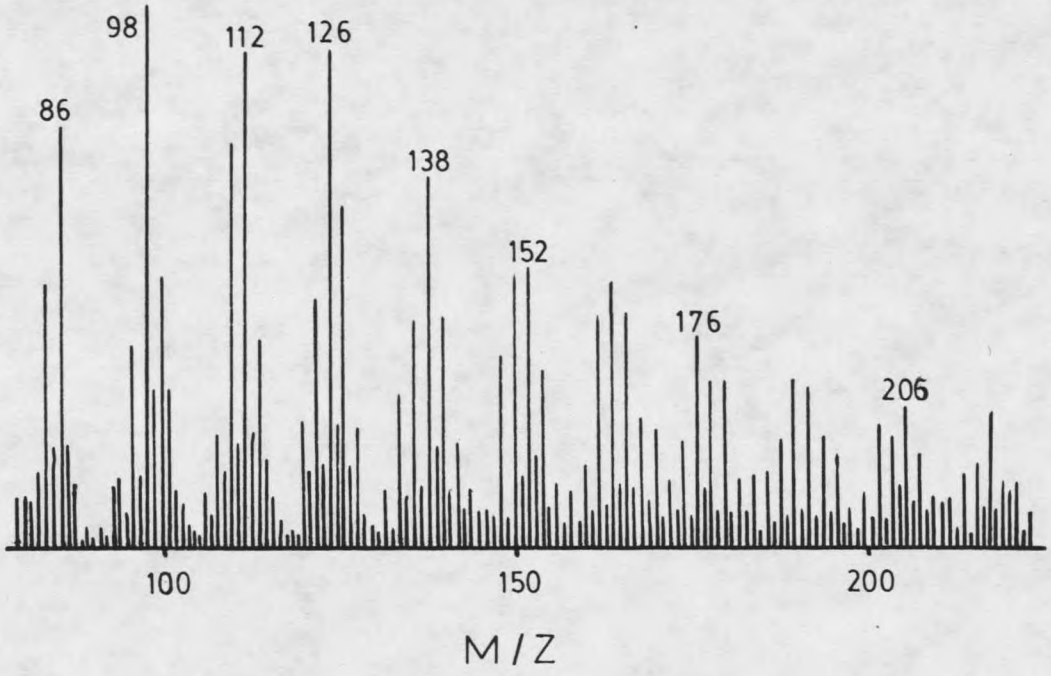

Figure 24. The HPECMS spectrum taken from the apex of the background signal in Figure 23.

This is followed by an apparent exponential decay of ion signal. The initial increase occurs with a concurrent decrease in intensity from the wall activated ions, m/z= 162 and 142.

There is insufficient experimental data to explain the increase in M^- intensity for fluoranil, however, the model of the HPECMS dynamics provides a guide for evaluating possible causes of this result. The intensity of the m/z = 180 ion is essentially the same in CH_4 and CO_2 as seen from time 0 and the extrapolated time of 25 minutes from Figure 23 (the actual value at 25 minutes was measured and found to be the same as the value at time 0). This suggests that the amount of neutral, M, available to form M^- is the same in both gases in a well equilibrated ion source. The large increase in M^- ion signal when switching from CH_4 to CO_2 can be due to only two possibilities; an increase in the amount of available neutral, M, or a decrease in the loss of M^- by neutralization processes.

The model, shown in Figure 1, provides two possible routes for increased availability of the neutral analyte in the case of fluoranil. First, we know that fluoranil forms unusual negative ions through wall assisted transformation of the neutral fluoranil molecule. It may be reasonable to expect that during the change-over period from CH_4 to CO_2, those wall related processes which form neutrals, W, may be perturbed. This in turn may lead to increased availability

of M, thereby providing greater M^- ion signals. Second, we have seen that Route A provides an increase in M^- signals through a recycling process of $M^-$to M through neutralization processes. Perhaps a disturbance in wall related processes as the result of a "cleansing" effect by CO_2 could initiate this recycling event. It seems unlikely, however, that an order of magnitude increase in signal strength could be brought about by one of these processes for increasing the amount of available neutral. This is because the typical HPECMS ion source is dominated by loss mechanisms such as recombination and neutralization at the source walls.

The probable cause for such a large increase in M^- ion intensity is a perturbation in the rate of loss of M^-. It has been shown that negative ion-positive ion recombination is a major mechanism of loss of negative ions. A change in the apparent recombination loss rate of M^- would certainly provide increased signal strengths. In Figure 23, it was shown that there was a significant increase in the negative ion background. These background negative ions will undergo recombination with positive ions with the same fast rate coefficient as the negative ions which originate from M. The loss of background negative ions through recombination with positive ions will result in a decrease in positive ion density. This loss of positive ions, if significant, would provide a decrease in the loss of M^-

through the process of recombination. The overall result is an increase in the amount of available M^- for detection.

The discussion presented in the preceding two paragraphs may not provide a definitive explanation for the observed increase in fluoranil signal during the change-over period from CH_4 to CO_2. It does, however, provide a basis for future experiments. It is interesting to speculate whether the addition of some compound to the buffer gas, which results in the production of a stable set of nonreactive negative ions, would be an effective technique for providing increased levels of analytical signal. An order of magnitude increase in detection of negative ions related to the analyte would certainly enhance the use of HPECMS in many applications.

SUMMARY

A series of electron capture spectra have been presented which contained unusual negative ions. The negative ions in these spectra, which do not arise from the princple electron capture process, have not been adequately explained in the literature. Explanations for these spectra have been provided here. Additionally, techniques for the elimination or control of secondary processes which lead to unexpected negative ions have been described. This has been for the purpose of providing simple spectra which reflect the principle electron capture process.

Four different pathways to the formation of unusual negative ions in a high pressure electron capture mass spectrometer ion source have been examined. These routes have been incorporated into a kinetic model which provides a qualitative and quantitative description of the ion source dynamics. Two of these routes for the formation of unusual negative ions have been proposed here for the first time.

Route A has been shown in the model, presented in Figure 1, to be a potential mechanism for production of unusual negative ions as the result of negative ion-positive ion recombination followed by an EC reaction of

the recombination product. Although no examples were presented which explicitly follow Route A, it has been suggested that the spectrum of Pentac is, in part, due to recombination reactions.

Route B involves the formation of unusual negative ions by way of recombination of positive ions with electrons with subsequent electron capture by the recombination generated neutral. Negative ions produced by Route B will provide competitive signals in EC spectra only if the EC rate coefficient of the analyte is slow. The contribution of signals by this route has been effectively demonstrated in the EC spectra of the trifluoroacetic anhydride derivatives of the isomers of aminoanthracene and aminophenanthrene.

The importance of radical-molecule reactions prior to electron capture is emphasized by Route C. Here, gas phase radicals, generated by the interaction of the electron beam with the buffer gas react with the analyte to form altered neutrals. Electron capture by the altered analyte may result in the formation of an even electron negative ion if a radical addition had occurred. An even electron negative ion would be expected to show increased stability over odd electron molecular negative ions. The EC spectra of tetracyanoethylene and tetracyanoquinodimethane have been shown to be dominated by negative ions which have originated from prior reactions of these molecules with gas

phase free radicals.

The final pathway in the kinetic model for the generation of unusual ions involves the formation of an altered neutral through a wall activated transformation of the analyte. Route D has the potential to produce very intense negative ions even though the EC rate coefficient of the parent molecule is very fast. The EC spectrum of fluoranil, chloranil, and Pentac are shown to be greatly affected by this mechanism.

The occurrence of unusual and unexpected negative ions in HPECMS has been shown to complicate the normal EC spectrum as they do not reflect the direct dissociative or resonance electron capture by the analyte. Generally, these complications are undesirable. However, the presence of unusual negative ions can also be beneficial. It has been shown that negative ions, produced by the routes shown in the model, are directly responsible for isomer-dependent EC spectra. The presence of unusual negative ions may, therefore, provide extremely valuable information in selected analytical applications. The model developed here may serve as a useful guide in the development of new analytical techniques in HPECMS which utilize the more sensitive routes toward negative ion production.

The second portion of this study has dealt with the development of techniques which may be used to eliminate or control the occurrence of unusual negative ions. The

modification of the ion source walls by coating with a layer of gold was found to provide no change in the observed EC spectrum of fluoranil. Additionally, the absorption of altered neutral species on the source walls was unchanged with surface modifications as demonstrated by the temporal profiles of reconstructed ion chromatograms.

Some of the EC spectra presented in this study indicate that many of the observed unusual negative ions are the result of using methane as the buffer gas. It was shown that the use of non-hydrocarbon buffer gases resulted in EC spectra which were generally free of unexpected negative ions. Although the spectra were simplified, the sensitivities obtained in helium, argon, and nitrogen were generally inadequate for trace analysis. Carbon dioxide, when used as the buffer gas, was found to provide simple spectra, demonstrated by a series of figures comparing EC results obtained carbon dioxide and methane. Additionally, ion intensities obtained from carbon dioxide were found to be greater than or equivalent to those observed from methane.

A discussion of the characteristics desireable in a buffer gas revealed that carbon dioxide might be uniquely suited for use in HPECMS. The ability of carbon dioxide to form short lived negative ion-molecule resonance states provides an added mode of electron energy attenuation which is not available to most buffer gases used in HPECMS. The

relative rate of collisional stabilization of ion energy, for a given ion, was found to proceed with exceptional efficiency in carbon dioxide. Support for the combined efficiencies of electron thermalization and collisional stabilization of carbon dioxide was found here in the relative EC sensitivities of various compounds in this buffer gas.

LITERATURE CITED

1. M.S.B. Munson and F.H. Field, *J. Amer. Chem. Soc.* 88, 2621 (1966).

2. A.G. Harrison, *Chemical Ionization Mass Spectrometry.* Chapter 2, CRC Press, Inc., Boca Raton, Florida (1983).

3. R.C. Daugherty and J. Dalton, *Org. Mass Spectrom.* 6, 1171 (1972).

4. D.F. Hunt, G.C. Stafford Jr., F.W. Crow and J.W. Russell, *Anal. Chem.* 48, 2098 (1976).

5. K.L. Busch, A. Norstrom, C.A. Nilsson, M.M.Bursey and J.R. Hass, *Env. Health Perspec.* 36, 125 (1980).

6. E.A. Stemmler and R.A. Hites, *Anal. Chem.* 57, 684 (1985).

7. D. Stockl and H Budzikiewicz, *Org. Mass Spectrom.* 17, 376 (1982).

8. L.R. Hilpert, G.D. Byrd and C.R. Vogt, *Anal. Chem.* 56, 1842 (1984).

9. D. Hunt and F.W. Crow, *Anal. Chem.* 50, 1781 (1978).

10. J.T. Martin, J.D. Barchas and K.F. Faull, *Anal. Chem.* 54, 1806 (1982).

11. K.E. Ibrahin, M.W. Couch, C.W. William, M.B. Budd, R.A. Yost and J.M. Midgley, *Anal. Chem.* 56, 1695 (1984).

12. D.B. Kassel, K.A. Kayganich and J.T. Watson, *American Society for Mass Spectrometry*, 34th Annual Conference, Cincinnati, OH (1986), Abstracts, p 523.

13. C.N. McEwen and M.A. Rudat, *J. Amer. Chem. Soc.* 101, 6470 (1979).

14. S. Dushman, in *Scientific Foundations of Vacuum Techniques*, ed. by J.M. Lafferty, p. 91. John Wiley & Sons, Inc., New York (1962).

15. *American Institute of Physics Handbook*, 3rd Edition, ed. by J.B. Marion and D.E. Grey, p. 184, McGraw-Hill, New York (1972).

16. C.N. McEwen and M.A. Rudat, *J. Amer. Chem. Soc.* 103, 4343 (1981).

17. H. Shimamori and H. Hotta, *J. Chem. Phys.* 85, 4480 (1986).

18. W.A. Prior, *Free Radicals*, part III, McGraw-Hill, New York (1966).

19. R.T. Morrison and R.N. Boyd, *Organic Chemistry*, 3rd Eddition, Chapters 3 and 6, Allyn and Bacon, Inc., Boston, MA (1975).

20. K.L. Denerjian, J.A. Kerr and J.G. Calvert, *Adv. Environ. Sci. Technol.* 4, 1 (1974).

21. S. Chowdhury, E.P. Grimsrud and P. Kebarle, *J. Phys. Chem.*, unpublished.

22. E.W. McDaniel, *Collision Phenomena in Ionized Gased*, pp. 503-506, Wiley, New York (1964).

23. S. Dushman, op. cit., p. 66.

24. E.W. McDaniel, op. cit., pp. 512-518.

25. W. Lindinger and D.L. Albritton, *J. Chem. Phys.* 62, 3517 (1975).

26. J.A. Kerr, in *Free Radicals*, ed by J.K. Kochi, Vol. 1, Chapter 1, John Wiley & Sons, New York (1973).

27. J.B.A. Mitchell and J.W. McGowan, in *Physics of Ion-Ion and Electron-Ion Collisions*, ed. by F. Brouillard and J.W. McGowan, p. 279. Plenum Press, New York (1983).

28. M.A. Biondi, in *Priciples of Laser Plasmas*, ed. by G. Bekefi, Chapter 4, John Wildy and Sons, New York (1976).

29. D. Smith and N.G. Adams, in *Physics of Ion-Ion and Electron-Ion Collision*, ed. by F. Brouillard and J.W. GcGowan, p. 501. Plenum Press, New York (1983).

30. C.A. Valkenburg, L.A. Krieger and E.P. Grimsrud, *J. Chem. Phys.* 86, 12 (1987).

31. M.W. Siegal, *Int. J. Mass Spectrom. & Ion Phys.* 46, 325 (1983).

32. B.W. Wilson, R.A. Pelroy and J.T. Cresto, *Mutat. Res.* 79, 193 (1980).

33. D.A. Later, M.L. Lee and B.W. Wilson, *Anal. Chem.* 54, 117 (1982).

34. T.H. Morton and T.A. Shaler, *American Society for Mass Spectrometry*, 36th Annual Conference, San Fransisco, CA (1988), Abstracts p. 677.

35. E.P. Grimsrud, *Anal. Chem.* 56, 1797 (1984).

36. E.P. Grimsrud, *J. Chromatogr.* 312, 49 (1984).

37. J.M. Warman and M.C. Saurer Jr., *J. Chem. Phys.* 62, 1971 (1775).

38. A.A. Christodoulides and L.G. Christophorou, *J. Chem. Phys.* 55, 4691 (1971).

39. L.G. Christophorou, K.S. Gant and J.K. Baird, *Chem. Phys. Letters* 30, 104 (1975).

40. M.T. Bowers and J.B. Laudenslager, in *Priciples of Laser Plasmas*, ed by G. Bekefi, Chepter 3, John Wiley & Sons, Inc., New York (1976).

41. M. Saber and R.C. Dunbar, *J. Amer. Chem. Soc.* 109, 3215 (1987).

42. I.K. Gregor and M. Guilhaus, *Int. J. Mass Spectrom. Ion Proc.* 56, 167 (1984).

43. E.P. Grimsrud, S. Chowdhury and P. Kebarle, *J. Chem. Phys.* 83, 8 (1985).

44. E.P. Grimsrud, G.C. Caldwell, S. Chowdhury and P. Kebarle, *J. Amer. Chem. Soc.*, 107, 4627 (1985).

45. R.K. Michum, J.P. Freeman, and G.G. Meisels, *J. Chem. Phys.* 62, 2465 (1975).